Doctoral Dissertation

Diverse Biomaterials Formation by Graft Polymer Approach

Kyohei NITTA

Department of Life and Functional Material Science,

Graduate School of Natural Science

Konan University

March 2016

Referee in Chief: **Professor Dr. Junji WATANABE**

Faculty of Science and Engineering, Konan University

Referees: **Professor Dr. Nobuya MACHIDA**

Faculty of Science and Engineering, Konan University

Professor Dr. Masahiro YAMAMOTO

Faculty of Science and Engineering, Konan University

Table of Contents

Chapter 1

General Introduction

Chapter 2

Solution Properties of Graft Copolymer with Poly(trimethylene carbonate) Oligo Segment

Chapter 3

Characterization of Temperature-Responsive Graft Copolymer with Polycarbonate Oligo Segment

Chapter 4

Synthesis and Evaluation of Surface Property of Amphiphilic Graft Copolymer Containing Different Oligo Segments

Chapter 5

Design and Synthesis of Amphiphilic Graft Hydrogel Having Hydrophobic Domain Formed by Multiple Physical Interactions

Chapter 6

Synthesis of Amphiphilic Polymer Gels Containing Poly(trimethylene carbonate) Segments and Evaluation of Its Molecular Incorporation Properties

Chapter 7

Chapter 1

General Introduction

1.1 Scope of Research

Biomaterials are defined as materials that can be adapted for use with elements that comprise biological bodies, such as biologically relevant molecules and cells, and can also be utilized in direct contact with the biological body [1]. In the polymer biomaterials field, molded articles, surgical materials, and polymeric drugs have been put to practical use [2].

For example, blood bags, artificial blood vessels, and syringes are made from molded commodity resins such as poly(vinyl chloride), polytetrafluoroethylene, and polypropylene. The surgical materials, suture thread, and bolts for the treatment of fractures are made from poly(lactic acid), hydroxyapatite, etc. In polymeric drugs, the drug delivery system (DDS) and gene therapy are well known and these techniques are aggregate introduced poly(ethylene glycol) (PEG) and liposome into copolymer. Biomaterials have wide-ranging applications, but the common properties required for ensuring interaction between the biological body and the material are biocompatibility, non-toxicity, antibiotic activity, strength, and functionality [3].

Biomaterials based on polymers have advantages over ceramic and metallic materials in terms of molecular design when considering interactions with biological bodies. Moreover, polymeric biomaterials have excellent transparency, weight, flexibility, and workability compared to metallic and ceramic biomaterials, and is adaptable to needs and technologies for greater sophistication and diversity. Therefore, to express functions for biomaterials, polymer design is assumed increasing importance in association with highly development of medical technology. Due to the constant efforts of researchers, many kinds of polymeric biomaterials have been developed and improved. The author focused on high functional devices, polymer colloids, polymer

membranes, and polymer gels composed of multicomponent copolymers (Figure 1.1). Three types of materials are expected and applied to biomaterial. The author designed and synthesized a novel amphiphilic graft copolymer by introducing functional group to change the physical and chemical properties. The graft copolymer was synthesized by the macromonomer method (Figure 1.2). The advantage of this method is that the hydrophilic–hydrophobic balance parameter could be controlled by altering the segment length and monomer composition ratio at the point of synthesis. The author conducted the study from the viewpoint of molecular design for the applications of biomaterials.

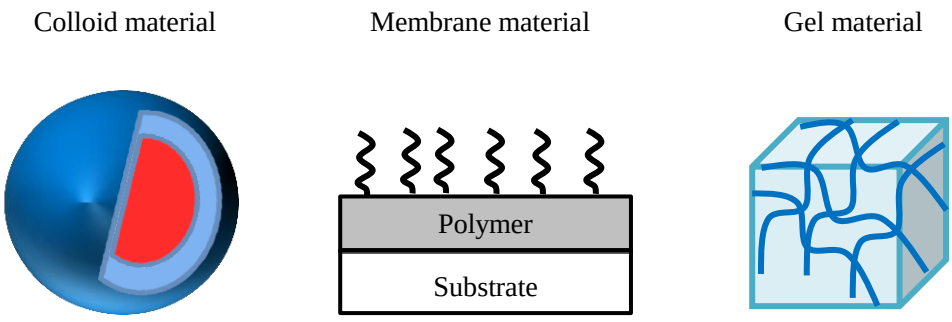

Figure 1.1. Illustrations of various polymeric materials.

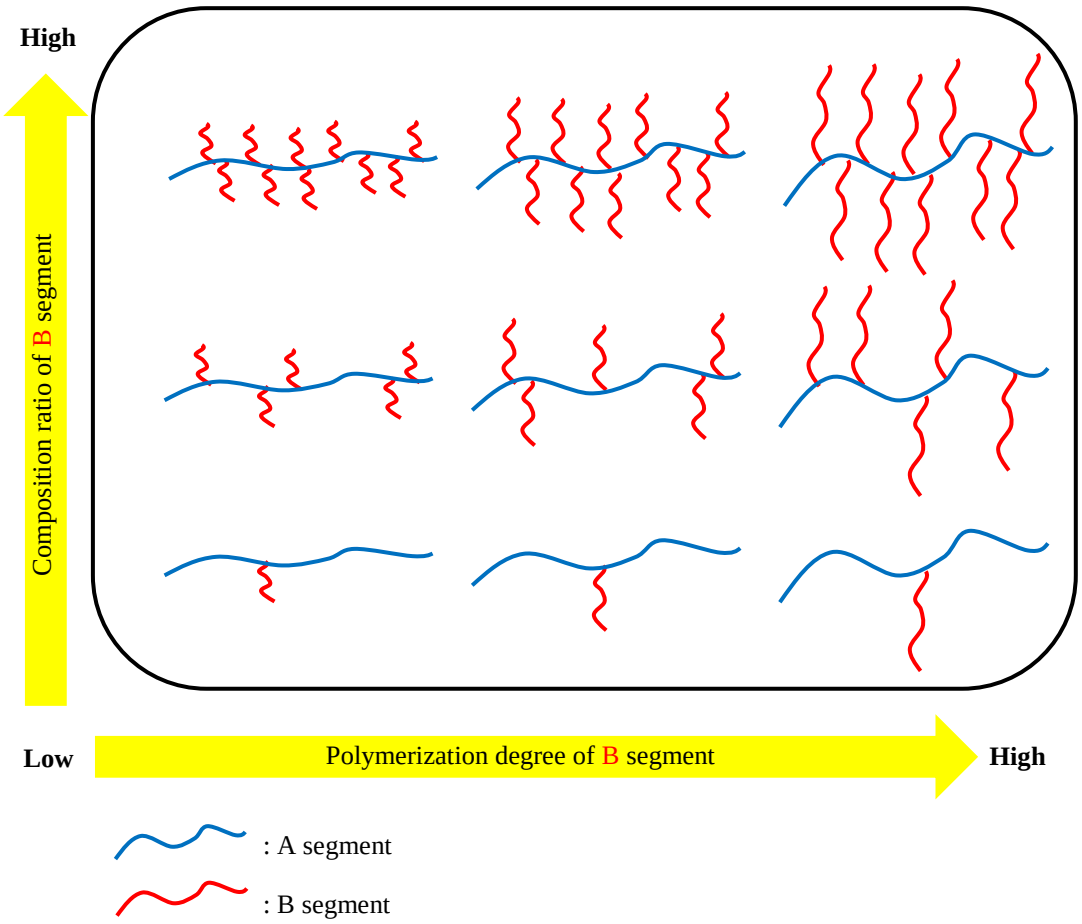

Figure 1.2. Illustration of the graft copolymer synthesized by the macromonomer method. Using this method, different graft copolymers can be obtained by altering the polymerization degree and composition ratio of the side chain.

1.2 Amphiphilic Copolymers

1.2.1 Amphiphilic Block Copolymers

Among copolymers, random copolymers are the most popular and have an irregular polymer structure formed by the connection of heterogeneous monomers (Figure 1.3(a)). On the other hand, block copolymers are constructed by covalent bonding between different polymer chains, so AB-type, ABA-type, and ABC-type copolymers are pattern (Figure 1.3(b and c)). The properties of block copolymer by polymer design are different by structure, ratio of components, polymerization degree, conjugation sequence, etc. Therefore, many types of phase-separated structures are formed and are expressed in novel functions under various systems. The study of block copolymers is actively researched. Amphiphilic block copolymers are composed of hydrophilic and hydrophobic segments and can be used to create novel functional polymeric materials [4–8]. For example, poly(hydroxethyl methacrylate)–*block*–polystyrene (PHEMA–*b*–PSt), a hydrophilic–hydrophobic diblock copolymer forms a lamellar layer and has excellent blood compatibility [9, 10]. The synthesis of block copolymers can be carried out by precise methods such as living polymerization [11–13].

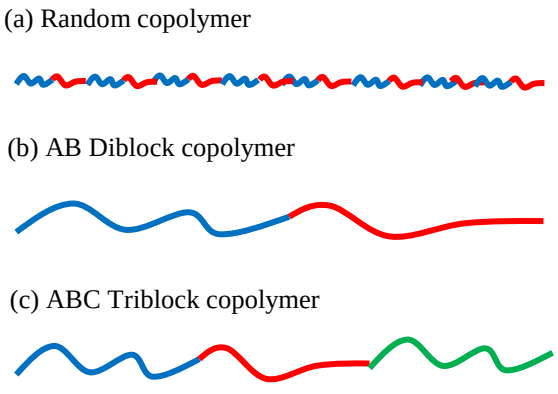

Figure 1.3. Illustrations of general random and block copolymers. (a) Random copolymer, (b) AB diblock copolymer, and (c) ABC triblock copolymer.

1.2.2 Amphiphilic Graft Copolymers

Graft polymerization introduces side chain polymers or oligomers in the main polymer chain, and the resulting copolymers are called star-shaped polymers, comb-shaped polymers, brush-shaped polymers, etc. The properties of graft copolymer can be changed by altering the number and length of the side chains. Polymer particle and substrate surface are able to introduce graft chains such as chemical reaction. Amphiphilic poly(dextran–*graft*–poly(lactic acid)) was reported to control the biodegradable rate in body [14]. Different polymer designs can be used to create novel functions. The synthesis of graft copolymers is classified into three main types, viz. the grafting-from method, grafting-onto method, and grafting-through method (macromonomer method) [15] (Figure 1.4). In the grafting-from method, the main chain

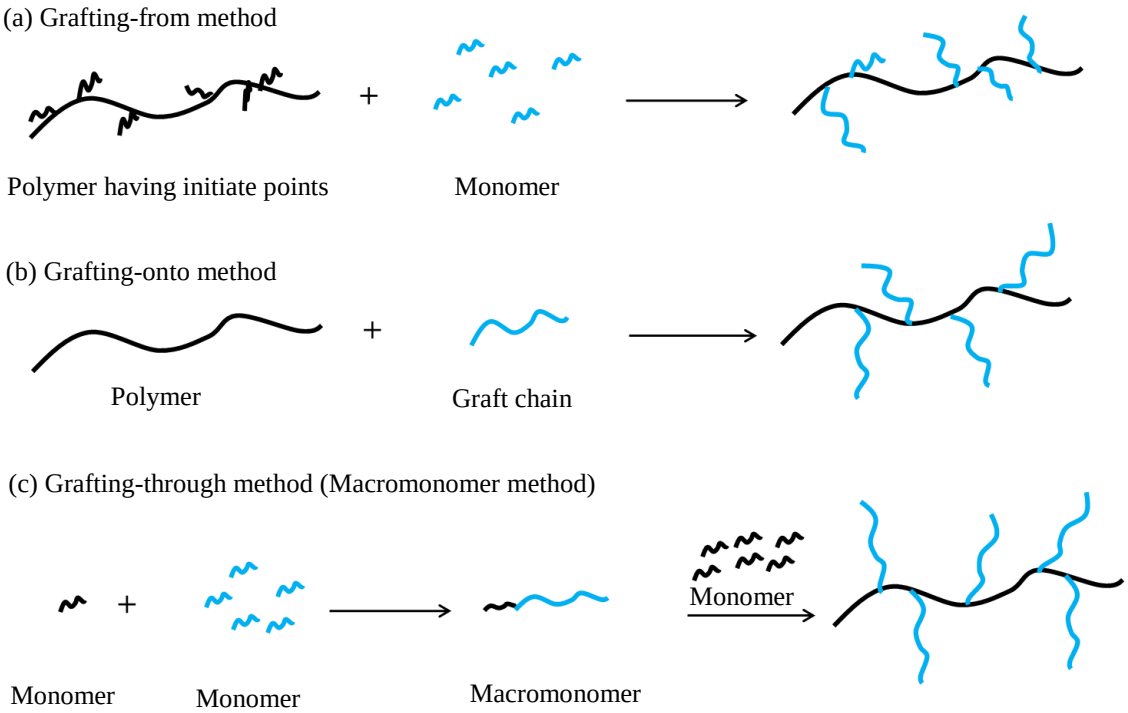

Figure 1.4. Illustrations of the synthesis methods of graft copolymers. (a) Grafting-from method, (b) grafting-onto method, and (c) grafting-through method (macromonomer method).

polymer is formed by building up from the reaction initiator, and then the monomer polymerizes onto this polymer (Figure 1.4(a)) [14]. This method is able to control the polymerization degree for precise polymerization, and can be used for the surface polymerization of materials using silane as the coupling agent [16].

The grafting-onto method introduces side chain polymers into the main chain polymer by chemical modification (Figure 1.4(b)). In this method, the length of the side chain is controlled, but controlling the introduction ratio is difficult because of the steric hindrance of the macromolecule.

The macromonomer method introduces polymerizable functional groups into the oligomer (or polymer) end group to form macromonomers (Figure1.4(c)). Subsequently, polymerization is carried out using the prepared macromonomers and monomer. The macromonomer method can easily control the composition ratio and provides a clear polymer structure (Figure 1.2) [17, 18].

These methods can be used to design various polymer structures. In this thesis, the author used the macromonomer method for polymer synthesis.

1.3 Main Polymer Biomaterials

1.3.1 Polymer colloids

Polymer colloids can be stably dispersed in solution and are widely applied in a variety of industries, including the food, medical, cosmetic, electrical, and paint industries. Microparticulated substances increase the surface area and are advantageous for functionality development. In medical fields, polymeric particles are used for diagnosis and in nano-capsules as drug- or gene-loading carriers. This technique is

called DDS. Injectable DDS can offset the side effects of drug molecules and is capable of spatially, quantitatively, and temporally controlled release. For example, Ringsdorf suggested a polymer backbone model in 1975 [4, 19]. This DDS model was still standard even now. This method was combining transport, drug, spacer, and solubilizer with polymer backbone. Polymer colloids were generally formed by microphase-separated structure by copolymer composed of hydrophilic segment and hydrophobic segment into one copolymer, wherein the hydrophilic segment is the outer shell and the hydrophobic segment is the inner core in aqueous solution [4–8, 20, 21]. In DDS, the hydrophilic segment is appropriate in biocompatible polymers for suppressing non-specific interactions with biomolecules such as proteins. A stimuli-responsive polymer capable of releasing the drug molecule is selected as the hydrophobic segment [22]. Kataoka *et al.* actively studied the DDS technique using hydrophilic PEG-modified copolymer carrier [23, 24]. A functional DDS carrier responsive to thermal, photochemical, and pH-related stimuli was recently studied [25–28].

1.3.2 Polymer Membranes

Polymer membranes are extensively used as molecular separation membrane, in water treatment, and in fuel cells. In the field of biomaterials, it is used in culture dishes, artificial joints, and dialysis machines [29]. The interface exists in all materials, , so the analysis of interface phenomenon is important. The biocompatibility of polymeric, ceramics, and metallic materials after polymer coating plays a role in the interface phenomenon. In the field of biomaterials, the poly(2-methacryloyloxyethyl phosphorylcholine) (PMPC) copolymer containing cellular membrane similar structure and the poly(2-methoxyethyl acrylate) (PMEA) copolymer having intermediate water

have attracted a lot of attention recently [30–35]. The poly(MPC–*co*–*n*-butyl methacrylate (BMA)) (PMB) copolymer showed different interface properties in air and water. This copolymer is achieved to express antithrombotic effect with materials *in vivo*, which materials put practical applications in medical front [33–35]. Therefore, ceramic or metallic biomaterials coated with MPC copolymers prevent the absorption of proteins and this ability is important for avoiding inflammation on using implants over long periods. Thus, the development of surface preparation agents having biocompatibility is imperative and is being actively pursued.

1.3.3 Polymer Hydrogels

Hydrogels are well known as water-absorbing bases for diapers, contact lenses, and greening deserts. In biomaterial fields, hydrogels are used in implantable materials, wound dressing, artificial muscle, and actuators, and their long-term impact are studied [36–38]. Polymer hydrogels form network structure by cross-linking between polymers. And the cross-link is classified based on the type of physical, chemical, and mechanical bonding [39, 40]. Physically cross-linked hydrogels have reversibly combination pattern as van der Waals force, electrostatic interaction, hydrogen bonding, and hydrophobic interaction, and volume changes such as swelling and shrinking can be caused by changing the external environment, salt concentration, electric field, temperature etc. Chemically cross-linked hydrogels are formed by irreversible covalent bonding, and are insulated from external influence. Mechanically cross-linking bridged site of topological gel is sliding on polymer network and increase mechanical strength. These hydrogels can load not only drug molecules but can also absorb solution such as culture media and bodily fluids. For example, a functional hydrogel-recognized by biomolecule

was reported to show swelling–shrinking behavior by formation and disassociation interaction of cross-linkage site by antigen-antibody reaction, thus the change in size by molecular recognition is applied for diagnosis system [41]. In this way, the inside of the hydrogel network is used the reaction domain, and the functional hydrogel is actively studied at present.

1.4 Poly(trimethylene carbonate)

Biocompatible and biodegradable polymers, such as poly(L-lactic acid) (PLA) and poly(ε-caprolactone) (PCL), have been widely studied for use as biomaterials (Figure 1.5) [14, 42–46]. In particular, PLA, which is derived from corn and potato, is obtained in large amounts using established industrial methods and is widely used for biomaterials, packaging films, vehicular components, etc. Although the PLA polymer has high mechanical strength because of its crystallinity, it has low compatibility with soft tissue due to its flexibility. Moreover, in degradable process of PLA, the noxious acid substrate to biological cell is formed. On the other hand, as an aliphatic polycarbonate, poly(trimethylene carbonate) (PTMC) is one of the hydrophobic polymers that has been investigated for biomedical applications [47–54]. PTMC has a number of advantageous properties that PLA and PCL do not have.

(a) PLA

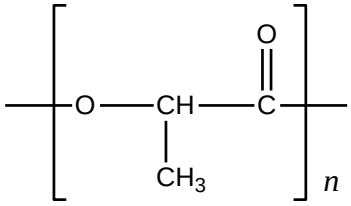

(b) PCL

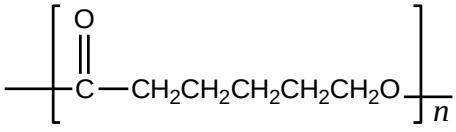

Figure 1.5. Chemical structures of (a) poly(L-lactic acid) (PLA) and (b) poly(ε-caprolactone) (PCL).

In this study, the author focused on the hydrophobic PTMC polymer. As a biodegradable polymer, PTMC is approved by the Food and Drug Administration and is a well-known biomaterial that is easily prepared from trimethylene carbonate (TMC) as cyclic monomer. TMC is polymerized at the hydroxyl group by a conventional ring-opening polymerization (ROP) technique using metal-free catalyst [55–57] (Scheme 1.1). The biodegradable PTMC indicates *in vivo* degradability by lipase enzyme without the formation of acidic degradation products, 1,3-propanediol and carbon dioxide . In addition, it has good biocompatibility, amorphous properties with a low glass transition temperature, and an easy and precise synthesis procedure. Therefore, the PTMC polymer as soft material is more compatible with soft tissues than the crystalline polymer. Conversely, in PTMC homopolymer, the fragile property is needed to compensate by copolymerization using other monomer. The materials of PTMC make it a promising candidate for use in tissue engineering, drug delivery systems, and surgical sutures. Watanabe *et al.* reported that polymer film created from block copolymer comprising PEG as the hydrophilic segment and PTMC as the hydrophobic segment has been selectively incorporated into an organic dye [51]. The fundamental mechanism for molecular incorporation is the spontaneous dynamic molecular motion of hydrophilic segments on the outermost surface. Therefore, surface enrichment with

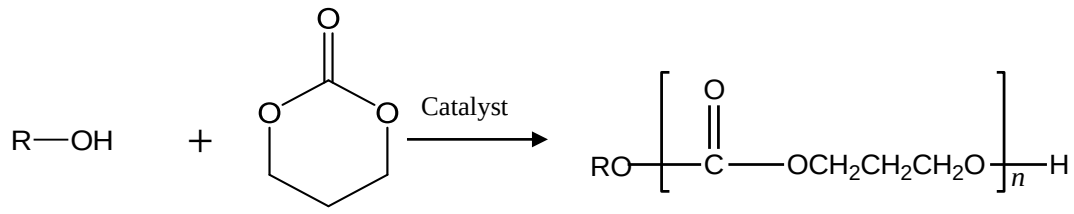

Scheme 1.1. Synthetic route towards the poly(trimetylene carbonate) (PTMC) copolymer.

hydrophilic segments would create an excellent interface between aqueous solutions and the PTMC membrane. Selectivity toward the organic dye could be achieved by changing the polarity of the dye molecules with respect to the hydrophobic environment created by the block copolymer. Thus, the PTMC derivative is designed and synthesized. Functionally, the PTMC copolymer is studied as a reverse temperature-responsive gel (PEG–PTMC diblock copolymer), surface preparation material (PTMC derivative) for biomaterials, and a DDS for protein loading and release (PTMC diols, poly(2-ethyl-2-oxazoline) (PEtOz)–*block*–PTMC, etc.) (Figure 1.6) [43, 52, 53, 58, 59]. Other amphiphilic polymers with hydrophobic and hydrophilic segments self-assemble to form hydrophobic domains in aqueous media. Thus, amphiphilic copolymers have enormous potential as DDS for enhancing drug-loading efficiency [60]. DDS vehicles in solution consist of stable core–shell structure formed by the aggregation of polymer chains. In many studies, biocompatible amphiphilic block copolymers have been designed using PEG, poly(methacrylic acid), and PMPC as the hydrophilic segment, and PLA, PCL, or PTMC as the hydrophobic segment [42, 43, 50, 61–63].

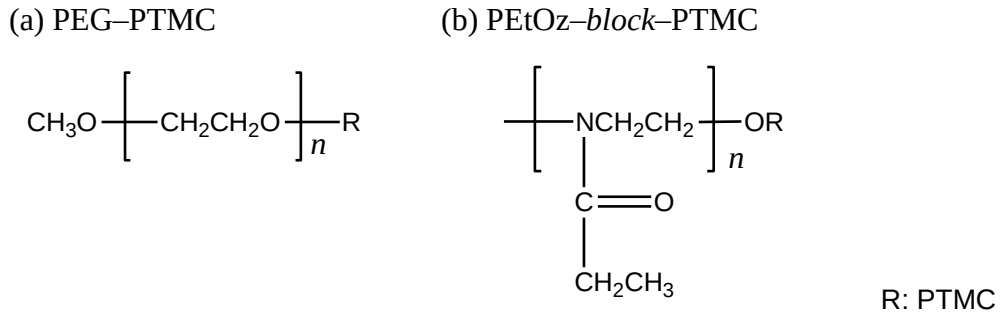

Figure 1.6. Chemical structures of (a) PEG–PTMC diblock copolymer and (b) PEtOz–*block*–PTMC.

1.5 Polymer Synthesis Method Used in This Study

1.5.1 Free Radical Polymerization

Free radical polymerization as an addition polymerization technique is a representative synthesis method in polymer science. In the case of the radical activated species, the polymerization is divided into four steps [15]. These elementary steps are called radical production, initiation, propagation, and termination via recombination or disproportionation. Initiators such as 2,2'-azobisisobutyronitrile and benzoyl peroxide were exposed to heat and light energy, which led to radical formation. This radical is reacted from vinyl monomer to vinyl monomer as chain-transfer reaction, and the active polymer grows to produce a polymer having high polymerization degree. Termination of active polymerization rapidly occurs by drawing hydrogen atoms or through recombination of polymers. As features of this polymerization method, the produced polymer has a high polymerization degree and a wide molecular weight distribution.

1.5.2 Ring-opening Polymerization

Cyclic monomers undergo ring-opening to overcome steric strain and is provided linear polymer by polymerizing reaction. Therefore, when the ring strain is high, polymerization proceeds to release the strain energy. The polymers using for biomaterials are PLA, poly(lactone), poly(dimethyl siloxane), PEG, poly(2-oxazoline), etc. [3, 42–46, 59]. These polymers are obtained by ROP. Polymerization by the ROP technique is easier and affords better yield than condensation polymerization.

1.6 Objective of this Thesis and Its Contents

This thesis is composed of seven chapters. The author conducted research on three types of materials such as polymer colloids, polymer membranes, and polymer gels (Figure 1.7). These materials were synthesized by macromonomer method and evaluated by material characterization in terms of polymer design for biomaterials. The author found that functionalities of these polymer materials were expected to apply for biomaterial fields.

Chapter 1 is a general introduction describing polymer biomaterials as colloids, hydrogels, and membranes. In the polymeric biomaterial section, to understand the polymeric biomaterial is more advantage than other materials and utilized biomaterials. In the polymer structure and materials section, the main copolymer is simple and is described by a study example. Moreover, we described reasons why some have chosen PTMC polymer and synthesis method in this study.

Chapter 2 describes polymer colloid gel formation from amphiphilic graft copolymers. This colloid gel spontaneously formed a micro network structure due to the driving forces of both hydrogen bonding and hydrophobic interactions in aqueous solution. For biomaterials, conventional polymer aggregation occurs due to molecular interactions, such as hydrophobic interactions, hydrogen bonding, and electrostatic interactions in solution. Polymer aggregation caused by several interactions has not been widely researched. Thus, the author had the objective of studying colloid particle preparation formed by from two type physical bonding and analyzed the solution properties. The author observed that hydrogen bonds dissociate upon heating and the particle size is changed. In addition, polymer colloids with different hydrophobic domain sizes were analyzed using the fluorescence probe method.

Chapter 3 describes about the functional polymer colloid preparation as basic design of graft copolymer in Chapter 2. Thermal responsiveness is one of the easily controlled external stimuli. The author focused on poly(*N*-isopropyl acrylamide) (poly(NIPAAm)) as a thermo-responsive polymer and designed the poly(*N*-hydroxyethyl acrylamide–*co*–NIPAAm–*co*–HEAA–PTMC) copolymer. This colloid gel derived from acrylamide polymer was investigated by reversibly altering the solution properties by hydration and dehydration under heating–cooling state. Furthermore, analysis of hydrophobic domains in the colloid gel was carried out using the fluorescence probe and fluorescence quenching methods.

Chapter 4 describes the molecular design of the polymer membrane for regulating surface properties. The author synthesized copolymers having hydrophilic and hydrophobic segments. The wettability of the amphiphilic random copolymer is maintained under the various conditions. Therefore, surface segregation by the polymer membrane is scarcely reported. The control of wettability, control of surface free energy, is important factors for affinity towards materials and biomolecules as well as adhesion–release. In Chapter 4, the author synthesized amphiphilic graft copolymers having different non-ionic segments by using the macromonomer method. Thus, the author conducted a study for controlling the wettability by altering the chain length and composition ratio of the hydrophobic PTMC segment. In terms of wettability, the surface property of the polymer membrane and the segment mobility of the copolymer were investigated by static contact angle measurements, microscopy observation, and differential scanning calorimetry analysis.

Chapter 5 describes the polymer design of hydrogels having a hydrophobic segment as the side chain. Conventional hydrogel composed of only hydrophilic segments

absorb low amounts of drug molecule and high amounts of water. In this chapter, the author attempted to improve the incorporation property of PTMC and the inhibition of swelling behavior by altering the cross-linking density. As a hydrophilic polymer, 2-acrylamidoglycolic acid (AGA) monomer with high hydrogen bonding was used as the main chain and the swelling ratio was controlled by physically cross-linking site and hydrogen bonding formation with hydroxyl, carboxyl, and amide groups. Thus, this prepared hydrogel with amphiphilic properties can be widely applied as a biocompatible and biodegradable soft material.

Chapter 6 describes the functionally of the improved hydrogel as a basic design of the amphiphilic graft gel in Chapter 5. The author selected three types of hydrophilic monomers, viz. 2-acrylamido-2-methylpropanesulfonic acid (AMPS), *N*-hydroxyethyl acrylamide (HEAA), and 2-hydroxyethyl acrylate (HEA). The purpose of this chapter was to examine the effectiveness of the soft material in terms of swelling ratio and model drug molecule loading. A number of different polar molecules were used and the selective molecule incorporative ability of each graft gel was evaluated by UV–Vis spectroscopy. These functional graft gels are expected to be used as DDS carriers, wound dressings, and adhesion prevention materials. The author synthesized amphiphilic graft gels by thermal polymerization or photo polymerization.

Chapter 7 is the conclusion of this thesis. The features of the amphiphilic graft copolymer introducing PTMC segment are summarized.

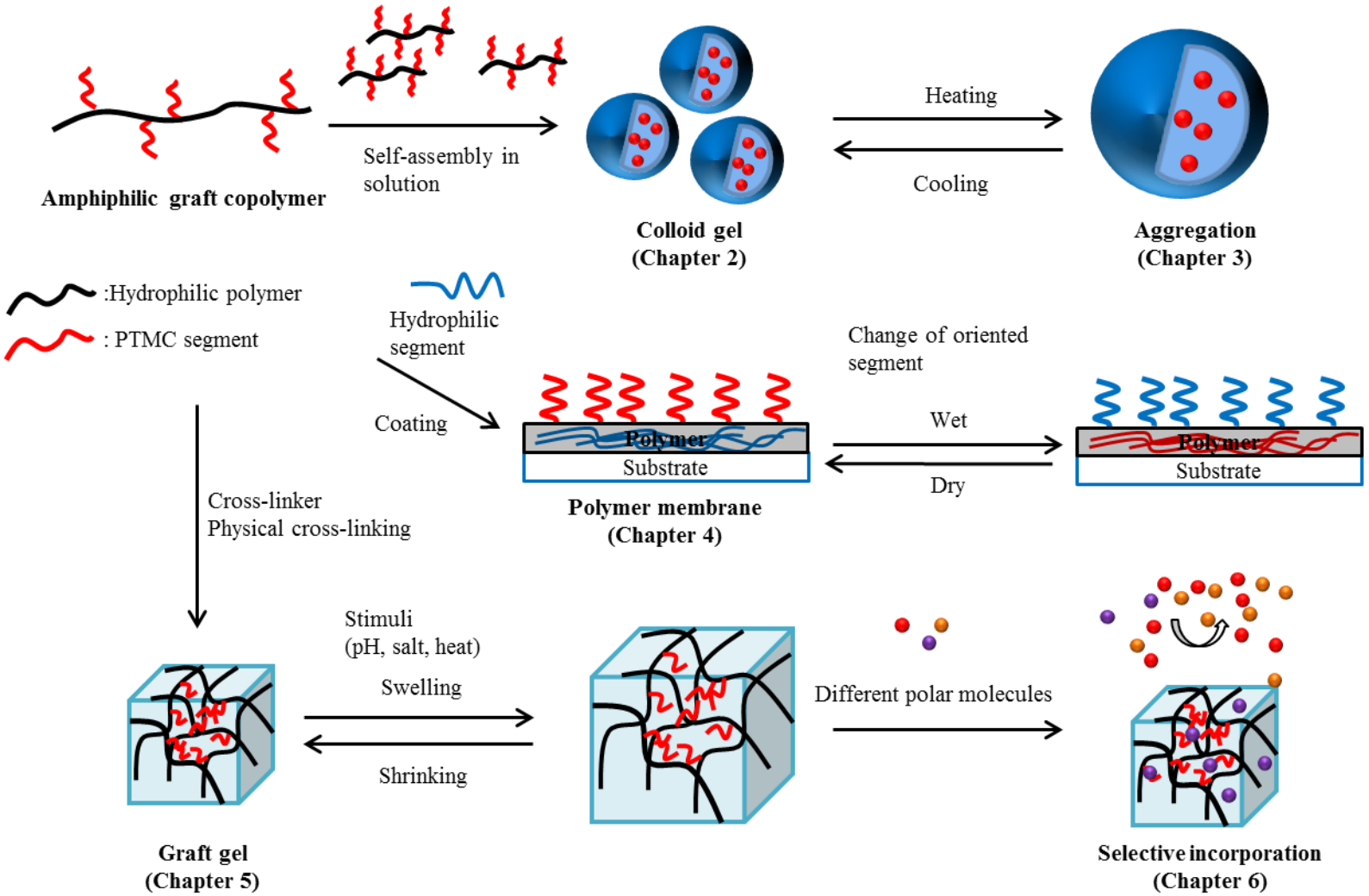

Figure 1.7. Illustration of the summary of this thesis.

1.7 Main Instruments Used for Characterization in This Study

The author used the following instruments listed below.

- Proton nuclear magnetic resonance (^{1}H NMR) spectrometer: Unity INOVA AS 500 MHz and Varian 300–MR (Varian Technologies Japan Co., Ltd., Tokyo, Japan).

- Fourier transform infrared spectroscopy (FT–IR) measurement device: FT/IR–4200, JASCO Co., Ltd., Tokyo, Japan.

- Gel permeation chromatography (GPC) measurement device; Shodex RI–71, UV–41, DS–4, and OVEN AO–30 (Showa Denko, Co., Ltd., Tokyo, Japan Showa Denko Co., Ltd., Tokyo, Japan) or UV–2075 Plus, RI–2031 Plus, PU–2080 Plus, AS–2055 Plus, and CO–2060 Plus (JASCO, Co., Ltd., Tokyo, Japan). All polymer samples and polystyrene as the standard substance were dissolved in *N*,*N*-dimethylformamide (DMF) at a concentration of 1 mg/mL in the presence of 10 mmol/L lithium bromide. GPC measurements were performed with a Shodex column (SB–804HQ or KD–804, Showa Denko Co., Ltd., Tokyo, Japan) with DMF eluent flow rate of 0.5 or 1.0 mL/min.

- Field-emission scanning electron microscopy (FE–SEM): VE–9800, KEYENCE Co., Ltd., Osaka, Japan. Sputter-coating with platinum: JFC–1600 AUTO FINE COATER, JEOL Co., Ltd., Tokyo, Japan.

- Atomic force microscopy (AFM): SPM–9700, SHIMADZU, Co., Ltd., Kyoto, Japan

- Differential scanning calorimetry (DSC) measurement device: Thermo Plus DSC8230, Rigaku Co., Ltd., Tokyo, Japan.

- Dynamic light scattering (DLS) measurement device: Zetasizer Nano ZS, Malvern Instruments Co., Ltd., Malvern, UK.

- Fluorescence spectrometer: F–2500 (Hitachi Co., Ltd., Tokyo, Japan.) or JASCO FP–8300 (temperature variable type) (JASCO Co., Ltd. Tokyo, Japan).

- Temperature variable UV–Vis spectrometer: JASCO V–650, JASCO Co., Ltd., Tokyo, Japan.

- Ultrapure water manufacturing equipment: Direct–Q 3 UV MILLIPORE, Japan Millipore Co., Ltd., Tokyo, Japan.

- Static contact angle measurement device: Drop Master 700 KYOWA Interface Science Co., Ltd., Saitama, Japan.

- Spin coater: SC–200, Oshigane Co., Ltd., Saitama, Japan.

1.8 References

[1] K. Ishihara, *Baiomateriaru Saiensu*, Tokyo Kagaku Dojin, **2003**.

[2] T. Furuzono and M. Okada, *Sinban Bijuaru-de Wakaru Baiomateriaru*, Shunjun-sha, **2006**.

[3] K. Ishihara, *Porima Baiomateriaru*, Korona-sha, **2009**.

[4] M. Hales, C. Barner-Kowollik, T. P. Davis, and M. H. Stenzel, *Langmuir* **2004**, *20*, 10809.

[5] J. Du and S. P. Armes, *Langmuir* **2009**, *25*, 9564.

[6] F. Yi and S. Zheng, *J. Phys. Chem. B* **2009**, *113*, 1857.

[7] F. J. Xu, J. Li, S. J. Yuan, Z. X. Zhang, E. T. Kang, and K. G. Neoh, *Biomacromolecules* **2008**, *9*, 331.

[8] Y. Iwasaki and E. Yamaguchi, *Macromolecules* **2010**, *43*, 2664.

[9] T. Okano, M. Katayama, and I. Shinohara, *J. Appl. Polym.* **1978**, *22*, 369.

[10] T. Okano, S. Nishiyama, I. Shinohara, T. Akaike, Y. Sakurai, K. Kataoka, T. Tsuruta, *J. Biomed. Mater. Res.* **1981**, *15*, 393.

[11] D. Neugebauer and K. Matyjaszewski, *Macromolecules* **2003**, *36*, 2598.

[12] P. Xu, H. Tang, S. Li, J. Ren, E. V. Kirk, W. J. Murdoch, M. Radosz, and Y. Shen, *Biomacromolecules* **2004**, *5*, 1736.

[13] S. Yusa, Y. Shimada, Y. Mitsukami, T. Yamamoto, and Yotaro Morishima, *Macromolecules* **2003**, *36*, 4208.

[14] K. Nagahama, Y. Mori, Y. Ohya, and T. Ouchi, *Biomacromolecules* **2007**, *8*, 2135.

[15] Kobunshi Gakkai-hen, *Kiso Kobunshi Kagaku*, Tokyo Kagaku Dojin, **2006**

[16] M. Kobayashi, Y. Terayama, H. Yamaguchi, M. Terada, D. Murakami, K. Ishihara, and A. Takahara, *Langmuir* **2012**, *28*, 7212.

[17] H. Shinoda, P. J. Miller, and K. Matyjaszewski., *Macromolecules* **2001**, *34*, 3186.

[18] H. Jeon, C. S. Lee, R. Pate, and J. H. Kim, *Appl. Mater. Interfaces* **2015**, *7*, 7767.

[19] Kobunshi Gakkai, *Doraggu Deribari Shisutemu*, Kyoritsu Shuppan, **2012**.

[20] S. Yusa, Y. Yokoyama, and Y. Morishima, *Macromolecules* **2009**, *42*, 376.

[21] H. Wei, W.-Q. Chen, C. Chang, C. Cheng, S.-X. Cheng, X.-Z. Zhang, and R.-X. Zhuo, *J. Phys. Chem. C* **2008**, *112*, 2888.

[22] J. Yan, Z. Ye, M. Chen, Z. Liu, Y. Xiao, Y. Zhang, Y. Zhou, W. Tan, and M. Lang, *Biomacromolecules* **2011**, *12*, 2562.

[23] A. Harada and K. Kataoka, *Prog. Polym. Sci.* **2006**, *31*, 949.

[24] M. Sanjoh, K. Miyata, R. J. Christie, T. Ishii, Y. Maeda, F. Pittella, S. Hiki, N. Nishiyama, and K. Kataoka *Biomacromolecules* **2012**, *12*, 3641.

[25] J. Rueda, S. Zschoche, H. Komber, D. Schmaljohann, and B. Voit, *Macromolecules* **2005**, *38*, 7330.

[26] J. V. M. Weaver, I. Bannister, K. L. Robinson, X. B.-Azeau, and S. P. Armes, *Macromolecules* **2004**, *37*, 2395.

[27] Q. Jin, F. Mitschang, and S. Agarwal, *Biomacromolecules* **2011**, *12*, 3684.

[28] S. Yusa, M. Sugahara, T. Endo, and Y. Morishima, *Langmuir* **2009**, *25*, 5258.

[29] K. Araki, M. Akashi, A. Takahara, and K. Kudo, *Yuki Kino Zairyo*, Tokyo Kagaku Dojin, **2006**.

[30] X. Lin, K. Fukazawa, and K. Ishihara, *Appli. Mater. Interfaces* **2015**, *7*, 17489.

[31] M. Tanaka, A. Mochizuki, N. Ishii, T. Motomura, and T. Hatakeyama, *Macromolecules* **2002**, *3*, 36.

[32] K. Fukazawa and K. Ishihara, *Appl. Mater. Interfaces* **2013**, *5*, 6832.

[33] S. Morita and M. Tanaka, *Langmuir* **2014**, *30*. 10698.

[34] W. Feng, S. Zhu, K. Ishihara, and J. L. Brash, *Langmuir* **2005**, *21*, 5980.

[35] K. Ishihara, T. Kitagawa, and Y. Inoue, *Biomater. Sci. Eng.* **2015**, *1*, 103

[36] M. L. O'Grady, P. Kuo, and K. K. Parker, *Appl. Mater. Interfaces* **2010**, *2*, 343.

[37] K. M. Park, Y. M. Shin, Y. K. Joung, H. Shin, and K. D. Park, *Biomacromolecules* **2010**, *11*, 706.

[38] Y. Takemoto, H. Ajiro, T. Asoh, and M. Akashi, *Chem. Mater*. **2010**, *22*, 2923.

[39] R. Yoshida, Kobunshi Geru, Kyoritsu Shuppan, **2004**

[40] Y. Hirokawa and S. Ida, Kinosei Geru-to Sono Oyo, Yoneda Shuppan, **2014**

[41] T. Miyata, M. Jige, T. Nakaminami, and T. Uragami, *Proc. Natl. Acad. Sci. USA.* **2006**, *103*, 1190.

[42] S. H. Kim, J. P. K. Tan, F. Nederberg, K. Fukushima, Y. Y. Yang, R. M. Waymouth and J. L. Hedrick, *Macromolecules* **2009**, *42*, 25.

[43] M. S. Kim, H. Hyun, G. Khang, and H. B. Lee, *Macromolecules* **2006**, *39*, 3099.

[44] B. G. Amsden, G. Misra, F. Gu, and H. M. Younes, *Biomacromolecules* **2004**, *5*, 2479.

[45] W. Fan, L. Wang, and S. Zheng, *Macromolecules* **2009**, *42*, 327.

[46] Z. Zhang, R. Kuijer, S. K. Bulstra, D. W. Grijpma, and J. Feijen, *Biomaterials* **2006**, *27*, 1741.

[47] N. Andronova and A.-C. Albertsson, *Biomacromolecules* **2006**, *7*, 1489.

[48] K. Terao, J. Miyake, J. Watanabe, and Y. Ikeda, *Mater. Sci. Eng. C* **2012**, *27*, 1741.

[49] F. Nederberg, B. G. G. Lohmeijer, F. Leibfarth, R. C. Pratt, J. Choi, A. P. Dove, R. M. Waymouth, and J. L. Hedrick, *Biomacromolecules* **2007**, *8*, 153.

[50] F. Nederberg, V. Trang, R. C. Pratt, A. F. Mason, C. W. Frank, R. M. Waymouth, and J. L. Hedrick, *Biomacromolecules* **2007**, *8*, 3294.

[51] J. Watanabe, H. Kotera, and M. Akashi, *Macromolecules* **2007**, *40*, 8731.

[52] J. Watanabe, S. Amemori, and M. Akashi, *Polymer* **2008**, *49*, 3709.

[53] B. Atthoff, F. Nederberg, L. Söderberg, J. Hilborn, and T. Bowden, *Biomacromolecules* **2006**, *7*, 2401.

[54] R. K. Srivastava and A.-C. Albertsson, *Macromolecules* **2007**, *40*, 4464.

[55] B. G. G. Lohmeijer, R. C. Pratt, F. Leibfarth, J. W. Logan, D. A. Long, A. P. Dove, F. Nederberg, J. Choi, C. Wade, R. M. Waymouth, and J. L. Hedrick, *Macromolecules* **2006**, *39*, 8574.

[56] H. Hyun, M. S. Kim, G. Khang, and H. B. Lee, *J. Polym. Sci Part A: Polym. Chem.* **2006**, *44*, 4235.

[57] F. He, H.-L. Jia, G. Liu, Y.-P. Wang, J. Feng, and R.-X. Zhuo, *Biomacromolecules* **2006**, *7*, 2269.

[58] K. Fukushima, R. C. Pratt, F. Nederberg, J. P. K. Tan, Y. Y. Yang, R. M. Waymouth, and J. L. Hedrick, *Biomacromolecules* **2008**, *9*, 3051.

[59] C. Kim, S. C. Lee, J. H. Shin, J.-S. Yoon, I. C. Kwon, and S. Y. Jeong, *Macromolecules* **2000**, *33*, 7448.

[60] R. A. Siegel and C. G. Pitt, *J. Controlled Release* **1995**, *33* 173.

[61] K. W. Nam, J. Watanabe, and K. Ishihara, *Biomacromolecules* **2002**, *3*, 100.

[62] T. Tyson, A. F.-Wistrand, and A.-C. Albertsson, *Biomacromolecules* **2009**, *10*, 149.

[63] K. Ishihara, Y. Iwasaki, and N. Nakabayashi, *Polym. J.* **1999**, *31*, 1231.

Chapter 2

Solution Properties of Graft Copolymer with Poly(trimethylene carbonate) Oligo Segment

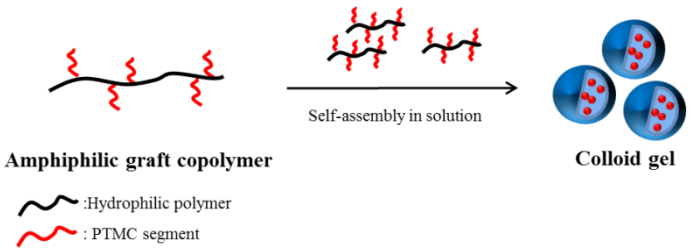

2.1 Introduction

Amphiphilic polymer with hydrophobic and hydrophilic segments self-assemble is known to form self-assembled structure having hydrophobic domain in aqueous media. Thus, amphiphilic copolymers have enormous potential as drug delivery systems (DDS) to enhance drug loading efficiency [1–3]. DDS vehicles in solution consist of a stable core–shell structure formed by the aggregation of polymer chains [1–10].

The author proposed and prepared an amphiphilic graft copolymer [11, 12]. The author evaluated the polarity of the hydrophobic domain formed by poly(*N*-hydroxyethyl acrylamide) (poly(HEAA)) grafted with poly(trimethylene carbonate) (PTMC), (Poly(HEAA–*graft*–PTMC) (PHET), in aqueous solution. The driving forces for the self-assembly are hydrogen bonding and hydrophobic interaction, and these properties can be adjusted by changing the composition ratio and the chain length of the macromonomer. Thus, PHET copolymers in aqueous solution could spontaneously form aggregates because of these driving forces [12].

In this chapter, the author prepared three kinds of amphiphilic graft copolymers. Two of these had similar hydrophobic chain lengths but different monomer composition ratios. The other combination had a similar total chain length, but different lengths of the hydrophobic segments. Thus, the effect of each molecular force could be evaluated in terms of polymer colloid formation for molecular encapsulation.

The author studied the properties of the PHET copolymers as well as their critical association concentrations (CAC) and partition equilibrium constants (K_v). The process of aggregation changes the properties of the solution, such as surface tension, turbidity, and light scattering intensity. Amphiphilic copolymer is known to forming micelle structure at lower CAC than surfactant of low molecular weight in aqueous solution.

Therefore, these amphiphilic copolymers are thermodynamicically stable [13]. Moreover, determining the values of CAC and K_v value is important for DDS, as they help in gauging the drug-loading ability of the aggregates. K_v value for partitioning of pyrene between the aqueous and aggregation phase represents one of the critical parameters related to aggregation stability. The CACs and K_v of the PHET copolymers were calculated by a fluorescence probe technique using the hydrophobic molecule pyrene, which is commonly employed to evaluate hydrophobic environments in aggregated structures [13–18]. The resulting data regarding the aggregate formation are extremely important for *in vivo* studies of this DDS vehicle in biomedical applications.

2.2 Experimental Section

2.2.1 Materials

In order to synthesize the macromonomer, the conventional ring-opening polymerization (ROP) was performed. Trimethylene carbonate (TMC) was purchased from Boehringer Ingelheim GmbH (Ingelheim, Germany). HEAA was provided by KOHJIN Co., Ltd. (Tokyo, Japan). 1,8-Diazabicyclo[5.4.0]undec-7-ene (DBU) (Kanto Chemical Co., Ltd., Tokyo, Japan) was used as a basic organocatalyst. The termination reaction of the ROP was performed using benzoic acid (Wako Pure Chemical Industries Co., Ltd., Osaka, Japan). To synthesize amphiphilic graft copolymers with the oligo PTMC segments, radical polymerization was carried out using 2,2′-azobis(isobutyronitrile) (AIBN; Tokyo Chemical Industry Co., Ltd., Tokyo, Japan) as the initiator. Pyrene was selected as a fluorescence probe and was purchased from Wako Pure Chemical Industries (Figure 2.1). All organic solvents were used as received.

2.2.2 Synthesis of HEAA–PTMC Macromonomer

Conventional ROP of TMC monomer from HEAA as initiator was first performed to obtain HEAA–PTMC macromonomer according to our previously reported procedure [11]. The synthesis of HEAA–PTMC macromonomers with 10 units of TMC was as follows: HEAA (102.8 μL, 1.0 mmol) and TMC (1.02 g, 10 mmol) were dissolved in methylene chloride (CH_2Cl_2) (30 mL). A solution of DBU (152.2 μL, 1.0 mmol) in

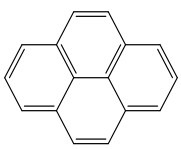

Figure 2.1. Chemical structure of pyrene.

CH_2Cl_2 was then added to the flask, and the solution was mixed. The final concentration of DBU was adjusted so as to not be greater than 30 mmol/L. The ROP was carried out under nitrogen atmosphere at room temperature for 24 h (Scheme 2.1). For the termination reaction, benzoic acid was added in order to inactivate the terminal hydroxyl group. The obtained solution including crude product was concentrated to 10 mL by rotary evaporation and was poured into a large amount of either a 2-propanol/water (2:1) mixture or undiluted 2-propanol in order to precipitate the resulting macromonomer. The final product was dried under reduced pressure to give in good yield. The degree of polymerization (DP) was calculated from the proton nuclear magnetic resonance (^{1}H NMR) spectrum. The synthesized HEA–PTMC macromonomers contained 10 or 50 TMC units. ^{1}H NMR (500 MHz, $CDCl_3$) δ: 2.1 (m, 2H, –CH_2–C*H*$_2$–CH_2–), 3.6 (q, 2H, –CH_2–C*H*$_2$–O–), 3.7 (t, 2H, –NH–C*H*$_2$–CH_2–), 4.2 (t, 4H, –O–C*H*$_2$–CH_2–C*H*$_2$–), 5.6 (d, 1H, CH_2=C*H*–C(=O)–O–), 6.1 (q, 1H, *H*–CH=CH–), 6.2 (br, 1H, –C(=O)–N*H*–CH_2–), 6.3 (d, 1H, H–C*H*=CH–).

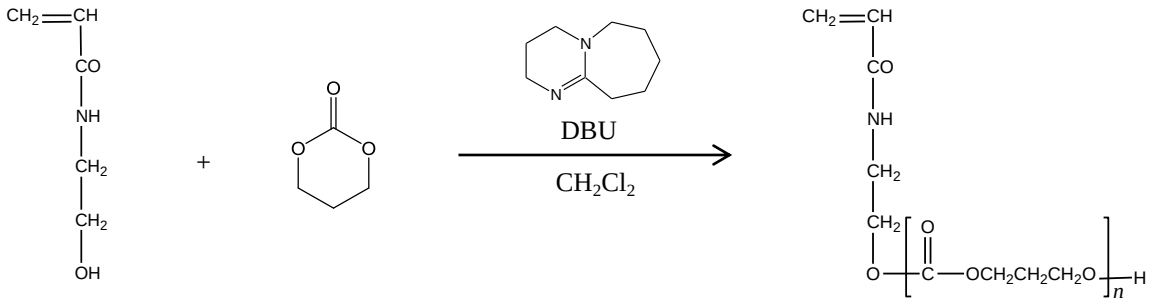

Scheme 2.1. Synthetic pathway of HEAA–PTMC macromonomer.

2.2.3 Synthesis of Amphiphilic Graft Copolymers; PHET Copolymers

The graft copolymer was synthesized using macromonomer method [12]. To prepare the graft copolymer, the free radical polymerization was carried out using AIBN, HEAA, and HEAA–PTMC macromonomer (Scheme 2.2). The reagents were each dissolved and mixed in *N*,*N*-dimethylformamide (DMF). The solution was degassed under reduced pressure and then was substituted by nitrogen gas. The mixture solution was heated at 70°C for 24 h. The reaction mixture was added to acetone/2-propanol (1:4 (v/v)), which is a poor solvent. The product was dried under reduced pressure. The composition ratio of HEAA to HEAA–PTMC macromonomer in the prepared graft copolymer was calculated from the ^{1}H NMR measurement. The number of graft chains in the copolymer was found to be approximately 1 to 10 mol%. The molecular weight was determined by gel permeation chromatography (GPC). ^{1}H NMR (500 MHz, DMSO-d_6) δ: 1.1–1.6 (br, 3H, –C*H*$_2$–C*H*–C(=O)–O–), 1.9 (m, 2H, –CH$_2$–C*H*$_2$–CH$_2$–), 3.4–3.5 (br, 4H, –NH–C*H*$_2$–C*H*$_2$–), 4.1 (t, 4H, –O–C*H*$_2$–CH$_2$–C*H*$_2$–O–), 7.2–7.9 (br, 1H, –C(=O)– N*H*–CH$_2$–).

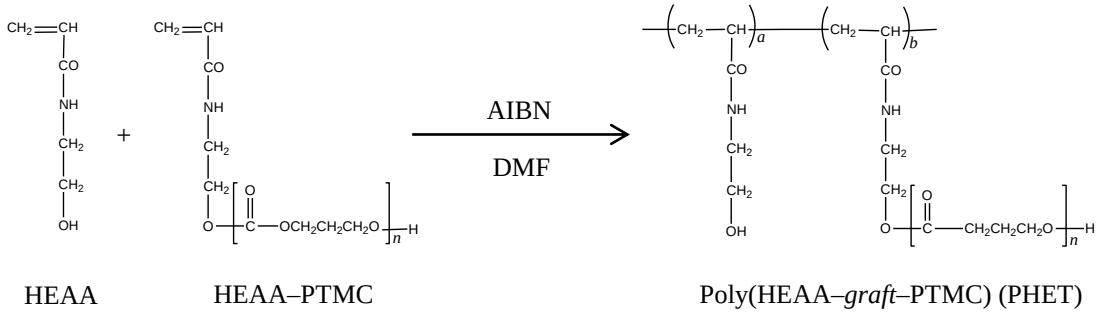

HEAA HEAA–PTMC Poly(HEAA–*graft*–PTMC) (PHET)

Scheme 2.2. Synthetic pathway of poly(HEAA–*graft*–PTMC) (PHET).

2.2.4 Particle Size and Thermal Stability

The synthesized graft copolymers spontaneously formed aggregates in aqueous media. In order to measure the size of these aggregates, the graft copolymer was dissolved in water, with ultrasonic agitation, for a short time, and then was filtered (pore size 0.8 μm). The copolymer solution was adjusted to a concentration at 1 mg/mL in water and dynamic light scattering (DLS) measurements were performed at temperatures ranging from 20 to 70°C.

2.2.5 Determination of CAC and Partition Equilibrium Constant (K_v)

In order to dissolve the hydrophobic pyrene probe in an aqueous solution, it was first dissolved in tetrahydrofuran (THF) at 1.2×10^{-3} mol/L [14, 16]. This solution was then added dropwise to water (6.0×10^{-7} mol/L) and vigorously stirred. THF was removed by rotary evaporation at 40°C for 2 h. A solution of the graft copolymer containing pyrene was then prepared. The final concentration of pyrene was 6.0×10^{-7} mol/L. Several graft copolymer solutions were prepared, with concentrations varying in the range of 10^{-5} to 1 mg/mL. The excitation spectrum of pyrene was measured using a fluorescence spectrophotometer at room temperature. The emission was measured at 373.0 nm with a slit-width of 5.0 nm and a scan speed of 300 nm/min.

2.3 Results and Discussion

2.3.1 Synthetic Results of Macromonomer and Amphiphilic Graft Copolymer

The polymerization of TMC was initiated from the hydroxyl end-group of HEAA. TMC monomer was polymerized by ROP with nucleophilic attack from the DBU-activated terminal hydroxyl group of HEAA [7–9, 19, 20]. Figure 2.2 shows the ^{1}H NMR spectrum of HEAA–PTMC10 in $CDCl_3$. The DP was calculated by integrating the ^{1}H NMR spectra and comparing the ratio of the vinyl proton (5.6 ppm) of HEAA to the methylene protons (2.1 ppm) of PTMC. The synthesized HEAA–PTMC macromonomer was used in a typical radical polymerization.

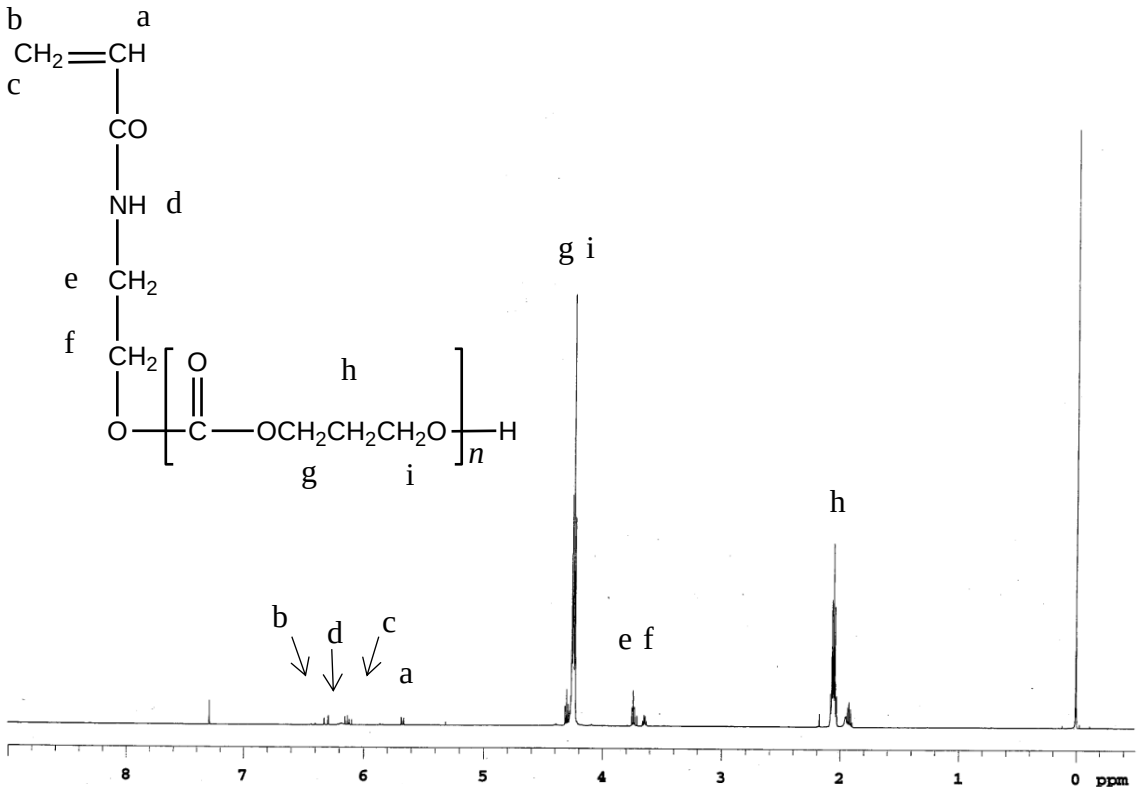

Figure 2.2. ^{1}H NMR spectrum of HEAA–PTMC10 macromonomer in $CDCl_3$.

Figure 2.3 shows the ^{1}H NMR spectrum of PHET in DMSO-d_6. Table 2.1 was displayed the results of the polymer synthesis. The sample code of PHET10–1 refers to the compound with macromonomer composition ratio of 1 mol% with approximately 10 repeating units of TMC in the macromonomer; the same system of nomenclature was applied to PHET10–10 and PHET50–1. Both the number of repeating units of TMC in the macromonomer and the composition ratio of the graft copolymer were calculated from the ^{1}H NMR spectrum. PHET10–1 and PHET10–10 were similar in terms of the number of repeating units of TMC, whereas PHET10–1 and PHET50–1 were similar in macromonomer composition. PHET10–10 had higher molecular weight and larger M_w/M_n than the others. The GPC result showed the effect of the interaction between the graft copolymers, because of the Tyndall phenomenon was observed on PHET10–10 solution in DMF. Particularly the interaction of PHET10–10 was much enhanced.

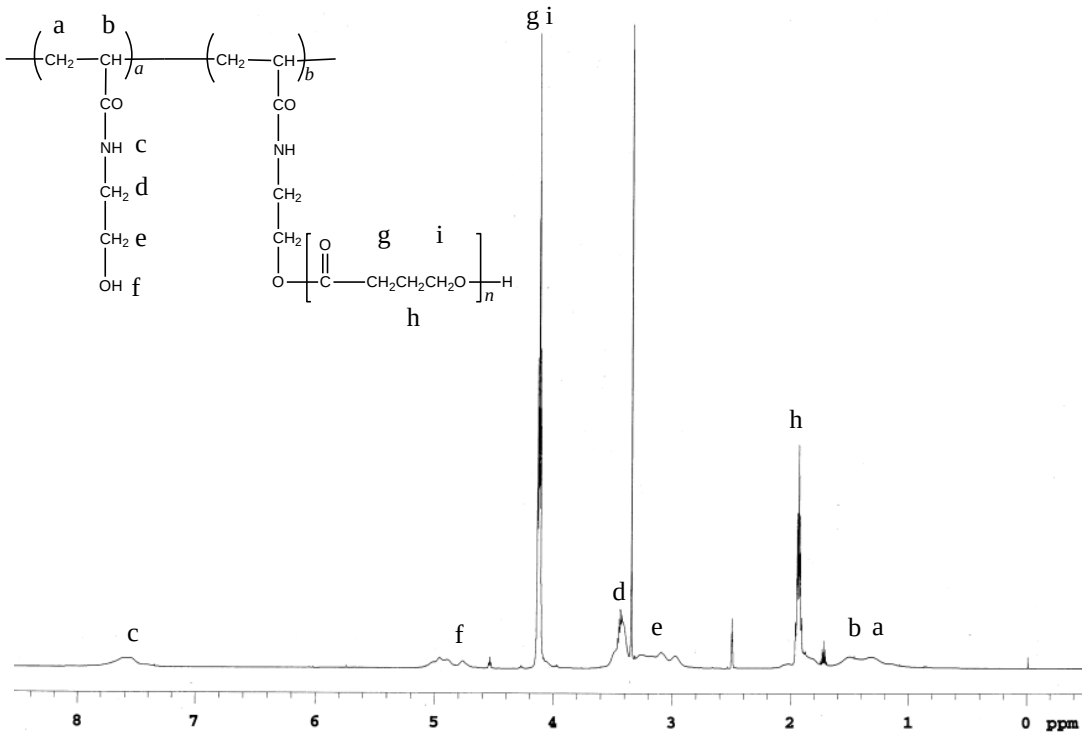

Figure 2.3. ^{1}H NMR spectrum of PHET in DMSO-d_6.

Table 2.1. Synthetic results for graft copolymers

Sample	DP of PTMC	Yield (%)	Composition ratio (mol%)[a)]		GPC		
			HEAA	HEAA–PTMC	M_n	M_w	M_w/M_n
Poly(HEAA)	–	93.9	100	0	18000	37000	2.0
PHET10–1	11	83.0	99.0	1.0	25100	47100	1.9
PHET10–10	9	63.8	91.6	8.4	79800	247000	4.2
PHET50–1	52	84.7	99.1	0.9	36700	94100	2.6

a) Determined by ^{1}H NMR.

2.3.2 Thermal Stability of Graft Copolymer Aggregates in Aqueous Media

The amphiphilic PHET graft copolymers spontaneously formed aggregates in aqueous media, driven by the hydrophobic interactions among the PTMC segments and the hydrogen bonding derived from HEAA. These aggregates consisted of a shell, covered with hydrophilic poly(HEAA) segments, and a core of PTMC domains. The particle size of the PHET copolymers at a concentration of 1 mg/mL in aqueous media was analyzed by DLS measurements.

In Figure 2.4, the particle sizes of PHET10–1, PHET10–10, and PHET50–1 were approximately 30.7, 70.2, and 300.1 nm at 25°C, respectively. For each PHET copolymer, the total amount of PTMC segments was different. For PHET10–1 and PHET10–10, the HEAA–PTMC macromonomer contents were significantly different, although the DP of the PTMC segment was almost the same. Therefore, these two copolymers should have different hydrophobic properties. By comparison with PHET10–1, PHET50–1 copolymer had a PTMC segment which DP was five times higher, although the macromonomer content was quite similar. This result indicated that the larger particle size observed was a result of the higher hydrophobicity caused by the PTMC environment. In addition, the small shoulder of the particle size distribution indicated that the unimer was formed due to the intramolecular aggregation of PHT.

The thermal stability of the particle as a function of temperature was measured using DLS (Figure 2.5). The temperature range was from 20 to 70°C. Both PHET10–10 and PHET50–1 remained highly stability and unchanging to dot hydrophobic domain formed by PTMC, but the particle size of poly(HEAA) and PHET10–1 increased in the interval from 60 to 70°C. By heating, it showed an unstable aggregate structure due to a disassociation of hydrogen bonding at higher temperatures. Therefore, in this

temperature range, the particle size of poly(HEAA) was about 80 nm. On the other hand, the particle size of PHET10–1 changed from about 115.0 nm to 140.0 nm in the process of forming the aggregate from the hydrophobic interaction of PTMC and its association through hydrogen bonding. In the case of colloid by forming graft polymer, the number of hydrophobic domain are scattered in colloid. Therefore, the particle size was increased by reorientation. This behavior indicated that graft copolymers as colloid gels were in swelled state. Additionally, the particle sizes reversibly increased and decreased to occur association-diassociation of physical cross-linking due to changes in temperature. The author considered that the physical cross-linking was dominant for the colloid gel association and disassociation.

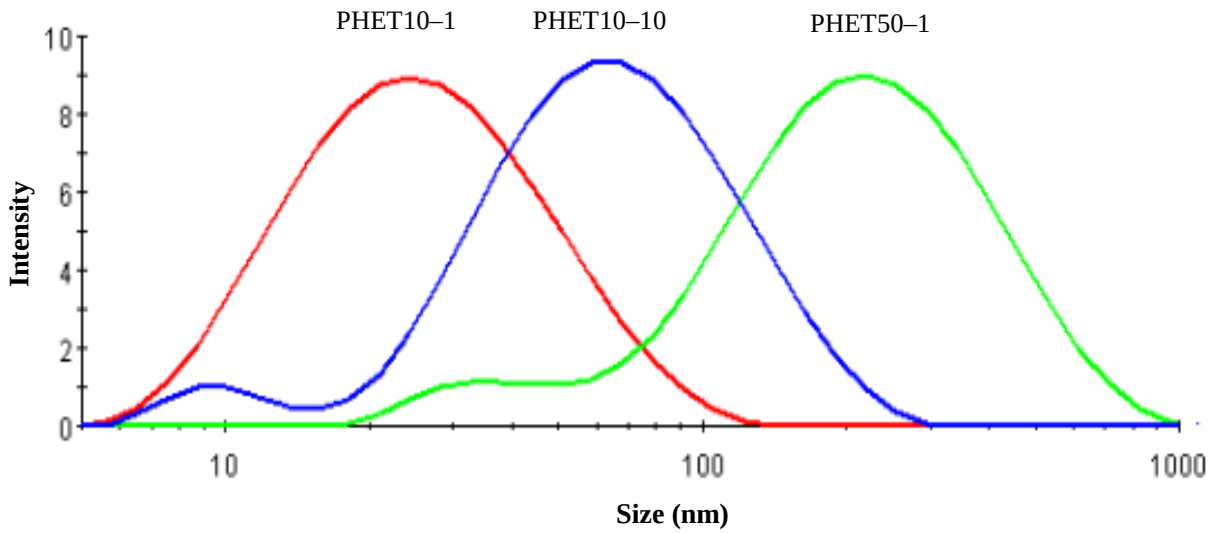

Figure 2.4. Particle size distribution of the PHET copolymers as determined by DLS measurement.

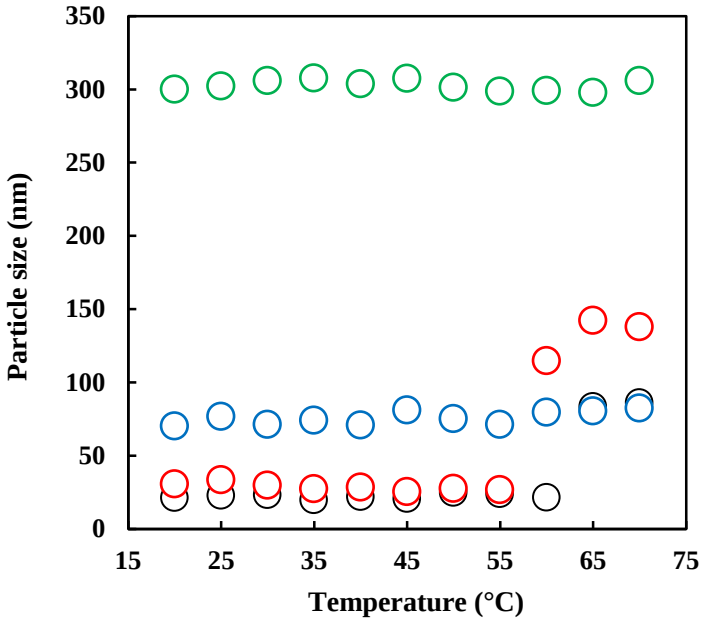

Figure 2.5. Change in particle size over the temperature range 20 to 70˚C. Poly(HEAA): ○, PHET10–1: ○, PHET10–10: ○, PHET50–1: ○.

2.3.3 Evaluation of Graft Copolymer Aggregate by Fluorescence Measurements.

The CAC and K_v values of the PHET copolymers were determined in aqueous media at different concentrations using fluorescence measurements, with pyrene as a hydrophobic fluorescent probe. The fluorescence spectrum of pyrene in solution is known to shift depending on the polarity of the surrounding environment [17, 20].

Florescence intensity was high with increasing the polymer concentration in aqueous media (Figure 2.6). The maximum value in the excitation spectra (λ_{ex}) of pyrene shifts from 333.5 to 336 nm, where it was considered that pyrene was incorporated into the hydrophobic PTMC domain. This shift in the excitation spectra was observed for all of the graft copolymers. The total intensities of the spectra varied depending on both the copolymer concentration and the total amount of hydrophobic PTMC segments.

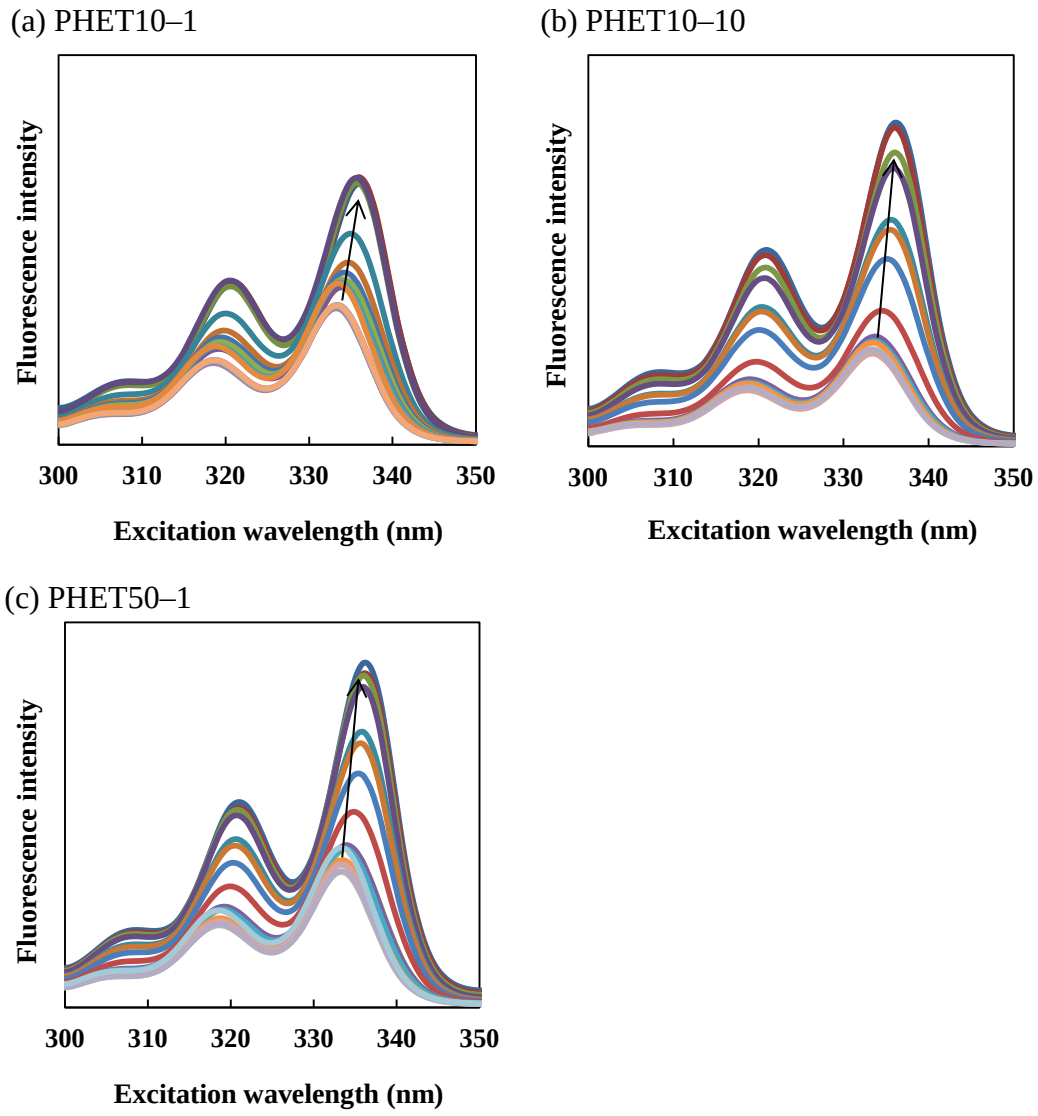

Figure 2.6. Excitation spectra of pyrene (6.0×10^{-7} mol/L) as a function of polymer concentration (10^{-5}–1 mg/mL) in aqueous solution. The samples were (a) PHET10–1, (b) PHET10–10, and (c) PHET50–1.

Figure 2.7 shows the fluorescence intensity ratio ($I_{336}/I_{333.5}$) in the pyrene excitation spectra at 373 nm versus the logarithm of the PHET concentration. Above the CAC, the fluorescence intensity increased exponentially, as the number of molecules of pyrene increased. So, the increase in signal due to the binding of pyrene becomes lager than the random error in determining the intensity of unbound component. On the other hand, below the CAC, absorption only occurred near the surface of the aggregates where the pyrene molecules cohered. The fluorescence intensity increased when pyrene followed by partitioning into the inner hydrophobic domain of aggregation [13]. This suggests that pyrene was solubilized in aggregation. The fluorescence intensity also increased by hydrophobic interaction between PTMC segment and pyreme with increasing PHET copolymer concentration. The increase in the intensity ratio indicated the onset of aggregate formation. Therefore, the CAC can be defined as the intersection of two straight lines in the low concentration range. The CAC values of PHET10–1, PHET10–10, and PHET50–1 were estimated to be approximately 8.9×10^{-2}, 3.2×10^{-3}, and 2.2×10^{-3} mg/mL, respectively (Table 2.2). The CAC of the graft copolymer decreased with increasing the chain length of PTMC and the macromonomer composition ratio. In the case of PHET10–1, the CAC had the lowest value among the copolymers, showing lower association forces. The repeating unit of TMC and the macromonomer composition both influenced the formation polymer colloids. In this case, the higher number of repeating units of TMC appears to be dominant; otherwise, a higher macromonomer composition would be necessary. The slope reached a plateau above 1.2 of $I_{336}/I_{333.5}$ for PHET10–10 and PHET50–1 samples, indicating that the hydrophobic domain was saturated with incorporated pyrene.

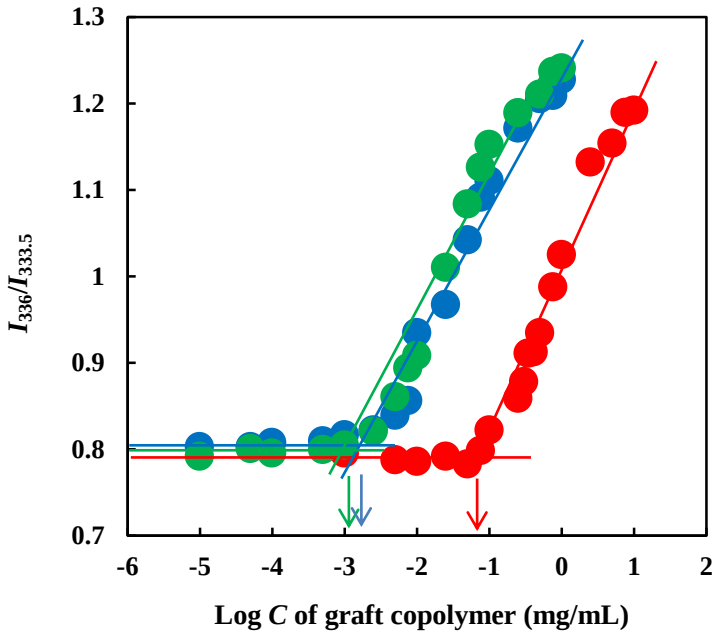

Figure 2.7. Plots of $I_{336}/I_{333.5}$ (from the pyrene excitation spectra) versus log C, where C is the concentration of the graft copolymers. PHET10–1: ●, PHET10–10: ●, and PHET50–1: ●.

To quantify the separation of pyrene into the hydrophobic domain during aggregation, Wilhelm *et al*. devised an equation to calculate the K_v value of the hydrophobic domain in graft copolymer aggregates [20]. The concentration of pyrene in the hydrophobic domain of the PHET copolymer was calculated using Equations (1)–(4), where $[Py]_A$ and $[Py]_w$ represent the concentrations of pyrene in the aggregated and aqueous phase, respectively. The binding of pyrene to aggregation is assumed to result from the simple equilibrium between the aggregation phase of volume (V_A) and the water phase of volume (V_w). The K_v value for pyrene was calculated from the ratio of the pyrene concentrations ($[Py]_A/[Py]_w$). In this approach, $[Py]_A/[Py]_w$ can be corrected

to the volume ratio of each phase:

which can be rewritten as

$$[\mathrm{Py}]_A/[\mathrm{Py}]_w = K_v(V_A/V_W) \quad (1)$$

Moreover, $[\mathrm{Py}]_A/[\mathrm{Py}]_w$ can be written as

$$[\mathrm{Py}]_A/[\mathrm{Py}]_w = K_v x(c - \mathrm{CAC})/1000\rho \quad (2)$$

where x is the weight fraction of the PTMC segment, c is the concentration of the graft copolymer, and ρ is the density of the PTMC aggregation domain, which is assumed to be the value of bulk PTMC (1.01 g/cm^3 ≅ g/mL).

$$[\mathrm{Py}]_A/[\mathrm{Py}]_w = (F - F_{\mathrm{min}})/(F_{\mathrm{max}} - F) \quad (3)$$

which can be rewritten as

$$K_v = \mathrm{slope} \times 1000\rho/x \quad (4)$$

where F_{min} and F_{max} correspond to the average magnitudes of the peak ratio in the region of high and low concentration ranges shown in Figure 2.8, respectively, and F is the fluorescence intensity ratio ($I_{336}/I_{333.5}$) in the intermediate concentration range of the conjugates [Equations (2) and (3)]. The slope was determined by a linear approximation and the K_v values were calculated using Equation (4).

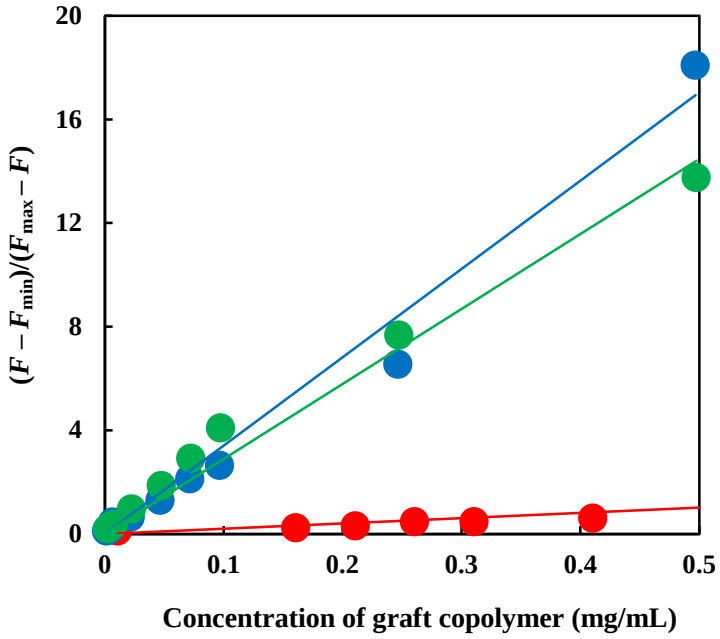

Figure 2.8. Plots of $(F - F_{min})/(F_{max} - F)$ versus concentration of graft copolymers. PHET10–1: ●, PHET10–10: ●, and PHET50–1: ●.

Table 2.2. The CAC and K_v of PHET copolymers

Sample	CAC (mg/mL)	$K_v/10^4$
PHET10–1	8.9×10^{-2}	2.0
PHET10–10	3.2×10^{-3}	8.0
PHET50–1	2.2×10^{-3}	9.8

The fluorescence study using pyrene also reflected the polymer structure, including the grafting degree and PTMC chain length. PHET10–10 and PHET50–1 had higher slope, as calculated by Equation (3), by changing each polymer concentration. The K_v values of PHET10–1, PHET10–10 and PHET50–1 were estimated to be approximately 2.0×10^{-4}, 8.0×10^{-4}, and 9.8×10^{-4} by Figure 2.8 and Equation (1)–(4). The K_v of PHET10–10 was four times as large as that of PHET10–1. The author concluded from these results that PTMC segments played a role in both molecular incorporation and cross-linking. Therefore, the K_v of PHET10–10 was not in agreement with the theoretical value. Table 2.2 summarized these results. The chain length of PTMC rather than the macromonomer composition ratio decreased the K_v values of graft copolymers. Therefore, the hydrophobic domain in PHET50–1 proved to have a more significant influence than in PHET10–10.

2.4 Conclusions

Amphiphilic graft copolymers with homogeneous graft chain lengths of PTMC segments were prepared using macromonomer method. These copolymer associations formed core–shell structures in an aqueous solution. The particle size of the poly(HEAA–*graft*–PTMC) (PHET) aggregates in aqueous solution was about 30.7–300.1 nm and was comparatively stable relative to changes in temperature. In particular, PHET10–1 and PHET10–10 have suitable particle sizes for common DDS. The CAC of the PHET copolymers were in the range of 2.0×10^{-3} to 8.9×10^{-2} mg/mL. The K_v values were dependent to the increase in TMC units. The author deduced that the particle size, CAC, and K_v values for the copolymers depended mostly on the chain length of the hydrophobic PTMC. The graft copolymer with a longer PTMC chain length underwent strong hydrophobic interactions, leading to an increase in the particle size and K_v. From these results, the function of the hydrophobic PTMC domains seemed to be slightly different according to the number of TMC repeating units. The author confirmed that the aggregates formed from the graft copolymers with PTMC domains may be used as potential drug delivery vehicles for loading hydrophobic molecules.

2.5 References

[1] C. Cheng, H Wei, J.-L. Zhu, C. Chang, H. Cheng, C. Li, S.-X. Cheng, X.-Z. Zhang, and R.-X. Zhuo, *Bioconjugate Chem.* **2008**, *19*, 1194.

[2] J. Li and P. Yang, *Langmuir* **2009**, *25*, 6385.

[3] J. Fan, F. Zeng, S. Wu, and X. Wang, *Biomacromolecules* **2012**, *13*, 4126.

[4] S. H, Kim, J. P. K. Tam, F. Nederberg, K. Fukushima, Y. Y. Yang, R. M. Waymouth, and J. L. Hedrick, *Macromolecules* **2009**, *42*, 25.

[5] M. S. Kim, H. Hyun, G. Khang, and H. B. Lee, *Macromolecules* **2006**, *39*, 3099.

[6] F. Nederberg, V. Trang, R. C. Pratt, A. F. Mason, C. W. Frank, R. M. Waymouth, and J. L. Hedrick, *Biomacromolecules* **2007**, *8*, 3294.

[7] K. W. Nam, J. Watanabe, and K. Ishihara, *Biomacromolecules* **2002**, *3*, 100.

[8] E. Akiyama, N. Morimoto, P. Kujawa, Y. Ozawa, F. M. Winnik, and K. Akiyoshi, *Biomacromolecules* **2007**, *8*, 2366.

[9] T. Tyson, A. Finne-Wistrand, and A.-C. Albertsson, *Biomacromolecules* **2009**, *10*, 149.

[10] K. Ishihara, Y. Iwasaki, and N. Nakabayashi, *Polymer* **1999**, *31*, 1231.

[11] K. Nitta, J. Miyake, J. Watanabe, and Y. Ikeda, *Trans. Mater. Res. Soc. Jpn.* **2012**, *37*, 349.

[12] K. Nitta, J. Miyake, J. Watanabe, and Y. Ikeda, *Biomacromolecules* **2012**, *13*, 1002.

[13] C.-T. Lee, C.-P. Huang, and Y.-D. Lee, *Biomacromolecules* **2006**, *7*, 1179.

[14] J. S. Cho, B. S. Kim, H. Hyun, J. Y. Youn, M. S. Kim, J. H. Ko, Y. H. Park, G. Khang, and H. B. Lee, *Polymer* **2008**, *49*, 1777.

[15] Y. Shibasaki, H. Sanada, M. Yokoi, F. Sanda, and T. Endo, *Macromolecules* **2000**, *33*, 4316.

[16] H. Hyun, J. W. Lee, J. S. Cho, Y. H. Kim, C. R. Lee, M, S. Kim, G. Khang, and H. B. Lee, *Colloids Surf., A: Physicochem. Eng. Aspects* **2008**, *313*, 131.

[17] C. Kim, S. C. Lee, J. H. Shin, J.-S. Yoon, I. C. Kwon, and S. Y. Jeong, *Macromolecules* **2000**, *33*, 7448.

[18] W. Mattanavee O. Suwantong, S. Puthong, T. Bunaprasert, V. P. Hoven, and P. Supaphol, *Appl. Mater. Interfaces* **2009**, *1*, 1076.

[19] R. A. Siegel and C. G. Pitt, *J. Controlled Release* **1995**, *33*, 173.

[20] M. Wilhelm, C-L. Zhao, Y. Wang, R. Xu, M. A. Winnik, J.-L. Mura, G. Riess, and M. D. Croucher, *Macromolecules* **1991**, *24*, 1033.

Chapter 3

Characterization of Temperature-Responsive Graft Copolymer with Polycarbonate Oligo Segment

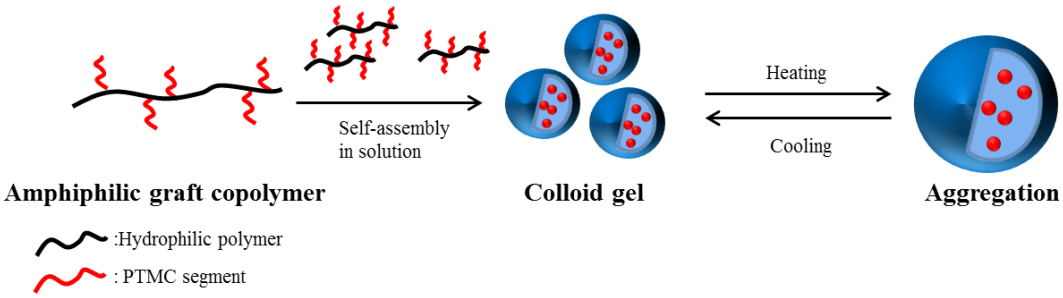

3.1 Introduction

Intelligent polymer colloids showing temperature and pH etc. responsiveness and increasing functionality have received much attention in biomedical and biomaterial fields [1–7]. A basic concept of preparing polymer colloids is the incorporation of amphiphilic properties into polymer chains. In the case of biomaterials, both biocompatibility and biodegradability are highly desirable properties. Aliphatic polyesters such as poly(L-lactic acid), poly(glycolic acid), and poly(amino acid) have these properties [8–12]. Therefore, these modified copolymers are widely investigated for functional biomaterial applications.

Poly(*N*-isopropyl acrylamide) (poly(NIPAAm)) is functional polymer that is well known for its thermosensitive properties, coil-globule transition, and lower critical solution temperature (LCST) of 32°C. Poly(NIPAAm) and its copolymers are widely studied for drug delivery systems (DDS) and tissue engineering [2–4, 13]. Accordingly, this study aims to increase the functionality of poly(NIPAAm) (such as thermosensitivity and enhancement of graft copolymer stability) by adding poly(trimethylene carbonate) (PTMC) as polymer side chains. Therefore, poly(NIPAAm) was copolymerized with the previously discussed PHET polymer as the third monomer unit. The resulting polymer could show LCST and higher stability at temperatures below the LCST.

In this chapter, poly(NIPAAm–*graft*–PTMC) (PNT) and poly((*N*-hydroxyethyl acrylamide (HEAA)–*co*–NIPAAm)–*graft*–PTMC) (PHNT) were designed and synthesized using macromonomer method (Figure 3.1). Using this method, both the segment length and composition ratio of the graft chain can be easily modified. Poly(HEAA–*graft*–PTMC) (PHET) copolymer in Chapter 2 is changing in property

such as hydrophobic–hydrophilic balance by addition to the temperature-responsive functionality. This is particularly useful in controlling the solubility of the polymers in water. The author investigated the solution property of the polymer colloids by fluorescence measurements using pyrene and cetylpyridium chrolide. Furthermore, the temperature-responsive property of colloid was evaluated by UV–Vis spectroscopy and dynamic light scattering (DLS) at various temperatures. These polymer colloids could be potential materials for designing temperature-responsive molecular carriers.

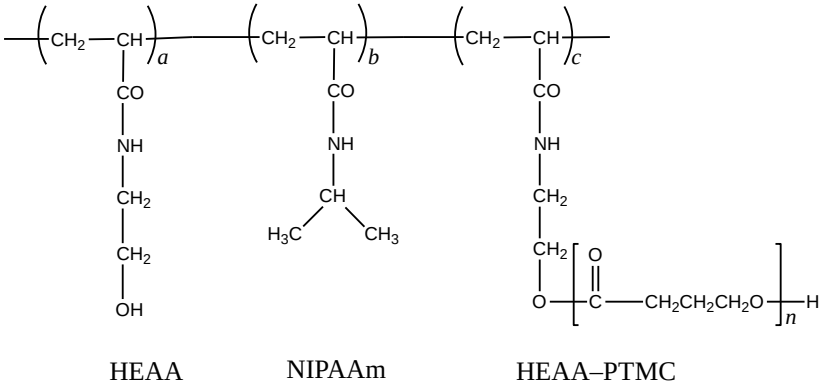

Figure 3.1. Chemical structure of poly((HEAA–*co*–NIPAAm)–*graft*–PTMC) (PHNT).

3.2 Experimental Section

3.2.1 Materials

N-Isopropyl acrylamide (NIPAAm) and HEAA were kindly supplied by KOHJIN Co., Ltd., Tokyo, Japan. Trimethylene carbonate (TMC) as a cyclic monomer was purchased from Boehringer Ingelheim Pharma GmbH, Ingelheim, Germany. 1,8-Diazabicyclo[5.4.0]undec-7-ene (DBU) as basic organic catalyst was obtained from Kanto Chemical Co., Ltd., Tokyo, Japan. Benzoic acid (Wako Pure Chemical Industries, Co., Ltd. Osaka, Japan) was used to ring-opening polymerization (ROP). 2,2′-azobis(isobutyronitrile) (AIBN) was used as an initiator for radical polymerization and was purchased from Tokyo Chemical Industry Co., Ltd, Tokyo, Japan. Pyrene was selected as a fluorescence probe and was purchased from Wako Pure Chemical Industries. Cetylpyridium chrolide (CPC) as quenching agent was purchased from Wako Pure Chemical Industries (Figure 3.2). Dichloromethane, *N*,*N*-dimethyl formamide (DMF), and all other organic solvents were used as received.

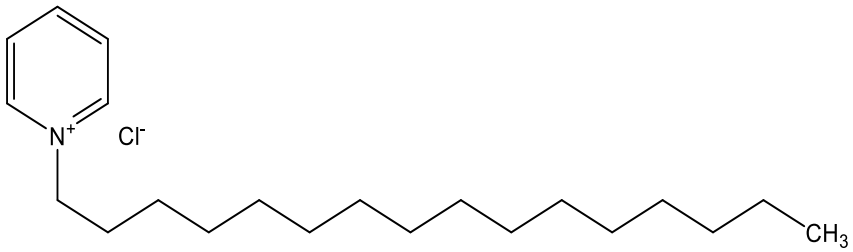

Figure 3.2. Chemical structure of CPC.

3.2.2 Synthesis of Hydrophobic Temperature-Responsive Graft Copolymers

The HEAA–PTMC macromonomer was synthesized using previously reported procedure [14]. The author prepared the macromonomer with approximately 10 repeating units of TMC. The DP of PTMC was calculated from the proton nuclear magnetic resonance (^{1}H NMR; 500 MHz) spectrum in $CDCl_3$.

The author synthesized the novel temperature-responsive graft copolymer by radical polymerization. AIBN, NIPAAm, and the HEAA–PTMC macromonomer were dissolved in DMF, and polymerization was performed at 70°C with nitrogen gas bubbling for 24 h. Furthermore, an additional graft copolymer was synthesized using AIBN, HEAA, NIPAAm, and HEAA–PTMC macromonomer. The reaction mixture was added to dichloromethane/*n*-hexane (1:4 (v/v)), which is a poor solvent. The product was dried under reduced pressure and the resulting material was dissolved in DMF, then dialyzed for 48 h at room temperature using preswollen dialysis membrane (approximate molecular weight cut off = 3,500 Da) to remove any residual solvent. The obtained copolymer solution was freeze-dried. The refined copolymer was analyzed by ^{1}H NMR and gel permeation chromatography (GPC).

3.2.3 Evaluation of Polymer Colloids at Lower Critical Solution Temperature

The LCST behavior of the polymers was determined by temperature variable UV–Vis spectrometer. The transmittance of each sample was measured at temperatures from 20°C to 70°C. The measurements were performed at heating rate of 1.2°C/min and 2.0 nm bandwidth. The change in particle size around the LCST was determined by dynamic light scattering (DLS) at various temperatures. The polymer concentration was 1 mg/mL in water.

3.2.4 Determination of Critical Association Concentration

The critical association concentration (CAC) was determined by using pyrene as a hydrophobic fluorescence probe. First, pyrene was dissolved in tetrahydrofuran (THF) at a concentration of 1.2×10^{-3} mol/L. The pyrene solution was then added to a large amount of water. After mixing, the THF was removed by rotary evaporation at 40°C for 2 h. The final concentration of pyrene was 6.0×10^{-7} mol/L [4, 15]. The copolymers were dissolved in the aqueous pyrene solution at various concentrations between 1.0×10^{-3} and 1 mg/mL. The fluorescence spectra were recorded on fluorescence spectrophotometer. The emission and excitation spectra of pyrene were monitored at various temperatures. The measurements were taken with a 5.0 nm slit width and 300 nm/min scan speed.

3.2.5 Estimation of Aggregation Number by Quenching Method

The aggregation number (N_{agg}) of copolymer was determined by CPC [5–7]. Pyrene was dissolved in THF at a concentration of 1.0×10^{-3} mol/L. The pyrene solution was added to water and then mixed. The THF was removed by rotary evaporator at 40°C for 2 h. Pyrene aqueous solution was adjusted at concentration of 1.0×10^{-6} mol/L. The copolymers were dissolved in the pyrene aqueous solution at various polymer concentrations of 0.1 mg/mL. CPC at various concentrations from 1.0×10^{-5} mol/L to 8.0×10^{-5} mol/L was added into polymer solutions. The fluorescence spectra were recorded on fluorescence spectrophotometer. The emission spectra of pyrene were monitored at 25°C. The measurements were taken width and 500 nm/min scan speed.

3.3 Results and Discussion

3.3.1 Synthesis of Temperature-Responsive Graft Copolymers

The HEAA–PTMC macromonomer was prepared by previously reported method [14]. The number of repeating units of TMC was controlled at approximately 10 (Table 3.1). Temperature-responsive graft copolymers having an oligo PTMC segment (PNT and PHNT) were synthesized by conventional radical polymerization. The resulting polymer was a colorless, viscose precipitate. Figure 3.3 shows the ^{1}H NMR spectrum of PHNT in DMSO-d_6. The composition ratio of macromonomer unit in the graft copolymer was calculated by comparing the integral value of the amide protons of NIPAAm and HEAA (7.1–7.4 ppm) and the methylene protons of PTMC (4.1 ppm). The composition ratio of the HEAA and NIPAAm units in PHNT was then compared to the integral value of the hydroxyl proton of HEAA (4.8 ppm) and the isopropyl protons of NIPAAm (1.0 ppm).

Table 3.1. Synthetic results of amphiphilic graft copolymers

Sample	DP of PTMC[a)]	Yield (%)	Composition ratio (mol%)[a)]			GPC[b)]		
			HEAA	NIPAAm	HEAA–PTMC	M_n	M_w	M_w/M_n
PNT[c)]	10.2	83.0	0.0	99.2	0.8	27700	107500	3.9
PHNT	10.1	84.7	26.4	72.7	0.9	23500	114000	4.7
PHN[d)]	—	94.3	28.0	72.0	—	29200	89600	3.4

a) Determined by ^{1}H NMR.

b) The calibration curve was prepared by using polystyrene standards.

c) PNT: Poly(NIPAAm–*graft*–PTMC)

d) PHN: Poly(HEAA–*co*–NIPAAm)

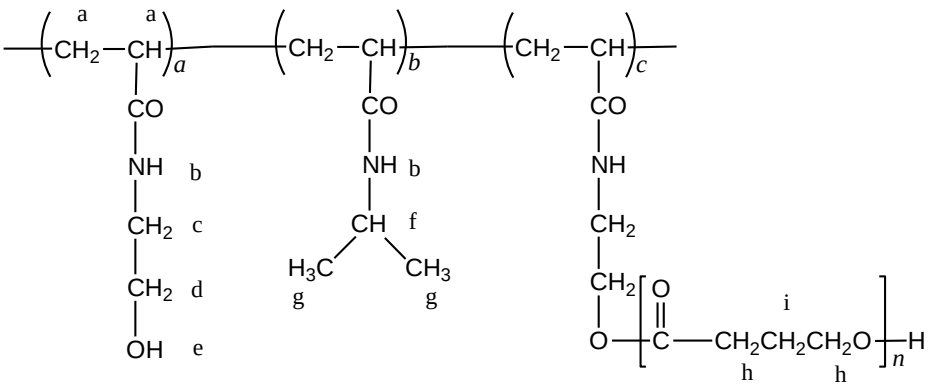

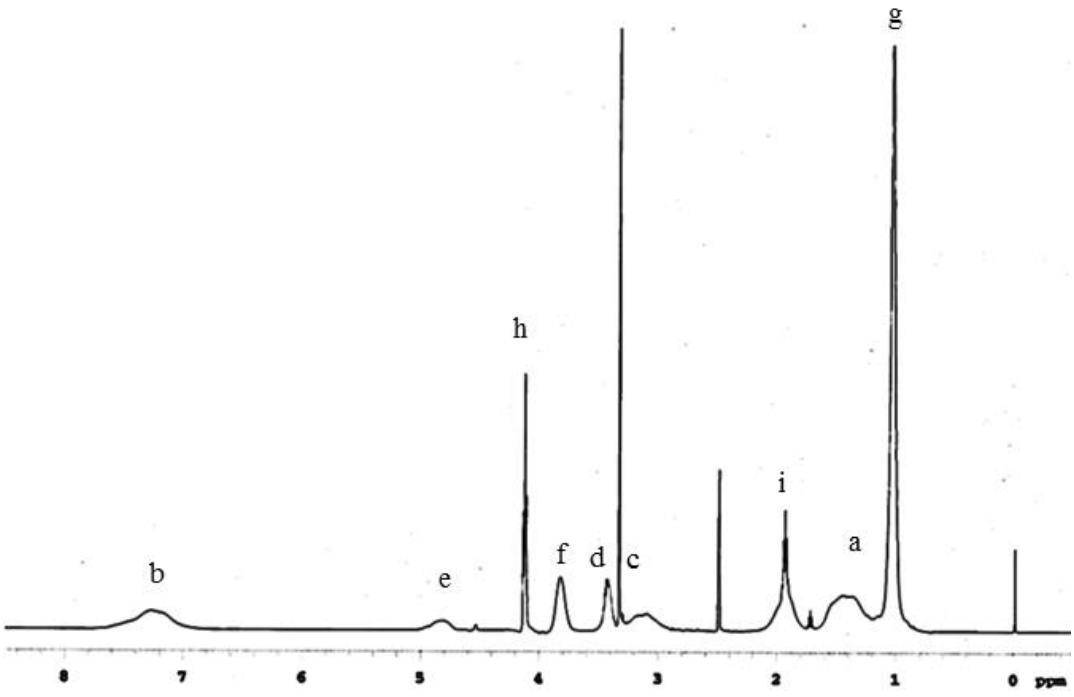

Figure 3.3. ^{1}H NMR spectrum of PHNT copolymer in DMSO-d_6.

3.3.2 Lower Critical Solution Temperature of the Temperature-Responsive Graft Copolymers

The LCST of the copolymers was determined by UV–Vis and DLS. Figure 3.4 shows the transmittance (%T) versus temperature curves measured by UV–Vis spectroscopy. The LCST of the poly(NIPAAm) homopolymer was approximately 32.0°C. The LCST of PNT was approximately 31.6°C with the introduction of the hydrophobic PTMC segment. Therefore, the incorporation of the hydrophobic macromonomer unit into PNT decreased the LCST in comparison to poly(NIPAAm). On the other hand, PHNT showed LCST of 43.0°C by a smooth phase transition. This was because the main chain of the copolymer, composed of NIPAAm units, was randomly substituted with hydrophilic HEAA units. Thus, the LCST of PHNT was higher than that of all hydrophobic chain, PNT. Poly(HEAA–*co*–NIPAAm) (PHN) showed LCST of approximately 53.0°C. The transmittance profile was slightly affected by increasing the amount of HEAA. The change in the composition ratio of the NIPAAm units influenced the LCST. The author concluded that the LCST was controlled by adding the composition of HEAA units.

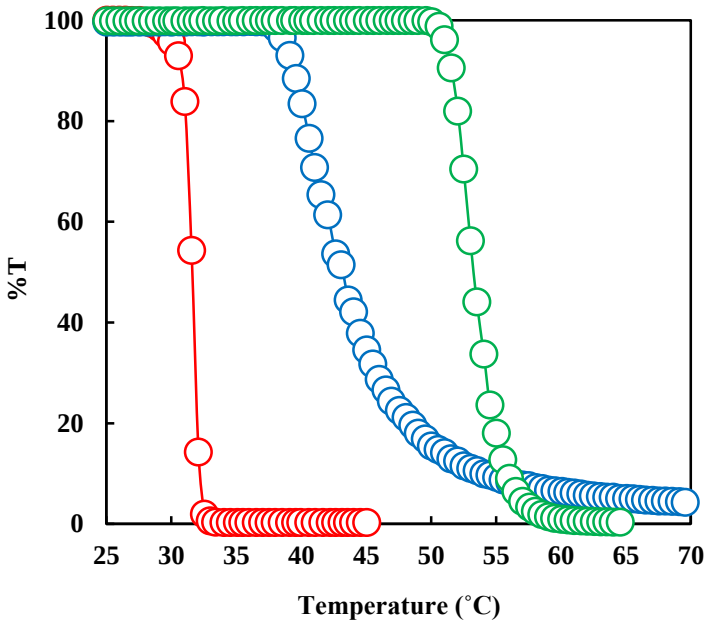

Figure 3.4. Transmittance versus temperature curves from PNT: ○, PHNT: ○, and PHN: ○. The aqueous solution was heated and monitored by UV–Vis spectroscopy. The polymer concentration was 1.0 mg/mL.

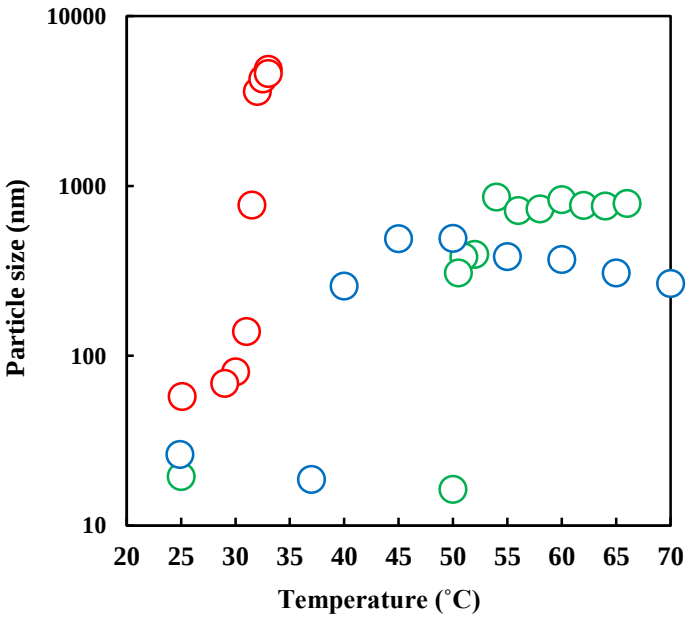

Figure 3.5. Particle size versus temperature curves from PNT: ○, PHNT: ○, and PHN: ○. The aqueous solution was heated and monitored by UV–Vis spectroscopy. The polymer concentration was 1.0 mg/mL.

DLS measurements were performed at various temperatures. The particle size increased with temperature as shown in Figure 3.5. Each particle size was single peak. At 25.0°C, the particle sizes of PNT, PHNT, and PHN were 57.5, 26.2, and 19.4 nm, respectively. The author inferred that the HEAA units decreased the particle size due to increasing cohesion forces resulting from hydrogen bonding in the particles. On the other hand, the hydrophobic interactions induced by the introduction of the PTMC segments caused intermolecular aggregation. At the LCST, these copolymers clearly showed that the aggregation was caused by the hydrophobic effects of the poly(NIPAAm) unit. Therefore, the particle sizes of PNT, PHNT, and PHN increased to 4,500, 491.2, and 858.7 nm, respectively. The PNT colloids with hydrophobic segments decreased in size and formed a large hydrophobic core due to aggregation of the NIPAAm units. This suggests that PNT copolymer fragmentation and reorganization occurred among the copolymers. After reaching the LCST, the PHNT copolymer formed similar aggregates among the copolymers; however, the hydrophilic HEAA units formed shell structure. Furthermore, heating lead to the breaking of hydrogen bonds between the acrylamide derivatives in the PHNT colloids, inducing copolymer reorganization. Therefore, the particle size of PHNT gradually decreased from approximately 491.2 to 265.3 nm. The PHN colloid without hydrophobic PTMC segments had a higher LCST than the other copolymers. Similar to PHNT, the particle size of PHN decreased from approximately 858.7 to 759.2 nm. Above the LCST, poly(NIPAAm) changed the hydrophobic properties of the copolymers and formed a stable hydrophobic core in the copolymer resulting in drastically increased particle size. The results suggest that the introduction of the PTMC segment and HEAA units prevented the formation of aggregates of more than 1000 nm in diameter among the

polymer colloids.

3.3.3 Characterization of Amphiphilic Temperature-Responsive Graft Copolymers

The CAC of the aqueous phase copolymers at various concentrations was determined by using pyrene as the hydrophobic fluorescence probe. The fluorescence spectra of the pyrene solutions were shifted by the polarity change. The excitation spectra of pyrene at 333 nm and 336 nm were recorded, and their ratio was plotted. Figure 3.6 shows the fluorescence intensity ratio (I_{336}/I_{333}) of pyrene excitation spectra versus the logarithm of copolymer concentration. The I_{336}/I_{333} values represent the hydrophobicity of the copolymers. At high concentrations the I_{336}/I_{333} value of PNT and PHNT, increased with concentration. This suggested that pyrene molecules were incorporated into the hydrophobic PTMC domain in the polymer aggregates and the CAC values were estimated. The intersection of the two straight lines in the low concentration range indicated to the CAC. The CAC values of PNT and PHNT were determined to be approximately 3.2×10^{-2} and 3.8×10^{-2} mg/mL, respectively. The CAC of PNT and PHNT with different main chains were almost identical. This indicated that NIPAAm and HEAA when used as the hydrophilic main chain did not affect the CAC at room temperature. Therefore, PHN as hydrophilic–hydrophilic copolymer was non-existent at the CAC.

When change in temperature at less than CAC values of each copolymer solution (2.5×10^{-2} mg/mL), the I_{336}/I_{333} values of PNT copolymer was drastically increased, but PHNT and PHN was gently increased (Figure 3.6). Approaching the LCST region, the I_{336}/I_{333} value of PNT and PHNT increased and then reached a plateau (similar to Figure 3.6). This result indicated that copolymers reached the critical association temperature.

On the other hand, the I_{336}/I_{333} values of the PHN copolymer did not plateau with temperature at 2.5×10^{-2} mg/mL. The author inferred that copolymer fragments gradually associated and formed hydrophobic domain comprising poly(NIPAAm) with increasing temperature.

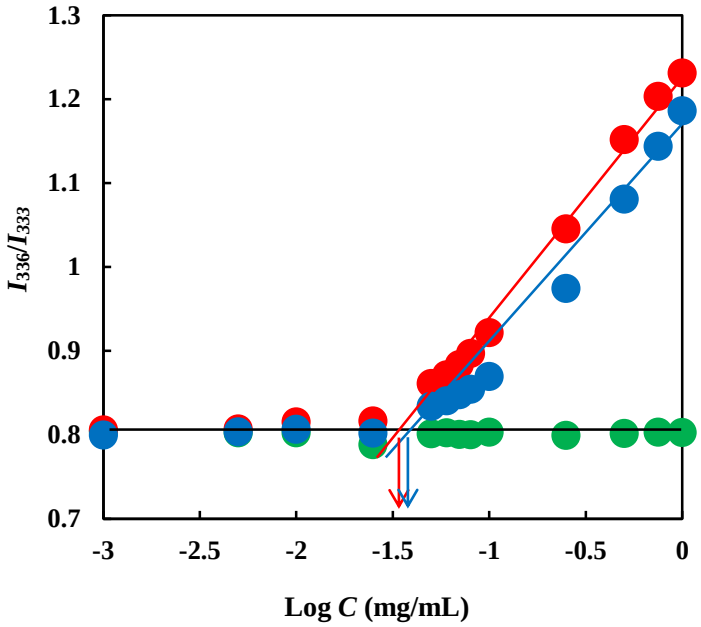

Figure 3.6. Plots of I_{336}/I_{333} (from the pyrene excitation spectra) versus log C for the formation of polymer aggregates of PNT: ●, PHNT: ●, and PHN: ●.

3.3.4 Estimation of Aggregation Number by Quenching Method

The N_{agg} was estimated by fluorescence quenching method using CPC and pyrene. This method is analyzed fluorescence decay curve by the fluorescence measurement and

has the advantage of unaffected between aggregation interactions. This experiment was performed on polymer solutions of concentration 0.1 mg/mL, PNT: 3.6×10^{-5} and PHNT: 4.3×10^{-5} mol/L. The fluorescence spectra were monitored at various concentration of CPC quencher (Figure 3.7). These emission intensities of spectral curves decreased as more increasing as quencher concentration. The modified Stern–Volmer plots for the copolymers are presents. Increasing CPC quencher, the emission intensity of pyrene decreased and the plots of the logarithm of the emission intensity ratio of pyrene in the absence (I_0) and presence (I) of CPC quencher ($\ln I_0/I$) was high. These plots are liner, thus, the author saw that the CPC in polymer colloid was served as the predominant host for pyrene. Table 3.2 summarized calculation results of Stern–Volmer equation. The N_{agg} is calculated and estimated by Stern–Volmer equation. The slope of the plots in Figure 3.8 is related to N_{agg} follow:

$$\ln (I_0/I) = [\text{CPC}]/[\text{Aggregation}]$$

$$[\text{Aggregation}] = [\text{Polymer}] - [\text{CAC}]/[N_{agg}]$$

where [CPC], [Aggregation], and [Polymer] represent each concentrations. [CAC] represents the critical association concentration in Figure 3.6. The N_{agg} was estimated by equation and those of PNT and PHNT were approximately 2.3 and 3.7, respectively. The author thought that hydrophobic interaction by PTMC segments and hydrogen bonding of NIPAAm units and HEAA were driving force for assembly.

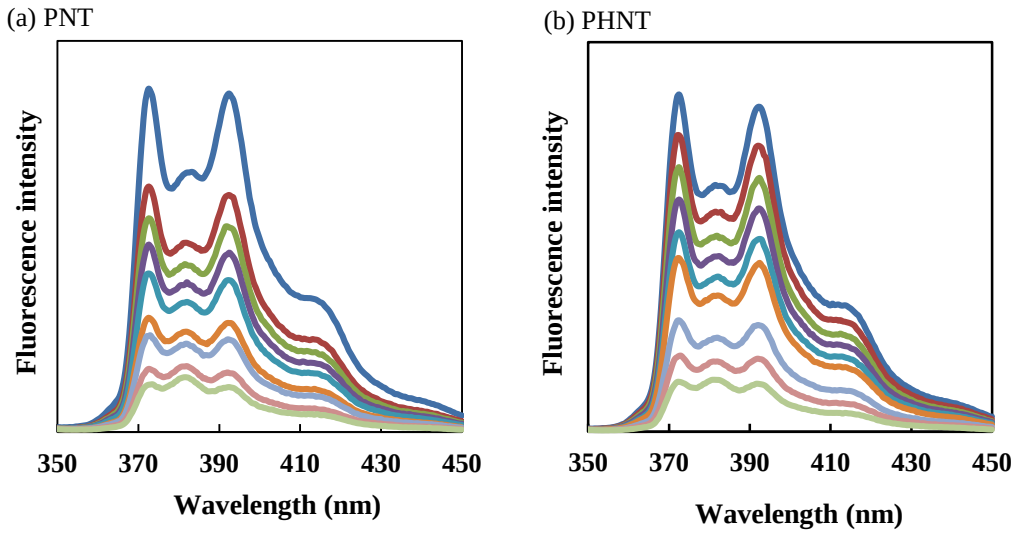

Figure 3.7. Fluorescence spectra of pyrene (1×10^{-6} mol/L) as a function of CPC concentration (1×10^{-4} – 8×10^{-4} mol/L) in the presence of polymer solution of (a) PNT (3.6×10^{-6} mol/L; 0.1 mg/mL) and (b) PHNT (4.3×10^{-6} mol/L; 0.1 mg/mL).

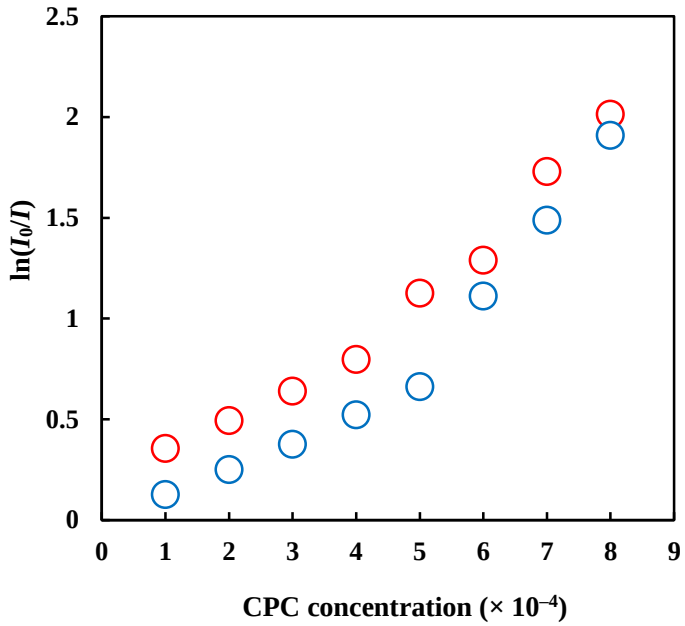

Figure 3.8. Plots of $\ln(I_0/I)$ versus concentration of CPC. Concentration of PNT and PHNT were 3.6×10^{-6} and 4.3×10^{-6} mol/L, respectively. PNT: ○ and PHNT: ○.

Table 3.2. Calculated results of N_{agg}

Sample	Concentration of copolymers (mol/L)	N_{agg} (25°C)
PNT	3.6×10^{-6}	2.3
PHNT	4.3×10^{-6}	3.7

3.4 Conclusions

Graft copolymers with temperature-responsive function were synthesized by conventional two-step polymerization and their structure was confirmed by ^{1}H NMR. By introducing NIPAAm units into the copolymer, the previously reported PHET copolymers possessed a thermal response. In this study, the author investigated the LCST and function of molecular incorporation by fluorescence probe techniques. By the introducing HEAA units into PNT, PHNT showed a LCST at 43.1°C and a decreased particle size compared to unmodified PNT. Above the LCST, the HEAA units of the copolymer formed a shell structure in aqueous media and reorganized into a stable colloid. The CAC values of PNT and PHNT were between 3.0×10^{-2} to 4.0×10^{-2} mg/mL and these aggregations was composed of the number of from approximately 10 to 20 copolymers. Furthermore, at 2.5×10^{-2} mg/mL (near the CAC), PNT and PHNT are gradually formed stable colloids at the LCST. From these results, the author expects that PHNT colloids having LCST and hydrophobic domains show potential applications environmentally responsive carriers.

3.5 References

[1] Y. Q. Yang, L. S. Zheng, X. D. Guo, Y. Qian, and L. J. Zhang., *Biomacromolecules* **2011**, *12*, 116.

[2] C. Cheng, H. Wei, J.-L. Zhu, C. Chang, H. Cheng, C. Li, S.-X. Cheng, X.-Z. Zhang, and R-X. Zuo, *Bioconjugate Chem.* **2008**, *19*, 1194.

[3] D.-G. Ahn, J. Lee, S.-Y. Park, Y.-J. Kwark, and K. Y. Lee, *Appl. Mater. Interfaces* **2014**, *6*, 22069.

[4] Y.-H. Hsu, W.-H. Chiang, C.-H. Chen, C.-S. Chern, and H.-C. Chiu, *Macromolecules* **2005**, *38*, 9757.

[5] K. Akiyoshi, S. Deguchi, H. Tajima, T. Nishikawa, and J. Sunamoto, *Macromolecules* **1997**, *30*, 857.

[6] K. Chandrasekar and G. Basker, *Biomacromolecules* **2007**, *8*, 1665.

[7] E. Akiyama, N. Morimoto, P. Kujawa, Y. Ozawa, F. M. Winnik, and K. Akiyoshi, *Biomacromolecules* **2007**, *8*, 2366.

[8] K. Fukushima, R.-C. Pratt, F. Nederberg, J.-P.-K. Tan, Y.-Y. Yan, R.-M. Waymouth, and J. L. Hedrick, *Biomacromolecules* **2008**, *9*, 3051.

[9] H. Qian, A.-R. Whol, J.-T. Crow, C.-W. Macosko, and T.-R. Hoye, *Macromolecules* **2011**, *44*, 7132.

[10] T. Akagi, M. Higashi, T. Kaneko, T. Kida, and M. Akashi, M, *Biomacromolecules* **2006**, *7*, 297.

[11] T. Akagi, P. Piyapakorn, M. Akashi, *Langmuir* **2012**, *28*, 5249.

[12] P. Piyapakorn, T. Akagi, M. Hachisuka, T. Onishi, H. Matsuoka, and M. Akashi, *Macromolecules* **2013**, *46*, 6187.

[13] E. Ho, A. Lowman, and M. Marcolongo, *Biomacromolecules* **2006**, *7*, 3223.

[14] K. Nitta, J. Miyake, J. Watanabe, and Y. Ikeda, *Trans. Mater. Res. Soc. Jpn.* **2012**, *37*, 349.

[15] J. S. Cho, B. S. Kim, H. Hyun, J. Y. Youn, M. S. Kim, J. H. Ko, Y. H. Park, G. Khang, and H. B. Lee, *Polymer* **2008**, *49*, 1777.

Chapter 4

Synthesis and Evaluation of Surface Property of Amphiphilic Graft Copolymer Containing Different Oligo Segments

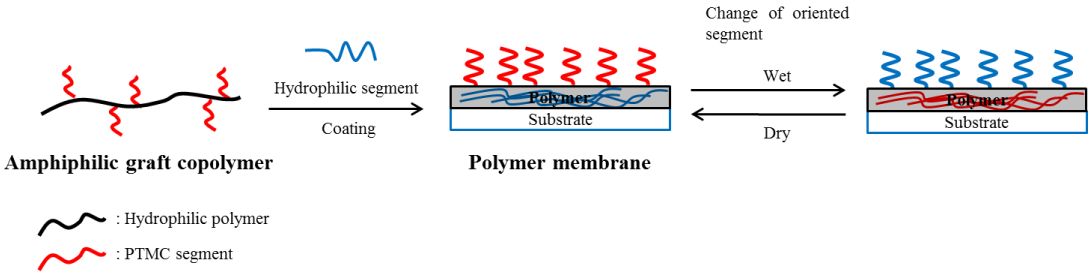

4.1 Introduction

Polymer membranes that have surface properties such as antifouling behavior are widely researched and applied to many material fields from marine to biomedical industries [1–4]. In the biomaterial field, however, there are growing concerns about the inflammation caused by protein adsorption between materials within the body. In such matters, molecular design is important for development, and as a result, functional materials such as polymers with excellent surface properties are the focus of many researchers, where the polymer's contact angles with water and the water structure in hydration polymers have been reported to be important for biomaterial [5–7]. Amphiphilic polymers with hydrophobic–hydrophilic properties are being actively researched to develop a method of suppressing non-specific protein adsorption [4, 7, 8]. As the antithrombogenic polymer, poly(ethylene glycol) (PEG) and zwitterionic polymers, such as poly(2-methacryloyloxyethyl phosphorylcholine) and poly(sulfobetaine methacrylate), are the most widely studied in the biomedical field. It is thought that the good hydration state, the exchange of bound water on the polymer surface in body to inducing electrostatic interaction through zwitterionic polymer and to forming hydrogen bonding by water molecule and ether oxygen atoms of PEG [3, 7–10]. Moreover, the solubility of copolymers in water increases upon increases in the number of ethylene glycol units incorporated into the polymer, even as the molecular weight increases. The control of amphiphilic polymer microstructures is also actively investigated in the field of tissue engineering. The self-assembled honeycomb structure of such polymers is suitable for use in cell cultures due to the resulting fitted membrane hardness and hydrogen bonding ability [11, 12]. Therefore, the design of functional polymer-based materials is required to control their wettability in response to their

external environment. In other studies, control of the friction and adhesion at the interface between polymers, polymer materials incorporating segments with different properties were reported [13–15]. These polymers were able to demonstrate significant switching of their surface responsive behaviors and wettability upon the introduction of external stimuli, such as immersion in solvents of varying polarities and changes in temperature.

Many reports have been published about polymer material characterizations of poly(ethylene glycol) monomethyl ether (mPEG) and poly(L-lactic acid) (PLA) amphiphilic diblock copolymer [16–19]. The author has reported amphiphilic graft copolymer composed of mPEG and poly(trimethylene carbonate) (PTMC) instead of PLA. As polymer design, the author focused on and selected biodegradable PTMC and biocompatible mPEG. Block copolymers composed of PTMC segments have been achieved and reported to rapidly modify their surface wettability under a wetting environment [20]. Therefore, the author designed and synthesized amphiphilic graft copolymers containing PTMC oligo segments and oligo(ethylene glycol) segments using a macromonomer method. Generally, the amorphous PTMC segment has high molecular mobility and PTMC block copolymer has stimulus-responsive upon changes to its external environment. The biodegradable polycarbonate, however, such as high molecular weight PTMC, could be susceptible to hydrolysis *in vivo* [20–22], which could lead to reduced function of the material. On the other hand, PTMC with a degree of polymerization (DP) between 10 and 50, does not undergo appreciable degradation in the presence of lipase enzyme [23, 24]. An oligo PEG segment can be incorporated into graft copolymer so that it segregates to the surface of the material. Hydrophilic and biocompatible PEG on the surface of polymeric materials decreases the hydrophobic

interactions of the materials and this property is important for their use at biointerfaces. As the main chain in graft copolymers, the author selected two types of monomers containing different functional groups, 2-hydroxyethyl acrylate (HEA) and 2-methoxyethyl acrylate (MEA). The chemical structure of HEA comprises a hydroxyl and ester group, while that of MEA has an ester and methoxy group, and poly(MEA) exhibits good biocompatibility and hydrophobicity [6–8, 25].

In this study, the author reports the synthesis of novel copolymers and investigates their surface responsive properties, such as surface morphology and wettability. The author synthesized PTMC macromonomer, and then prepared further ternary graft copolymers. The hydrophobic–hydrophilic balance of these materials was controlled by the composition ratio of PTMC oligo and mPEG oligo segments. The polymer membrane was studied in terms of its surface morphology and roughness. These copolymers were evaluated using differential scanning calorimetry and contact angle measurements to estimate their phase separation and surface responsiveness towards surface enrichment due to the mobility of the polymer segments.

4.2 Experimental Section

4.2.1 Materials

2-Methoxyethyl acrylate (MEA), 1,8-diazabicyclo[5.4.0]undec-7-ene (DBU), benzoic acid, and 2,2'-azobis(isobutyronitrile) (AIBN) were purchased from Wako Pure Chemical Industries, Co., Ltd., Osaka, Japan. The hydrophilic macromonomer, poly(ethylene glycol) methyl ether methacrylate (mPEGMA: M_n = 950 and polymerization degree of ethylene glycol units: 19.5), was purchased from Sigma-Aldrich Corp., St. Louis, MO, USA. Trimethylene carbonate (TMC) and 2-hydroxyethyl acrylate (HEA) were purchased from Tokyo Chemical Industry Co., Ltd, Tokyo, Japan. Dichloromethane, *N*,*N*-dimethyl formamide (DMF), and all other organic solvents were used as received.

4.2.2 Synthesis of HEA–PTMC Macromonomer

Conventional ring-opening polymerization (ROP) of TMC monomer using HEA initiator was initially performed in order to obtain the HEA–PTMC macromonomer according to our previously reported procedure [26]. The synthesis of the HEA–PTMC macromonomer with 10 units of TMC proceeded as follows: HEA (105.7 μL, 1.0 mmol) and TMC (1.02 g, 10 mmol) were dissolved in dichloromethane (CH_2Cl_2) (10 mL). A solution of DBU (152.2 μL, 1.0 mmol) in CH_2Cl_2 was then added to the flask, and the solution was mixed. The ROP was carried out under a nitrogen atmosphere at room temperature for 24 h. Benzoic acid was added to the reaction mixture in order to inactivate the terminal hydroxyl group and terminate the reaction. The obtained solution was poured into a large amount of either a 2-propanol/water (2:1) mixture or undiluted 2-propanol in order to precipitate the desired macromonomer product. The viscous

product was dried under reduced pressure to give the product in stable yield. The degree of polymerization (DP) was calculated using proton nuclear magnetic resonance (^{1}H NMR) spectroscopy. The synthesized HEA–PTMC macromonomers contained 10 or 20 TMC units. ^{1}H NMR (300 MHz, $CDCl_3$) δ: 2.1 (m, 2H, –CH_2–C*H*$_2$–CH_2–), 3.6 (q, 2H, –CH_2–C*H*$_2$–O–), 3.7 (t, 2H, –C(=O)–O–C*H*$_2$–CH_2–), 4.2 (t, 4H, –C*H*$_2$–CH_2–C*H*$_2$–), 5.8 (d, 1H, CH_2=C*H*–C(=O)–O–), 6.1 (q, 1H, *H*–CH=CH–), and 6.4 ppm (d, 1H, H–C*H*=CH–).

4.2.3 Synthesis of Poly(HEA–*graft*–HEA–PTMC–*co*–mPEGMA) Copolymer

To synthesize poly(HEA–*graft*–HEA–PTMC–*co*–mPEGMA) (PHPT) copolymer (Figure 4.1(a)), radical polymerization was carried out using AIBN, HEA, HEA–PTMC, and mPEGMA. The reagents were each dissolved in DMF, and their solutions combined. The mixture was refluxed at 70 °C for 24 h. The crude product was poured into a large volume of a hexane/2-propanol (2:1) mixture to precipitate the resulting copolymer, which was separated from the supernatant by decantation. The copolymer was dried under reduced pressure to give a colorless and sticky product. Chemical structures were confirmed by ^{1}H NMR spectroscopic analysis and the molecular weight was determined by gel permeation chromatography (GPC). ^{1}H NMR (300 MHz, DMSO-d_6) δ: 1.2 (br, 3H, –CH_2–C(C*H*$_3$)–C(=O)–O–, 1.2–1.9 (br, 2H, –C*H*$_2$–CH–C(=O)–O– and 2H, –C*H*$_2$–C(CH_3)–C(=O)–O–, 1.9 (m, 2H, –C(=O)–O–CH_2–C*H*$_2$–CH_2–O–), 2.2 (1H, –CH_2–C*H*–C(=O)–O–), 3.2 (s, 3H, –CH_2–CH_2–O–C*H*$_3$), 3.4 (m, 2H,– C(=O)–O–CH_2–C*H*$_2$–O–CO–)3.5 (s, 4H, –O–C*H*$_2$–C*H*$_2$–O–), 3.6 (m, 2H,–C(=O)–O–CH_2–C*H*$_2$–OH), 3.9 (2H,–C(=O)–O–C*H*$_2$–CH_2–O–), 4.1 (m, 4H, –C(=O)–O–C*H*$_2$–CH_2–C*H*$_2$–O–), and 4.6–4.8 (br, 1H, –O–CH_2–CH_2–O*H*) [27, 28].

4.2.4 Synthesis of Poly(MEA–*co*–HEA–PTMC–*co*–mPEGMA) Copolymer

To synthesize poly(MEA–*graft*–HEA–PTMC–*co*–mPEGMA) (PMPT) copolymer (Figure 4.1(b)), radical polymerization was carried out using AIBN, MEA, HEA–PTMC, and mPEGMA. The reagents were each dissolved in DMF, and their solutions combined. The mixture was refluxed at 70°C for 24 h. The crude product was poured into a large volume of a hexane/2-propanol (2:1) mixture to precipitate the resulting copolymer, which was separated from the supernatant by decantation. The copolymer was dried under reduced pressure to give a colorless and sticky product. Chemical structures were confirmed by ^{1}H NMR spectroscopic analysis and the molecular weight was determined by GPC. ^{1}H NMR (300 MHz, DMSO-d_6) δ: 1.0 (br, 3H, –CH_2–C(CH_3)–C(=O)–O–, 1.2–1.9 (br, 2H, –CH_2–CH–C(=O)–O– and br, 2H, –CH_2–C(CH_3)–C(=O)–O–, 1.9 (m, 2H, –C(=O)–O–CH_2–CH_2–CH_2–O–), 2.2 (1H, –CH_2–C*H*–C(=O)–O–), 3.2 (s, 3H, –CH_2–CH_2–O–CH_3), 3.4 (m, 2H,–O–CH_2–CH_2–O–C(=O)–O– and 3.5 (s, 4H, –O–CH_2–CH_2–O–), s, 2H,–C(=O)–O–CH_2–CH_2–O–), and 4.1 (s, 2H, –C(=O)–O– CH_2–CH_2–O– and m, 4H, –C(=O)–O–CH_2–CH_2–CH_2–O–) [27, 28].

(a) PHPT

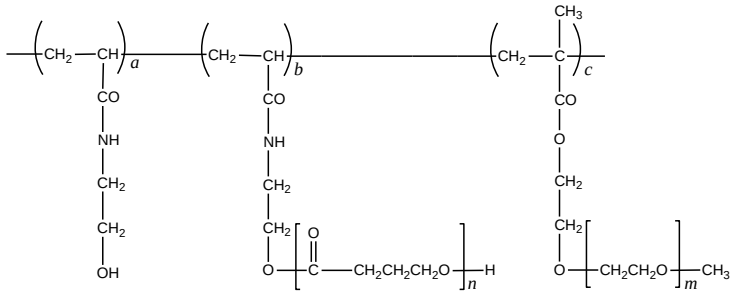

(b) PMPT

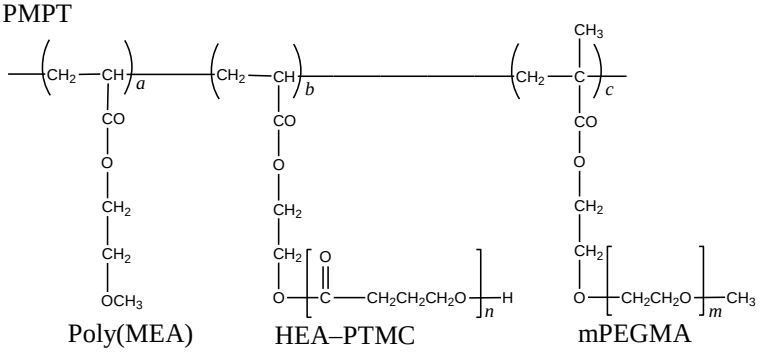

Figure 4.1. Chemical structures of (a) poly(HEA–*graft*–HEA–PTMC–*co*–mPEGMA) (PHPT) and (b) poly(MEA–*co*–HEA–PTMC–*co*–mPEGMA) (PMPT).

4.2.5 Thermal Analysis by Differential Scanning Calorimetry Measurement

The thermal properties of the graft copolymers were investigated using differential scanning calorimetry (DSC). DSC measurements were performed using a heat–cool–heat cycle. The glass transition temperatures (T_g) of the graft copolymers were recorded from −50 to 150°C at a scanning rate of 10°C/min. Liquid nitrogen was used to cool the sample as required at the lower temperatures.

4.2.6 Observation of Surface Morphology

A glass substrate was coated with polymer dissolved in acetone. The concentration of polymer solution was 1 w/v%. The coating of the polymer on the substrate was achieved using a spin coater (rotation speed of 3000 rpm/min for 60 s), then the polymer-coated substrates were dried under reduced pressure. The author observed the stored polymer-coated glass substrate in dry state. For study by scanning electron microscopy (SEM), the glass substrate was fixed using carbon tape on the sample stage, then electro-conductive paste (DOTITE; Fujikura Kasei Co., Ltd., Tochigi, Japan) was spotted onto the corner of the sample. All samples were sputter-coated with platinum prior to observation. The accelerating voltage set at 2.0 kV. To observed surface roughness, atomic force microscopy AFM measurements were performed immediately at room temperature in air. The scan size measured was $5 \times 5\ \mu m^2$. For the surface response experiments, the samples were immersed in solvent, such as water, ethanol, or hexane, for 2 h, and then dried by blowing air over the sample.

4.2.7 Surface Properties Evaluated by Static Contact Angle Measurement

The copolymers were dissolved in acetone at a concentration of 1 w/v%. The solution was coated onto a glass substrate using a spin coater (rotation speed: 3000 rpm, time: 60 s). After drying under reduced pressure overnight, the static contact angle was measured. The substrate was treated with several solvents, such as water, ethanol, and hexane, for 2 h. The contact angle of the immersed substrate was then measured after drying by nitrogen gas flow. All measurements were taken at a temperature of 25 ± 0.5 °C and humidity of 35–45%.

4.3 Results and Discussion

4.3.1 Synthesis of Amphiphilic Graft Copolymer Having Different Oligo Segment

The HEA–PTMC copolymers were synthesized using a conventional ROP technique. Two polymerization conditions were employed, where the feed ratios of [TMC]/[HEA] were 10 and 20, and the DP of PTMC, calculated by ^{1}H NMR spectroscopy, was approximately 10 and 20, respectively. Figure 4.2 shows the ^{1}H NMR spectrum of HEA–PTMC10 [26], where the integral ratios of the vinyl proton (5.8 ppm) of HEA with respect to the methylene protons (2.1 ppm) of PTMC were compared.

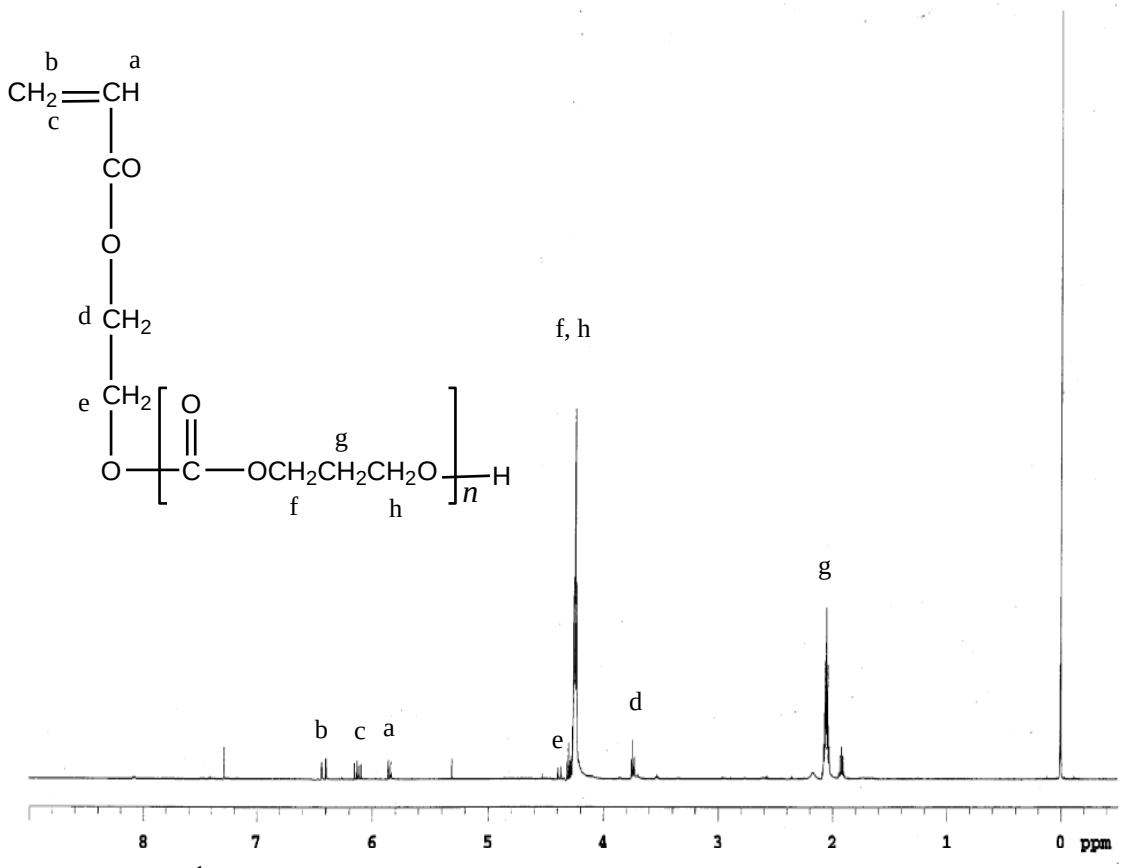

Figure 4.2. ^{1}H NMR spectrum of HEA–PTMC10 macromonomer in $CDCl_3$.

The amphiphilic graft copolymers, PHPT and PMPT, were synthesized by a free radical polymerization method over 24 h. Figure 4.3 shows the ^{1}H NMR spectra of the PHPT and PMPT copolymers. Table 4.1 summarizes the synthetic condition and results utilized and obtained in this work. The naming convention used is based on the acronym P‘M’PT*n*–*b*, where ‘M’ represents the monomer incorporated (H = HEA and M = MEA), ‘*b*’ describes the PTMC macromonomer composition, and ‘*n*’ represents the DP of PTMC. For example, PHPT10−2 refers to a graft copolymer with a poly(HEA) main chain, DP of PTMC of 10 and macromonomer composition feed ratio of 2 mol%. The objective copolymers were obtained, but the polymer yield decreased from approximately 90 to 40% with increases in the feed ratio of the macromonomer composition. The polymer composition ratios were calculated using ^{1}H NMR spectroscopy in DMSO-d_6 by comparing the integral ratios of the HEA protons to those of PTMC and mPEGMA. These results indicated that the polymer composition was clearly dependent upon the monomer composition in the feed. The average molecular weight distributions (M_w/M_n) were evaluated by GPC measurements. Wide distributions were observed in DMF with increasing macromonomer composition, and a Tyndall phenomenon could be confirmed. The author hypothesize that the hydrophobic interactions between PTMC molecules resulted in the spontaneous formation of aggregates in DMF, therefore, the estimated molecular weights were larger than expected.

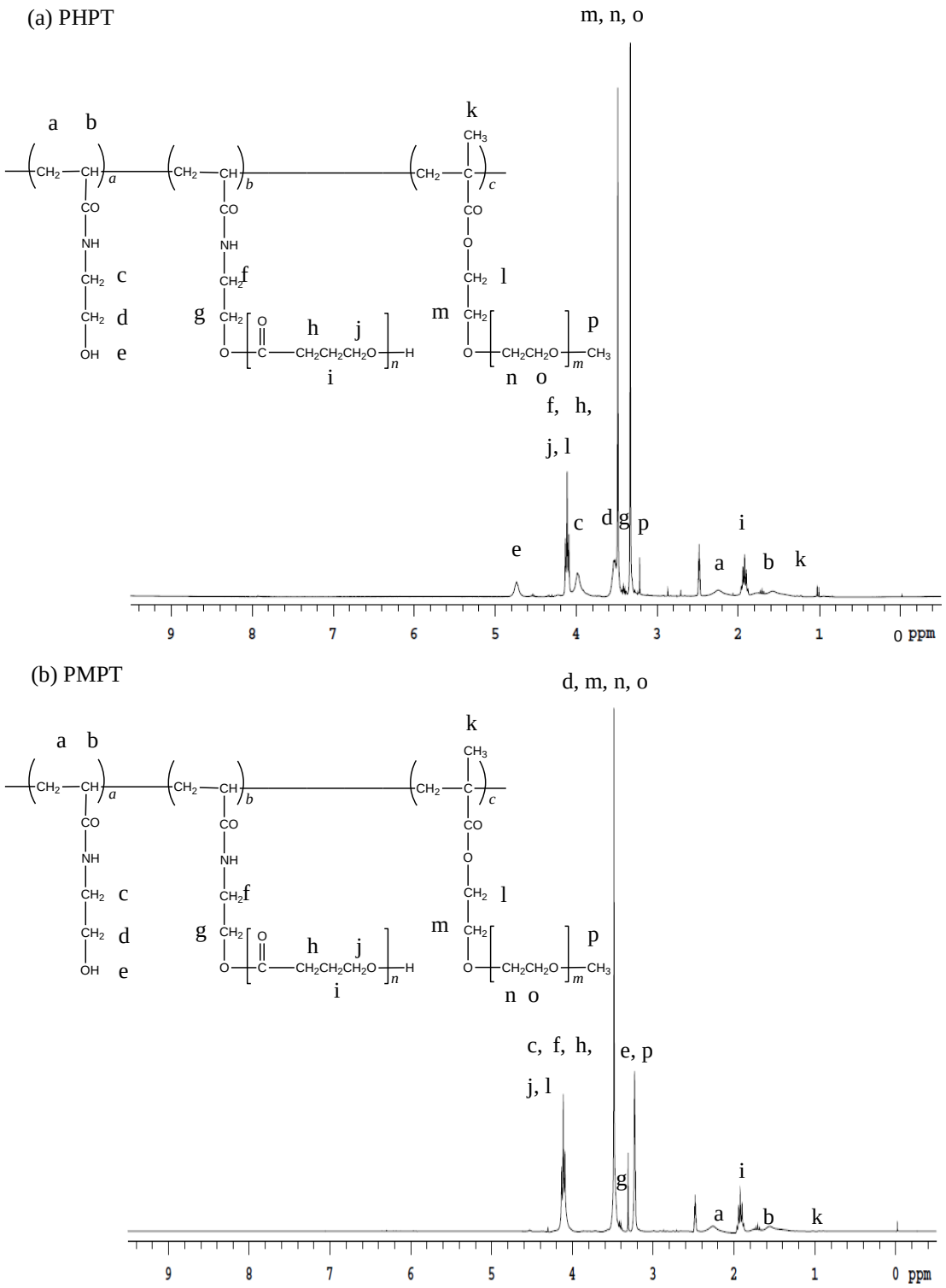

Figure 4.3. ^{1}H NMR spectra of (a) PHPT and (b) PMPT in DMSO-d_6.

Table 4.1. Synthetic results of amphiphilic graft copolymers

Sample	Yield (%)	DP of PTMC	Composition ratio (mol%)			Molecular weight			T_g	Solubility in water [a)]
			Main monomer	Macromonomer	mPEGMA	M_n	M_w	M_w/M_n		
Poly(HEA)	85.6	–	100	–	–	68800	120700	1.8	–21.0	○
PHP	78.6	–	95.0	–	5.0	93400	181100	1.9	–49.7	○
PHT20–5	68.9	20	94.7	5.3	–	79100	104400	1.3	n.d.	×
PHPT10-2	89.6	11	93.1	2.1	4.8	37900	135000	3.6	–29.8	○
PHPT10-5	40.7	12	87.4	6.4	6.2	50000	119800	2.4	–39.3	○
PHPT10-10	58.0	12	81.9	12.0	6.1	112900	329700	2.9	–38.0	○
PHPT20-2	71.9	21	92.6	2.0	5.4	22300	71100	3.2	–48.7	○
PHPT20-5	69.6	21	87.5	6.3	6.2	18500	74200	3.9	–37.8	×
PHPT20-10	53.1	21	81.9	11.2	6.9	74600	280000	3.8	–46.8	×
Poly(MEA)	68.1	–	100	–	–	23200	70100	3.0	–42.7	×
PMP	73.8	–	95.4	–	4.6	108900	227300	2.1	–52.9	○
PMT20–5	51.9	20	94.9	5.1	–	47800	83200	1.7	n.d.	×
PMPT10-2	75.3	11	92.4	2.2	5.4	39100	148800	3.8	–43.0	×
PMPT10-5	45.1	12	90.7	4.6	4.7	43400	93200	2.2	–47.2	×
PMPT10-10	54.0	12	85.6	9.3	5.1	117700	380200	3.2	–43.5	×
PMPT20-2	59.8	21	90.4	2.8	6.8	33300	104700	3.1	–46.4	×
PMPT20-5	48.5	21	87.6	6.3	6.1	29900	105000	3.4	–47.1	×
PMPT20-10	49.2	21	85.4	8.6	6.0	17100	82700	4.8	–37.8	×

a) Each copolymer was immersed in water at concentration of 1 w/v%. ○:Soluble and ×: insoluble.

4.3.2 Thermal Analysis of Amphiphilic Graft Copolymers

Glass transition temperatures (T_g) were estimated from DSC thermograms. The copolymer samples were heated from 20–150°C prior to DSC measurement, and recorded at 10°C/min over the temperature over the temperature range of –100 to 150°C. The T_g of poly(HEA) and poly(MEA) were recorded at –21.0 and –42.7°C, respectively. It is well known that PTMC is an amorphous polymer, and therefore, the T_g process was observed at temperatures below room temperature. In addition, PEG is known to induce semi-crystallization, and the T_g of PEG is dependent on its molecular weight [29–31]. For graft copolymers having PTMC segments, the DSC curve attributed to T_g was observed across the range of –49 to –29°C (Table 4.1 and Figure 4.4). These results were corresponded with previously reported literature results [29, 32, 33]. The T_g was therefore not dependent on the segment length and composition ratio of the PTMC macromonomer. In a section of the copolymer, the T_g of polymer backbone (poly(HEA) and poly(MEA)), PTMC, and mPEGMA were not individually detected to show compatibility (Figure 4.4). From these results, the DSC data suggested that PTMC had high molecular mobility.

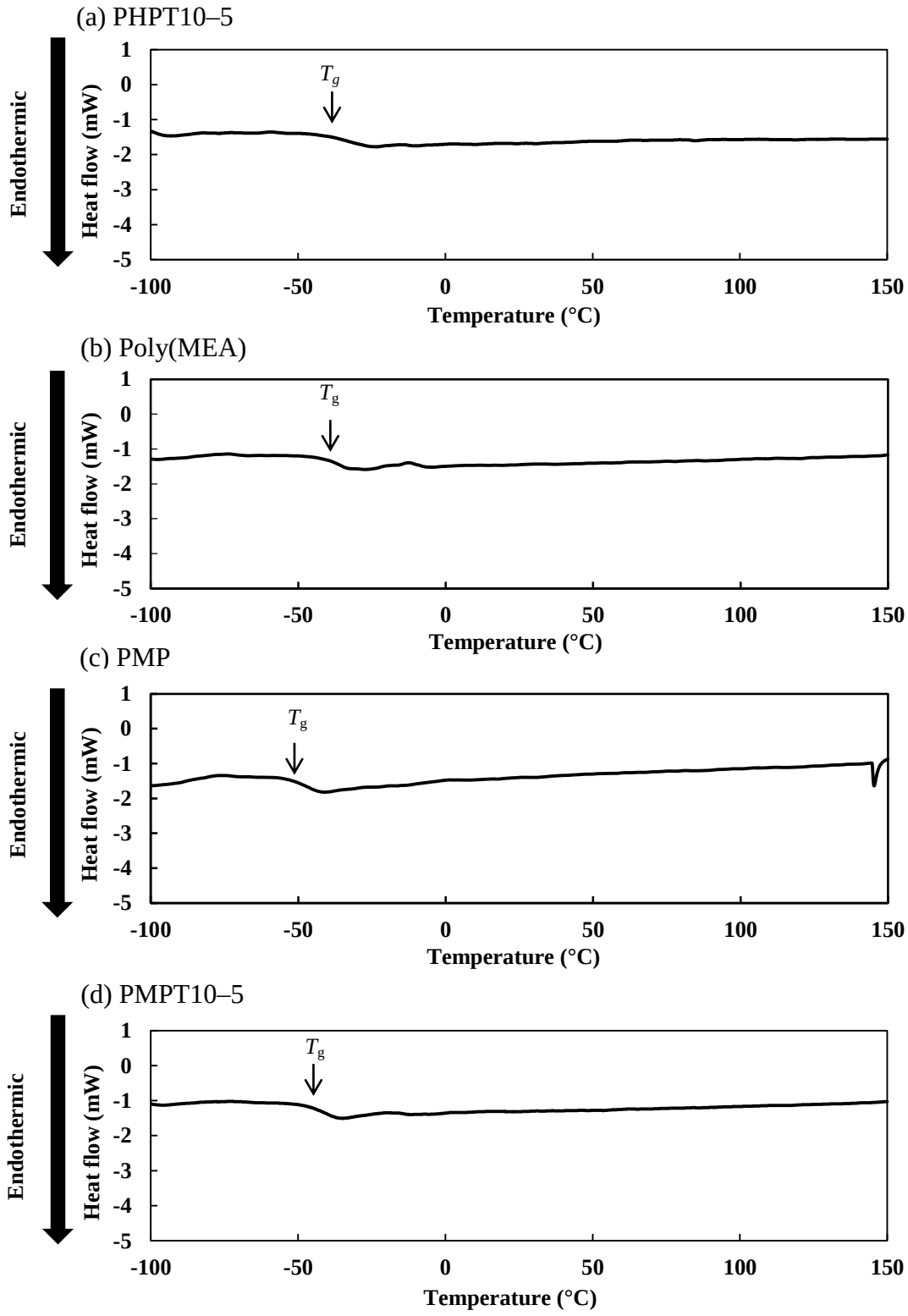

Figure 4.4. DSC thermograms of (a) PHPT10–5, (b) poly(MEA), (c) PMP, and (d) PMPT10–5.

4.3.3 SEM Observation of Polymer Thin Membrane

SEM studies were performed to investigate the homogeneity of the polymer membrane by spin coating. Membrane samples for analysis were prepared using a spin coating method to deposit an acetone solution of the polymer onto a glass substrate. Figure 4.5 shows SEM images of PHPT20–5 and PMPT20–5. The morphologies of the polymer membrane were not related in the monomer and macromonomer composition ratio. The author hypothesized that the polymer coated these glass slides homogeneously, so therefore the amount of polymer aggregation was low.

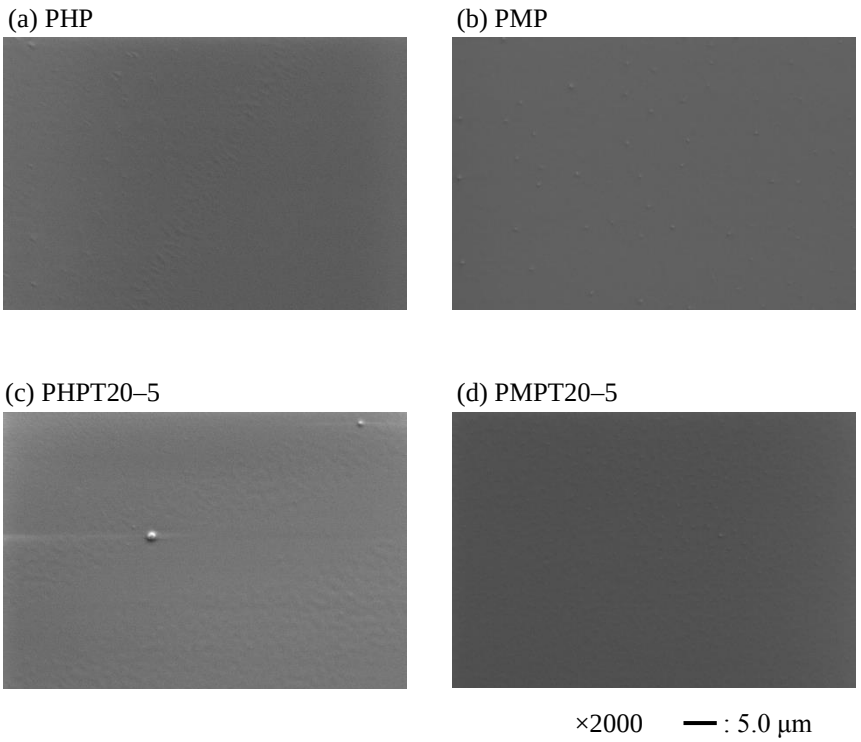

Figure 4.5. SEM images of (a) PHP, (b) PMP, (c) PHPT20–5, and (d) PMPT20–5. (Scale bar: 5.0 μm)

3.4. Evaluation of Surface Characterization by Static Contact Angle Measurement

The surface wettability of the graft copolymers was investigated by measuring their static contact angles with water droplets under various conditions, including dry, wet, and after immersion in different polar solvents. The contact angle of the water droplet on the polymer membrane was measured over a time period of 60 s. At polymer concentrations of 1 w/v%, poly(HEA–*co*–mPEGMA) (PHP), PHPT10–2, PHPT10–5, PHPT10–10, PHPT20–2, poly(MEA–*co*–mPEGMA) (PMP), PMPT10–2, and PMPT10–5 were all soluble in water (Table 4.1). The static contact angle of an acetone-coated glass substrate (control sample) ranged from 37.6° to 35.7° over 60 s.

The molecular orientation of the amphiphilic copolymer composed of hydrophilic and hydrophobic segments was oriented in order to minimize the interfacial free energy of the water–polymer interface. In this study, the wettability of the polymer-coated substrate changes from hydrophobic to more hydrophilic. Figure 4.7 and Figure 4.8 show the contact angles of polymer-coated glass substrates versus time in dry conditions (stored under reduced pressure). In Figure 4.7(a), the contact angle of PHPT10–2 ranged from 24.9° to 21.8° over 60 s. On the other hand, the contact angle of the polymer membrane increased upon the introduction of a PTMC segment. Furthermore, this change in wettability was dependent on the composition ratio of PTMC segment. In PHPT20–2, the initial contact angle was 28.3°, and it reduced to 21.0° after 10 s. The contact angle of PHPT10–5 and PHPT20–5, however, decreased from 45.0° to 34.0° over 60 s. A surface segregation phenomenon was observed for PHPT10‑10 and PHPT20–10, but the changes in contact angles were low, with changes of 54.1° to 49.1° and of 53.5° to 48.6° observed, respectively. Surface enrichment of the co-polymer with PEG and HEA units was suppressed by increases in the amount of

hydrophobic interactions, because the composition ratio of the PTMC macromonomer was increased. When the polymer membrane was in contact with water, hydrophilic segments such as PEG and poly(HEA) rapidly moved to the outermost surface of the polymer membrane. Figure 4.8(a) shows the changes in contact angles observed upon introducing poly(HEA) as the main chain component of the polymer. The contact angles of polymers incorporating poly(HEA) and PHP showed contact angles in the range of 44.4°–42.0° and 14.4°–10.7°, respectively. The contact angle of PHT20–5 with a PTMC segment exhibited a very rapid change from 47.0° to 36.2°.

In the case of the PMPT polymer, the polymer-coated substrates immediately exhibited surface responsive behaviors (Figure 4.7(b)). This behavior depended on the length of the PTMC segment incorporated into the polymer. In PMPT10–2 and PMPT20–2, the contact angle changed from 29.7° to 17.4° and from 26.9° to 15.7°, respectively. The contact angle of PMPT10–5 and PMPT20–5 ranged from 44.8° to 23.3° and from 47.7° to 20.5°, respectively. However, PMPT10–10 and PMPT20–10 showed different behaviors, where the contact angle of PMPT20–10 (from 53.0° to 26.7°) was lower than that of PMPT10–10 (from 59.9° to 40.9°) over 60 s. From these results, the author suspects that the molecular mobility of the PTMC segment in PMPT20–10 is high and the mPEG segment was aggregated on the polymer surface. In the PMPT-coated surface, the water droplet initially spread faster in all of the samples studied (Figure 4.7(c)). Figure 4.8(b) shows the contact angles of the poly(MEA) copolymers. The contact angles of the polymers with MEA backbones decreased in the initial stages of measurements, where the changes in the contact angles of poly(MEA), PMP, and PMT20–5 were 31.9°–24.8°, 17.7°–12.7°, and 47.7°–38.4°, respectively.

Upon introducing oligo PTMC and mPEG segments, fast surface responses were

achieved, and large changes in the contact angles were observed within only a few seconds. Moreover, by introducing a hydrophobic PTMC segment into the poly(MEA) copolymer, the change in contact angle was much larger than for that of PHPT. Upon hydration with a water droplet, PTMC segments were immediately shielded from the water interface as PTMC migrated into the polymer, and mPEG segments were concentrated to form a PEG layer at the outermost surface [34]. Therefore, the surface of copolymer containing PTMC and mPEG segments rapidly changed and became more hydrophilicity.

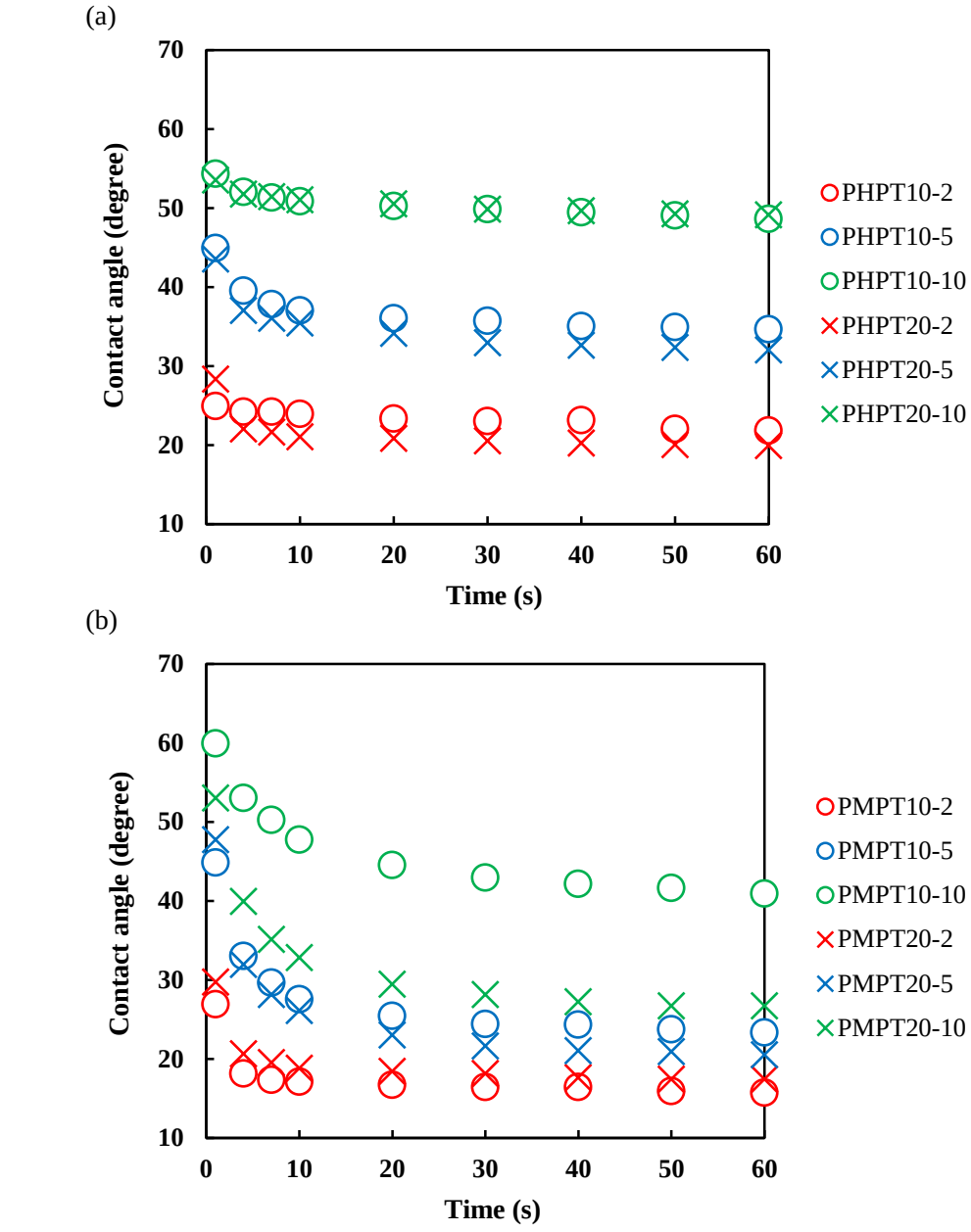

(c) PMPT10–10

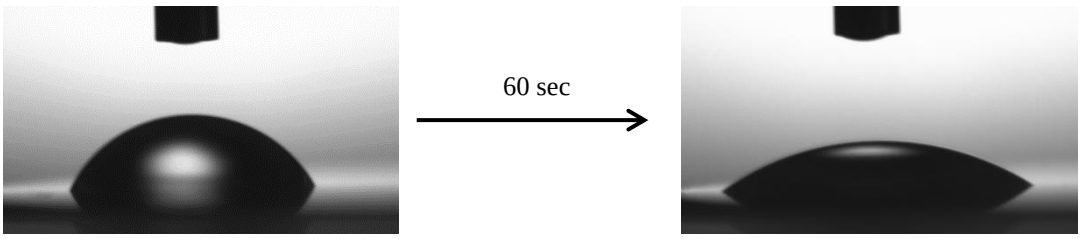

Figure 4.7. Static contact angles of (a) PHPT and (b) PMPT on a glass substrate. (c) A water droplet images on polymer membrane.

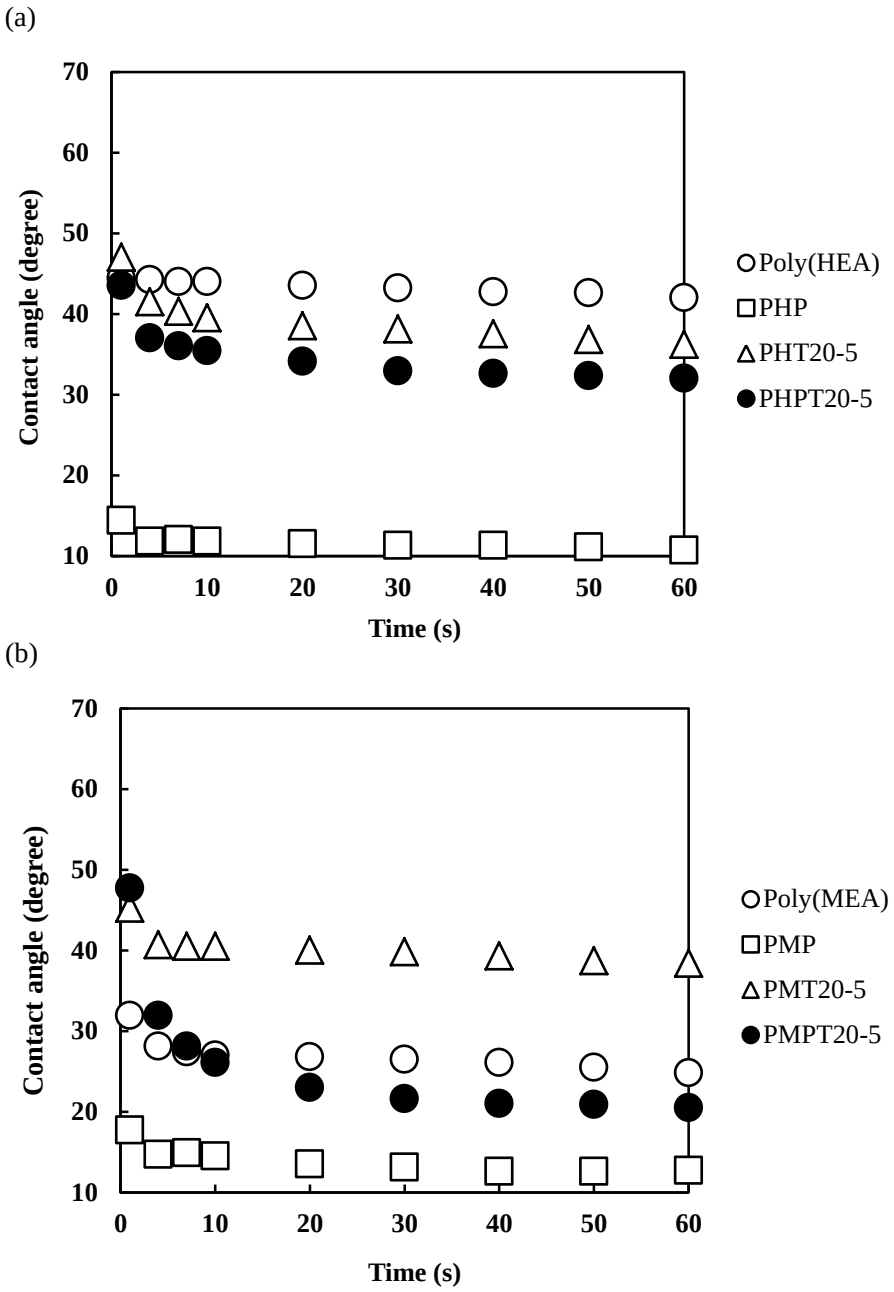

Figure 4.8. Static contact angles of (a) poly(HEA) copolymers and (b) poly(MEA) copolymers on a glass substrate.

Figure 4.9 shows the AFM images, and surface morphologies of the poly(HEA) and poly(MEA) copolymers in air. The surface roughness was different for each polymer system. In the case of poly(HEA), the surface height was in the range of 0.81–12.58 nm and the morphology was flat (Figure 4.9(a)). The author thought that the membrane do not enough prepared of poly(HEA)-coated substrate. The contact angle of the hydrophilic poly(HEA) was higher than that of hydrophobic poly(MEA). The height of PHPT20–5 containing PTMC and mPEG segment was observed to be between 49.54 to 105.49 nm, and the surface was rough (Figure 4.9(b)). The rough surface of this polymer-coated substrate expressed fast surface enrichment property. Figure 4.9(c)–(f) shows the surface roughness of poly(MEA) copolymers by AFM measurement. The surfaces obtained had homogenous heights in each sample, where that of poly(MEA), PMP, PMT20–5, and PMPT20–5 were approximately 17.89–39.93 nm, 12.35–28.33 nm, 23.25–53.25 nm, and 10.84–32.11 nm, respectively. It was hypothesized that the changes in contact angles of poly(MEA) copolymers were not dependent on their surface roughness and morphologies. The author thought that the polymer surface was formed the random morphology by composition of each monomers and macromonomers.

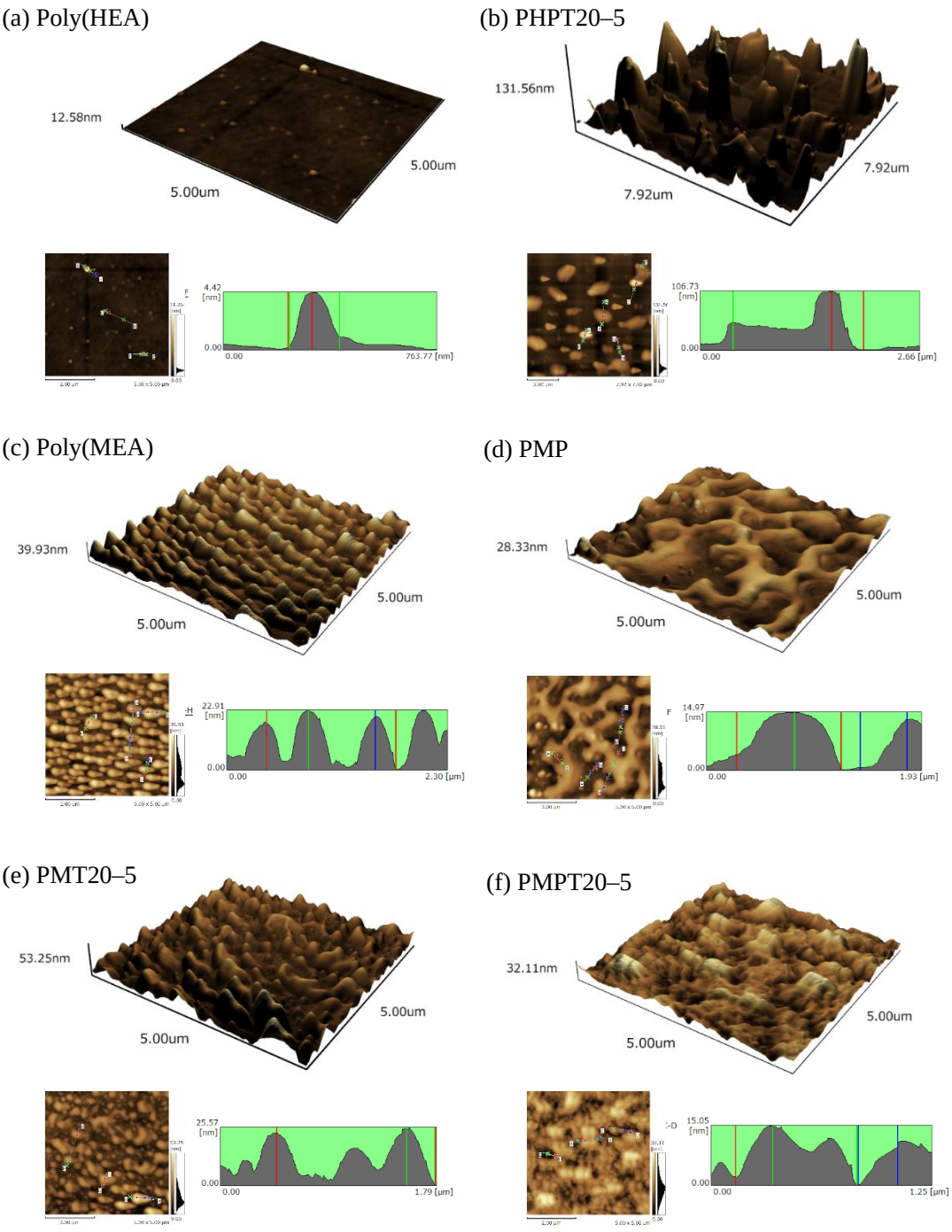

Figure 4.9. AFM images of the surface roughness and surface height of (a) poly(HEA), (b) PHPT20–5, (c) poly(MEA), (d) PMP, (e) PMT20–5, and (f) PMPT20–5 (Scan area: 5.0 × 5.0 μm^2).

To investigate the environmental responsiveness of the polymer surfaces, the polymer-coated substrates were immersed in several different solvents, including water, ethanol, and hexane. The wet condition was measured the contact angle by immersed into water and the contact angle was immediately measured after subjecting the surface to a flow of nitrogen gas for a few seconds. Non-coated glass substrates were immersed into ethanol or hexane for 2 h, and the wettability measured after this process did not changed over 60 s. The contact angles for these control surfaces treated with water, ethanol, and hexane were approximately 34.6°–31.6°, 31.9°–31.5°, and 51.7°–48.8°, respectively. Table 4.2 summarizes change in the contact angle in various conditions for 2 h. When the poly(HEA) and poly(MEA) coated substrate was immersed into hexane, the contact angle rapidly decreased above approximately 10°. In the case of immersed into ethanol and hexane, the contact angle of PHP and PMP did not change. The initial contact angle of homopolymer and copolymer introducing mPEG segment changed in depend on immersed solvent polarity. On the other hand, the initial contact angle of PHT20–5, PHPT20–5, PMT20–5, and PMPT20–5 introducing PTMC was recovered to hydrophobicity by the nitrogen gas flow, and then that of the copolymers changed in the contact angle for 60 s. The contact angle was drastically decreased by introducing mPEG segment content in the PHT20–5 and PMT20–5. Figure 4.10 shows the contact angles of PHPT20–5 and PMPT20–5 treated with various solvents for 2 h. When these substrates were immersed in water, the contact angle changed quickly from 51.9° to 26.8° over 60 s (Figure 4.10(a)). The sample immersed into ethanol maintained its initial contact angle, with values in the range of 50.8° and 41.8° over 60 s. The contact angle of PHPT20–5 treated with hexane started at 47.2° and decreased to 37.4°. These results demonstrate the rapid reorientation of PTMC segments on the polymer surface under nitrogen gas flow, and the contact angle

changing as the surface becomes hydrophilic upon contact with the water droplet for only a few seconds. In Figure 4.10(b), it can be seen the contact angle value recovered to what was observed under dry conditions. The contact angle of the PMPT20–5 polymer-coated substrate changed from 60.2° to 25.1° even after immersion in water, so the contact angle was immediately shifted to the hydrophobic side chain. In the case of immersion into ethanol and hexane, the contact angle recovered to 65.4° and 58.7°, and then decreased to 34.7° and 37.6°, respectively. These results indicated that the hydrophobic moieties of the copolymers PHPT20–5 and PMPT20–5 rapidly concentrated on the surface of the polymer.

Table 4.2. Change in the static contact angles in various conditions for 60 s

Sample	Contact angle in dry condition (degree)		Contact angle after immersion into solvent for 2 h (degree)					
			Water		Ethanol		Hexane	
	1 s	60 s	1 s	60 s	1 s	60 s	1 s	60 s
Poly(HEA)	44.4	42.0	–	–	–	–	40.2	27.3
PHP	14.4	10.7	–	–	48.5	41.6	43.4	37.5
PHT20–5	47.0	36.2	57.0	43.6	54.7	47.4	52.9	44.2
PHPT20–5	43.5	32.0	51.9	26.8	50.8	41.8	47.2	37.4
Poly(MEA)	31.9	24.8	–	–	–	–	40.6	26.9
PMP	17.7	12.7	–	–	65.3	60.0	58.8	54.3
PMT20–5	51.4	44.2	46.7	30.6	54.8	40.4	57.8	47.7
PMPT20–5	47.7	20.5	60.2	25.1	65.4	34.7	58.7	37.6

(a) PHPT20–5

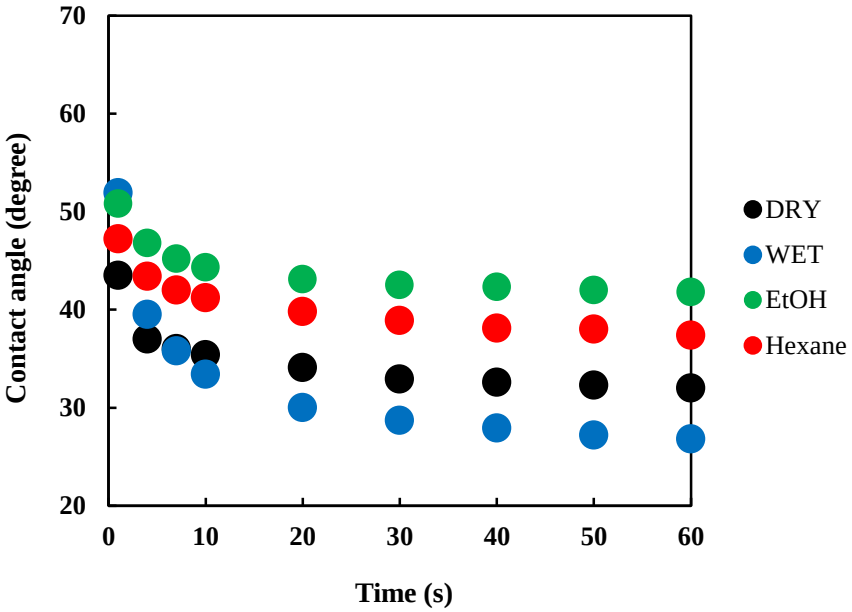

(b) PMPT20–5

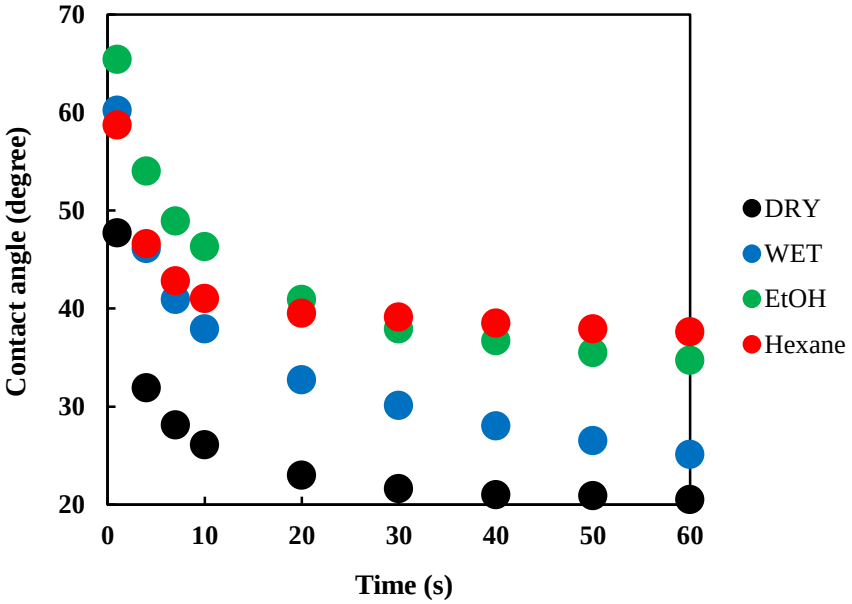

Figure 4.10. Static contact angles of (a) PHPT20–5 and (b) PMPT20–5 on a glass substrate. The samples were immersed into water (WET), ethanol, and hexane for 2 h, and then the contact angle was measured after exposure to a flow of nitrogen gas.

Figure 4.11–13 show AFM images of poly(MEA) copolymer-coated substrates treated by several solvents for 2 h. The surface roughness of poly(MEA) copolymer-coated substrates treated with several solvents was observed by AFM. The measurement was performed at room temperature in air. With regards to solubility in water, ethanol, and hexane, PMT20–5 and PMPT20–5 were insoluble in water, while PMP, PMT20–5, and PMPT20–5 were insoluble in ethanol. All of the samples were insoluble in hexane. In the case of the samples immersed in water, the hydrophilic moieties in the copolymer became enriched on the polymer surface. The membranes formed somewhat smooth structures with heights of the roughness for PMT20–5 and PMPT20–5 in the range of 3.83–16.50 nm and 4.00–12.31 nm, respectively (Figure 4.11). In the case of ethanol, the mPEG segment migrated to the ethanol and polymer interface. The surface morphologies on PMP, PMT20–5, and PMPT20–5 were island structures, with heights in the range of 1.85–5.60 nm, 3.71–9.99 nm, and 4.00–13.60 nm, respectively (Figure 4.12). When all samples were immersed into hexane for 2 h, all of the monomer units in copolymer were insoluble and fixed. The surface roughness was seen to be the most enhanced (Figure 4.13). The heights of poly(MEA), PMP, PMT20–5, and PMPT20–5 were approximately 6.24–54.07 nm, 8.60–56.22 nm, 8.06–26.10 nm, and 7.01–29.51 nm, respectively. However, the differences in roughness values of the samples were not related to the changes in wettability observed.

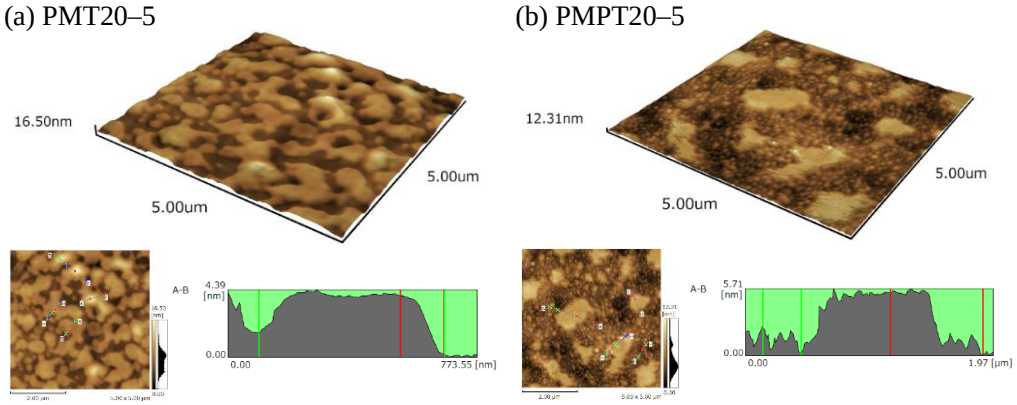

Figure 4.11. AFM images of the surface roughness and surface height after immersion into water for 2 h of (a) PMT20–5 and (b) PMPT20–5(Scan area: $5.0 \times 5.0\ \mu m^2$).

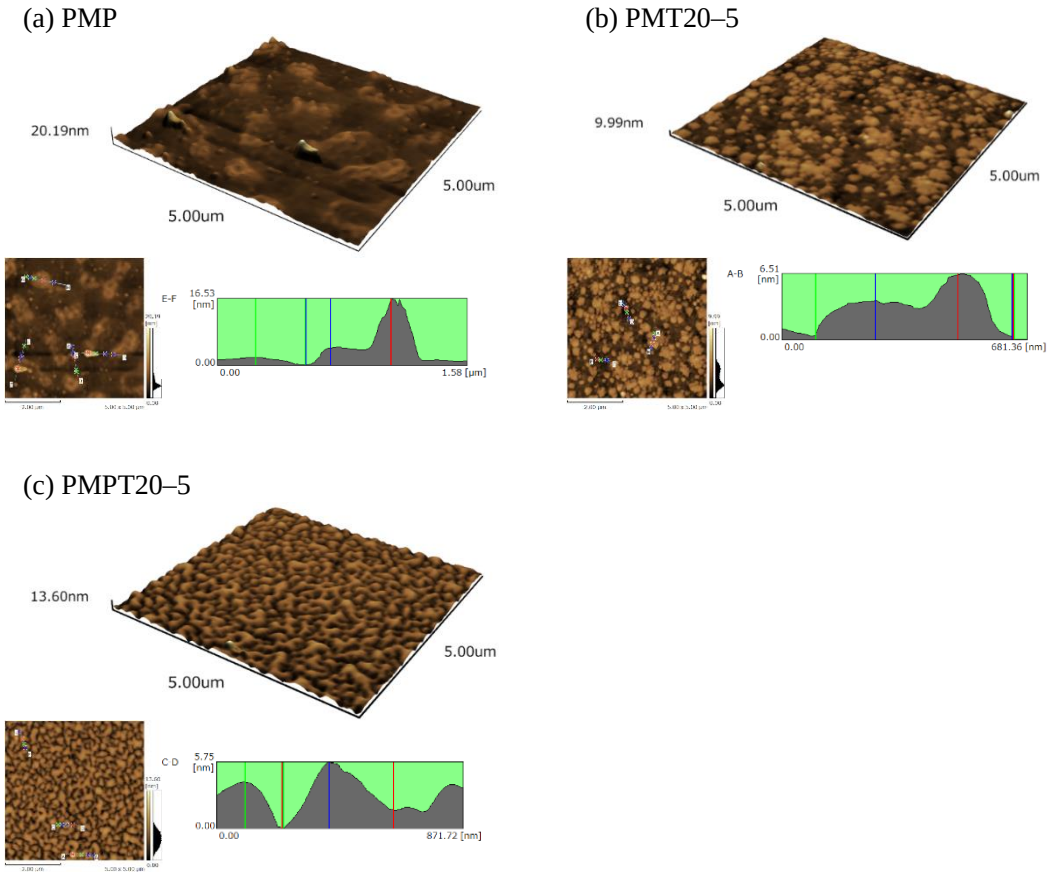

Figure 4.12. AFM images of the surface roughness and surface height after immersion into ethanol for 2 h of (a) PMP, (b) PMT20–5, and (c) PMPT20–5 (Scan area: 5.0 × 5.0 μm^2).

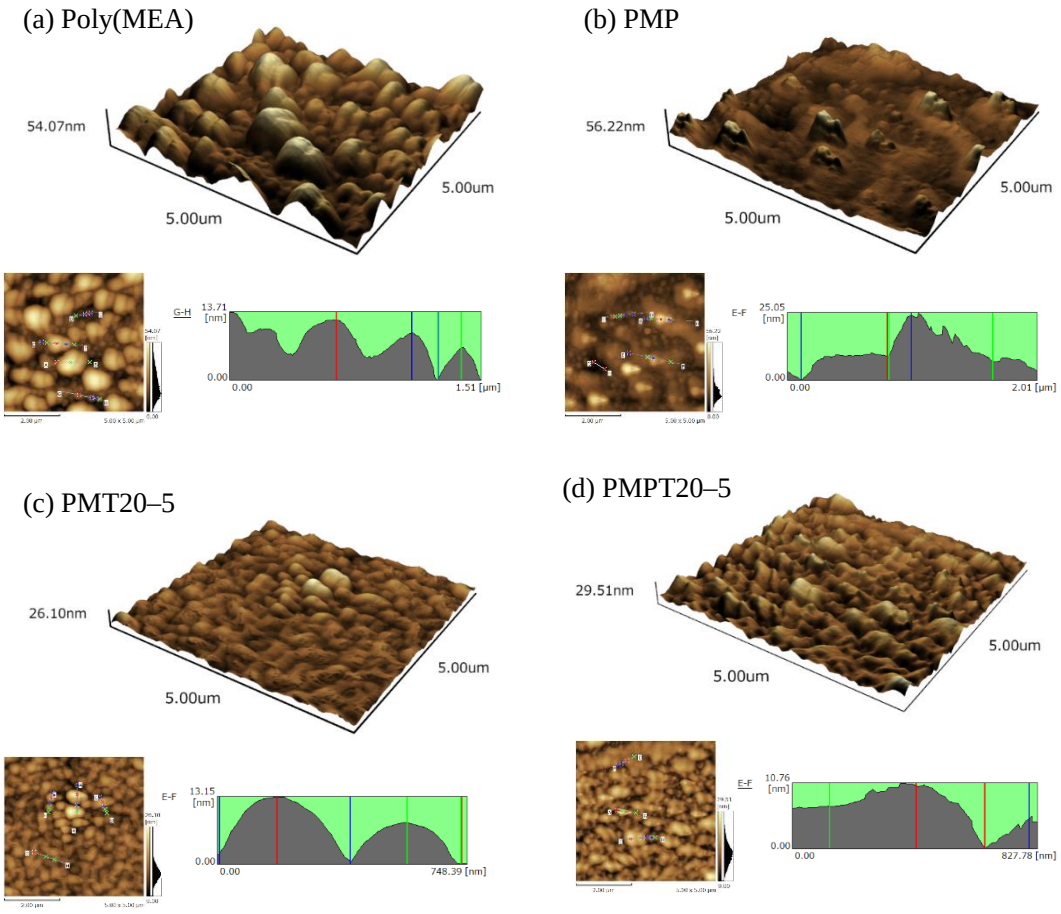

Figure 4.13. AFM images of the surface roughness and surface height after immersion into hexane for 2 h of (a) poly(MEA) (b) PMP, (c) PMT20–5, and (d) PMPT20–5 (Scan area: 5.0 × 5.0 μm^2).

In general, when the polymer-coated substrates were immersed in different solvents, the contact angle changed depending on the polarity of the solvent. However, in the cases where the copolymer incorporated oligo PTMC and mPEG segments, the contact angle rapidly returned to its initial stage after exposure to nitrogen gas flow. Upon immersion into water, the hydrophobic PTMC segments on the polymer surface migrated inside the polymer membrane, and hydrophilic mPEG segments were enriched on the surface to decrease the free energy of the interface. The author hypothesize that the amorphous PTMC segments inside the polymer membrane became concentrated on the surface upon exposure to nitrogen gas flow for few seconds due to their high molecular mobility (Figure 4.14). This switching behavior was further seen to be a repeatable responsive property. From these results, the surface properties of the amphiphilic graft copolymer can be seen, such as their rapid environmental responsiveness and reversible control of its hydrophilic-hydrophobic balance.

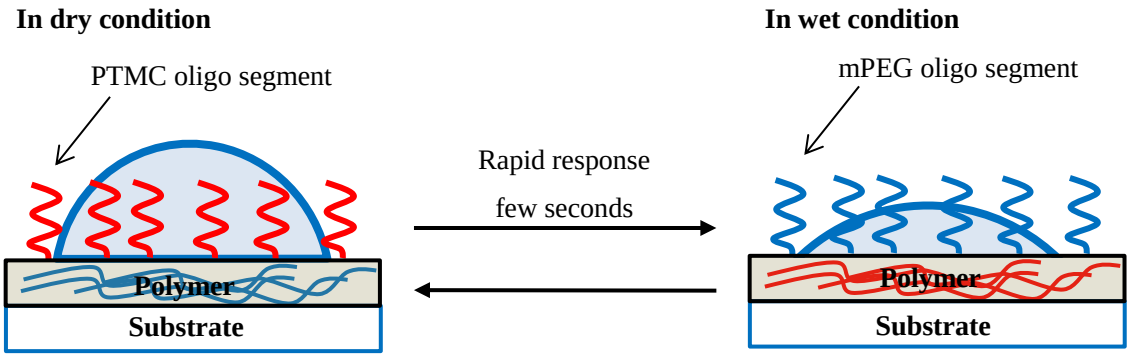

Figure 4.14. Illustration of the rapid and responsive surface copolymer switching behavior.

4.4 Conclusions

The author reports the design and synthesis of novel amphiphilic graft copolymers containing oligo PTMC and mPEG segments by a macromonomer method. By tuning the polymer polarity through the incorporation of main chain hydrophilic 2-hydroxyethyl acrylate or hydrophobic 2-methoxyethyl acrylate, the wettability of the polymer membranes prepared by spin coating was investigated. PTMC copolymers showed glass transition temperatures below 0°C. These copolymers showed flexible mobility of its segment at room temperature. The contact angle in air observed rapidly changed upon alterations in the length of PTMC incorporated and the composition ratio. These observations were caused by reorientation of the different polar segments within the polymer membrane upon contact with water. However, from the results of AFM measurements, it can be seen that the switching behavior of the contact angle was not dependent on the surface roughness of the membrane due to the composition ratio of side chains and immersing in solvents. The rapid environmental responsiveness of PTMC and mPEG segments was further shown to be reversible, and demonstrated a control of the hydrophilic-hydrophobic balance on the graft copolymer. By selecting appropriate functional monomers for polymer backbones, the graft copolymers incorporating oligo PTMC and mPEG segments are expected to have applications as more intelligent surface responsive materials. These biocompatible graft copolymers with surface responsiveness have potential uses as surface modifiers for medical and biomaterial applications.

4.5 References

[1] B. Zuo, Y. Hu, X. Lu, S. Zhang, H. Fan, and X. Wang, *J. Phys. Chem. C* **2013**, *117*, 3396.

[2] M. Kobayashi, Y. Terayama, H. Yamaguchi, M. Terada, D. Murakami, K. Ishihara, and A. Takahara, *Langmuir* **2012**, *28*, 7212.

[3] S. Lee and N. D. Spencer, *Langmuir* **2008**, *24*, 9479.

[4] I. Toki, M. Komatsu, Y. Shimizu, and Y. Hara, *J. Appl. Polym. Sci.* **2013**, *127*, 3657.

[5] C. Leng, H.-C. Hung, S. Sun, D. Wang, Y. Li, S. Jiang, and Z. Chen, *Appl. Mater. Interfaces* **2015**, *7*, 16881.

[6] M. Tanaka and A. Mochizuki, *J. Biomed. Mater. Res. A* **2004**, *68*, 684.

[7] K. Sato, S. Kobayashi, M. Kusakari, S. Watahiki, M. Oikawa, T. Hoshiba, and M. Tanaka, *Macromol. Biosci*. **2015**, *15*, 1296.

[8] S. Morita and M. Tanaka, *Langmuir* **2014**, *30*, 10698.

[9] B. Dizman, M. O. Elasri, and L. J. Mathias, *Biomacromolecules* **2005**, *6*, 514.

[10] R. Zhang, A. Seki, T. Ishizone and H. Yokoyama, *Langmuir*, **2008**, *24*, 5527.

[11] K. Ishihara, H. Oshida, Y. Endo, T. Ueda, A. Watanabe, and N. Nakabayashi, *J. Biomed. Mater. Res.* **1992**, *26*, 1543.

[12] D. R. Lu, S. J. Lee, and K. Park, *Biomater. Sci. Polym. Edn*. **1991**, *3*, 127.

[13] M. K. Vyas, K. Schneider, B. Nandan, and M. Stamm, *Soft Matter* **2008**, *4*, 1024.

[14] Y. G. Takei, T. Aoki, K. Sanui, N. Ogata, Y. Sakurai, and T. Okano, *Macromolecules* **1994**, *27*, 6163.

[15] T. Chen, R. Ferris, J. Zhang, R. Ducker, and S. Zauscher, *Prog. Polym. Sci.* **2010**, *35*, 94.

[16] O. Mert, E. Doganci, H. Y. Erbil, and A. S. Demir, *Langmuir* **2008**, *24*, 749.

[17] A. Diaz, L. del Valle, L. Franco, J.R. Sarasua, F. Estrany, and J. Puiggalí, *Mater. Sci. Eng. C* **2014**, *42*, 517.

[18] H. Ajiro, Y. Takahashi, M. Akashi, and T. Fujiwara, *Polymer* **2014**, *55*, 3591.

[19] M. Kallrot, U. Edlund, and A.-C. Albertsson, *Biomaterials* **2006**, *27*, 1788.

[20] J. Watanabe, H. Kotera, and M. Akashi, *Macromolecules* **2007**, *40*, 8731.

[21] J. Cai and K. J. Zhu, *Polym. International* **1997**, *42*, 373.

[22] J. Cai, K. J. Zhu, and S. L. Yang, *Polymer* **1998**, *39*, 4409.

[23] S. J. Buwalda, L. B. Perez, S. Teixeira, L. Calucci, C. Forte, J. Feijen, and P. J. Dijkstra, *Biomacromolecules* **2011**, *12*, 2746.

[24] K. Nitta, J. Miyake, J. Watanabe, and Y. Ikeda, *Trans. Mater. Res. Soc. Jpn.* **2013**, *38*, 629.

[25] T. Hirata, H. Matsuno, D. Kawaguchi, N. L. Yamada, M. Tanaka, and K. Tanaka, *Phys. Chem. Chem. Phys.* **2015**, *17*, 17399.

[26] K. Nitta, J. Miyake, J. Watanabe, and Y. Ikeda, *Trans. Mater. Res. Soc. Jpn.* **2012**, *37*, 349.

[27] A. Diaz, M. O. Elasri, and L. J. Mathias, *Biomacromolecules* **2005**, *6*, 514.

[28] W. Steinhauer, R. Hoogenboom, H. Keul, and M. Moeller, *Macromolecules* **2013**, *46*, 1447.

[29] Y. Feng and S. Zhang, *J. Polym. Sci. A: Polym. Chem.* **2005**, *43*, 4819.

[30] M. G. Carstens, C. F. van Nostrum, A. Ramzi, J. D. Meeldijk, R. Verrijk, L. L. de Leede, D. J. A. Crommelin, and W. E. Hennink, *Langmuir* **2005**, *21*, 11446.

[31] H. Wang, J. H. Dong, and K. Y. Qiu, *J. Polym. Sci. A: Polym. Chem.* **1998**, *36*, 695.

[32] T. Tyson, A. Finne-Wistrand, and A.-C. Albertsson, *Biomacromolecules* **2009**, *10*, 149.

[33] R. B. Trinca and M. I. Felisberti, *Euro. Polym. J.* **2015**, *62*, 77.

[34] H. Otsuka, Y. Nagasaki, and K. Kataoka, *Biomacromolecules* **2000**, *1*, 39.

Chapter 5

Design and Synthesis of Amphiphilic Graft Hydrogel Having Hydrophobic Domain Formed by Multiple Physical Interactions

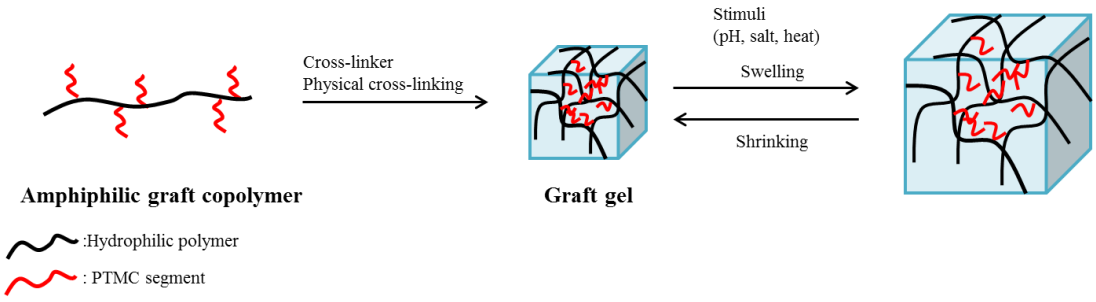

5.1 Introduction

Polymeric hydrogels are widely researched biomaterials. In order to develop various applications, plenty of hydrogel designs were proposed to improve their properties. Various cross-linking structures are investigated in terms of chain entanglement, molecular interaction, and molecular weight between cross-link points. Double network gels, hydrogen bonding gels, and tetra-poly(ethylene glycol) gels are researched [1–3]. In this chapter, an amphiphilic hydrogel cross-linked via physical interactions, such as hydrophobic interaction and hydrogen bonding, was designed and prepared. The author focused on the incorporation of graft gel as functional pendant segment into the hydrogel. For example, Kaneko *et al.* reported poly(*N*-isopropyl acrylamide)-grafted hydrogel having fast response rate to temperature [4]. Furthermore, hydrogel based on amphiphilic macromonomer was reported by Xu *et al* [5]. This hydrogel was formed by the aggregation of micelles into the hydrogel upon temperature change.

The hydrophobic poly(trimethylene carbonate) (PTMC) segment is easily and precisely synthesized by ring-opening polymerization (ROP) technique. Additionally, PTMC has been widely investigated in the biomaterials field because of its biodegradability by lipase and its amorphous property [6, 7].

In this chapter, the author examined the graft gel that includes the amphiphilic polymeric hydrogel with the PTMC macromonomer as the hydrophobic graft segment (Figure 5.1(a)). Graft hydrogels with a polymerization degree of PTMC ranging from 10 to 50 and grafting ratio from 1 to 10 mol% were prepared. The hydrophilic–hydrophobic balance was controlled by altering the above two parameters. In addition, poly(2-acrylamidoglycolic acid) (PAGA) was selected as the hydrophilic main chain. PAGA has numerous advantages such as hydrogen bonding ability, pH sensitivity, and

the presence of multiple reactive groups.

The author investigated the fundamental properties of the amphiphilic graft hydrogel. It spontaneously formed three-dimensional structure via physical interaction. Therefore, the favorable behavior of the hydrogel was changed by the hydrophobic effect and its physical properties were examined by swelling ratio measurement and scanning electron microscopy (SEM). The functional property of molecular loading was monitored by UV–Vis measurement using hydrophobic dye. The graft gel having PTMC segments is suitable for molecular adsorbent applications and this function is important for biomaterials and environmentally friendly materials.

(a) Graft gel

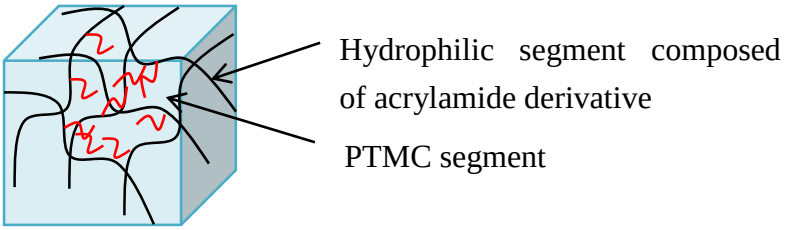

(b) GAT

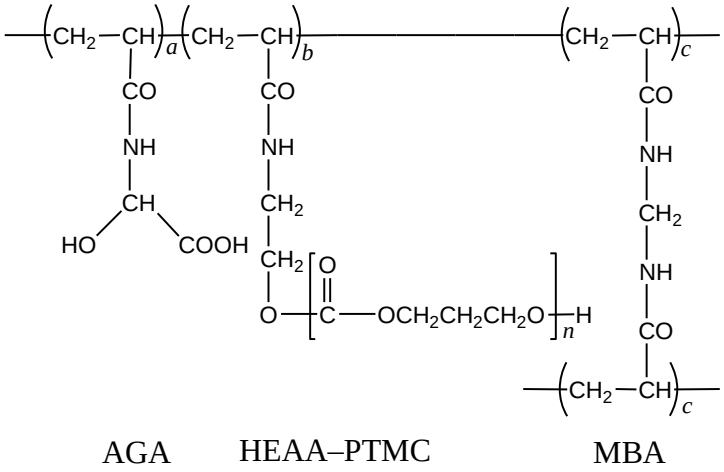

Figure 5.1. (a) Illustrations of the graft gel including PTMC segment. (b) Chemical structure of poly(AGA–*co*–HEAA–PTMC) (GAT) graft gel.

5.2 Experimental Section

5.2.1 Materials

For ROP, trimethylene carbonate (TMC), as cyclic monomer, and 1,8-diazabicyclo[5.4.0]undec-7-ene (DBU), as organic catalyst, were purchased from Tokyo Chemical Industry, Co., Ltd., Tokyo, Japan. *N*-Hydroxyethyl acrylamide (HEAA) was kindly supplied by KOHJIN Co., Ltd., Tokyo, Japan. In order to terminate the polymerization, benzoic acid (Wako Pure Chemical Industries, Ltd., Osaka, Japan) was used. For free radical polymerization, 2-acrylamidoglycolic acid monohydrate (AGA; Sigma-Aldrich Corp., St. Louis, MO, USA) was used as the monomer. 2,2'-Azobis(isobutyronitrile) (AIBN, Tokyo Chemical Industry Co., Ltd.) was used as the initiator for radical polymerization. *N*,*N*'-Methylenebis(acrylamide) (MBA, Wako Pure Chemical Industries, Ltd.) was used as a cross-linker. For confirmation of hydrogen bonding, urea was employed (Wako Pure Chemical Industries, Ltd.). Solutions with different pH values were prepared under the following buffer solutions: pH 3.0: glycine and HCl, pH 5.0: citric acid and NaOH, pH 7.1: phosphate buffered saline (PBS), pH 9.0: Na_2CO_3 and $NaHCO_3$, and pH 11.0: Na_2HPO_4 and NaOH. PBS (Dulbecco's PBS) was purchased from Life Technologies Corp., Waltham, MA, USA. Other reagents were purchased from Wako Pure Chemical Industries. To investigate the drug incorporation function of the hydrogel, Basic Blue 7 (BB7) (Tokyo Chemical Industry, Co., Ltd.) was used as a model drug. All organic solvents were used as received.

5.2.2 Synthesis of Poly(AGA–*co*–HEAA–PTMC) Graft Gel

The HEAA–PTMC macromonomer was prepared according to a previously reported

procedure [8]. The author prepared the macromonomer with approximately 10, 20, and 50 repeating units of TMC. The DP of PTMC was calculated from the ^{1}H NMR spectrum in $CDCl_3$.

To prepare the graft gel, free radical polymerization was carried out using AIBN, AGA, MBA, and HEAA–PTMC macromonomer (Figure 5.1(b)). The reagents were each dissolved in *N*,*N*-dimethylformamide (DMF), and then, their solutions were mixed. The total concentration of initiator, monomer, and macromonomer was 1.5 mol/L. The solution was degassed under reduced pressure and then was substituted by nitrogen gas. The mixture solution (1 mL) was heated at 70°C for 9 h in a 2.2 mL sample tube. To remove unreacted compounds, the crude product was immersed into a DMF/water mixed solution (DMF:water = 1:1) and into ultrapure water. Chemical structures were confirmed by FT–IR measurements. IR (in ATR mode, cm^{-1}): 3000–3500 (–C(=O)–NH–, and –OH), 1740 (–C=O), 1650 (–COOH), and 1240 (–C–O–C–).

5.2.3 Swelling Ratio Measurement

The prepared hydrogel was lyophilized and put into a nylon mesh bag. Before and after immersion in solutions at 37°C, the weight of the hydrogel was measured. The swelling ratio of the hydrogel was calculated by the following equation:

$$\text{Swelling ratio (\%)} = (W_s - W_d)/W_d \times 100$$

where W_s and W_d are the weights of the swollen hydrogel and the dried hydrogel, respectively. The pH values of each buffer solution were approximately 3.0, 5.0, 7.1, 9.0, and 11.0, respectively. The change in the swelling ratio of the hydrogel in different pH

solutions was measured after a 2 h interval for each solution. To confirm hydrogen bonding in the hydrogel, the change in swelling ratio was measured by using urea (2 mol/L). In addition, the hydrogel was heated in boiling water at 70°C [11].

5.2.4 Observation of Surface and Interior Morphology of Hydrogel

The lyophilized hydrogel was observed by SEM. The cut hydrogel was fixed by carbon tape on a sample stage, and then electro-conductive paste (DOTITE; Fujikura Kasei Co., Ltd., Tochigi, Japan) was spotted onto the corner of the sample. The sample was sputter-coated with platinum prior to the observation.

5.2.5 Evaluation of Model Drug Incorporation in Hydrogel

To evaluate the molecular loading function, hydrophobic BB7 (λ_{max} = 616 nm, solubility in water: 2.0 g/dL) was used as a model drug (Figure 5.2). The amount of drug loading was evaluated from absorbance values at 616 nm obtained from UV–Vis spectroscopy [9]. The BB7 aqueous solution was prepared with ultrapure water. The final concentration of BB7 was 10^{-5} mol/L. The swollen hydrogel (10 mg/mL at dried gel) was immersed into BB7 aqueous solution at room temperature. The UV–Vis spectrum of the supernatant was monitored at given times.

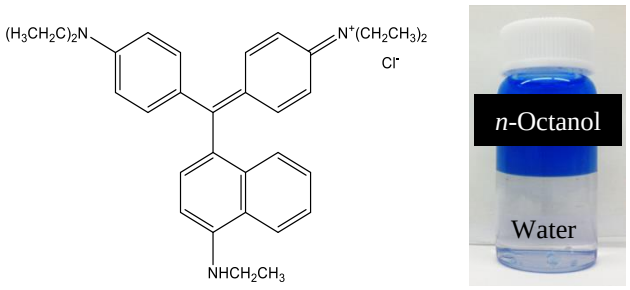

Figure 5.2. Chemical structure of BB7.

5.3 Results and Discussion

5.3.1 Preparation of Graft Gel Having PTMC Segments

The HEAA–PTMC macromonomer was synthesized by using DBU as basic organic catalyst. The feed ratio of [TMC]/[HEAA] was 10, 20, and 50. The DPs of PTMC calculated by ^{1}H NMR were 9, 19, and 49, respectively. In the ^{1}H NMR spectrum, the methylene signal on the PTMC (t, 4H, –C*H*$_2$–CH$_2$–C*H*$_2$–) shifted from around 4.5 to 4.2 ppm and the presence of the amide group of HEAA (br, 1H, –C(=O)–N*H*–CH$_2$–) was confirmed, showing no side-reactions. The product state of HEAA–PTMC was a clear viscous liquid when the DP of PTMC was 10 or 20. On the other hand, it was a white wax when the DP was 50. The product state was well correlated with the molecular weight of PTMC, indicating a corresponding enhancement of the molecular interaction.

The hydrogel with PTMC segments was prepared in a test tube by free radical polymerization using AIBN as the initiator. Unreacted chemicals such as AGA and the macromonomer were sequentially removed by immersing into DMF, ultrapure water, or their solution for three days. These solvents were replaced several times. The color of the resulting hydrogel was clear light yellow, derived from PAGA. All macromonomers having PTMC were insoluble in water and their appearance was a white precipitate in water. Therefore, the author expected that the unreacted macromonomer was completely removed from the hydrogel, and then the amphiphilic property of the hydrogel was examined. The chemical structure was confirmed by FT–IR measurement (Figure 5.3). The amide groups derived from AGA and HEAA–PTMC were observed at 3000–3500 cm^{-1}. In addition, the stretching vibration peaks of PTMC were observed at 1240 and 1740 cm^{-1} [10]. Therefore, the author concluded that the poly(AGA–*co*–HEAA–PTMC) graft gel was prepared. Table 5.1 summarizes the preparative condition for the graft gels.

The sample code was abbreviated as GAT*n*–*b*, where "*b*" represents the PTMC macromonomer composition. The "*n*" represents the DP of PTMC. For example, GAT10−1 refers to the graft hydrogel with a DP of PTMC and a macromonomer composition of approximately 10 and 1 mol%, respectively.

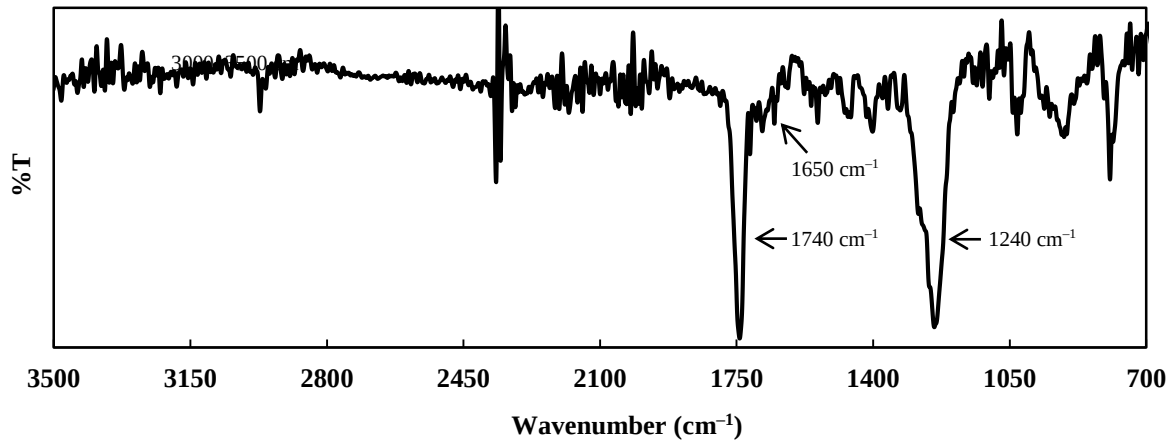

Figure 5.3. FT–IR spectrum of GAT50–1 graft gel.

Table 5.1. Preparation of amphiphilic graft hydrogels

Sample	Feed ratio (mol%)			
	AGA	HEAA–PTMC macromonomer	(DP)[1)]	MBA
PAGA gel–0	100	0	—	0
PAGA gel–1	100	0	—	1
PAGA gel–3	100	0	—	3
PAGA gel–5	100	0	—	5
GAT10–1	99	1	(9)	3
GAT10–5	95	5	(9)	3
GAT10–10	90	10	(9)	3
GAT20–1	99	1	(19)	3
GAT20–5	95	5	(19)	3
GAT20–10	90	10	(19)	3
GAT50–1	99	1	(49)	3
GAT50–5	95	5	(49)	3

[1)] The DP of PTMC was calculated by ^{1}H NMR.

5.3.2 Change in Swelling Ratio of Graft Gel

Swelling ratio was measured by using the nylon mesh bag method. Figure 5.4 shows swelling ratios of hydrogels obtained under various conditions. First, the author investigated the dependence on the MBA concentration. PAGA gel–0, PAGA gel–1, PAGA gel–3, and PAGA gel–5 represent sample codes for MBA concentrations of 0, 1.0, 3.0, and 5.0 mol%, respectively. The maximum swelling ratio of PAGA gel–0 was about 2,300% within 6 h. Maximum swelling ratios of PAGA gel–1, PAGA gel–3, and PAGA gel–5 were about 1,550, 1,450, and 900% within 6 h. By increasing the MBA concentration, tight cross-linking occurred in the polymer solution, and AGA, as an acrylamide derivative, formed cross-linking points by hydrogen bonding. Therefore, by increasing the MBA concentration, the swelling ratio of each sample in water decreased.

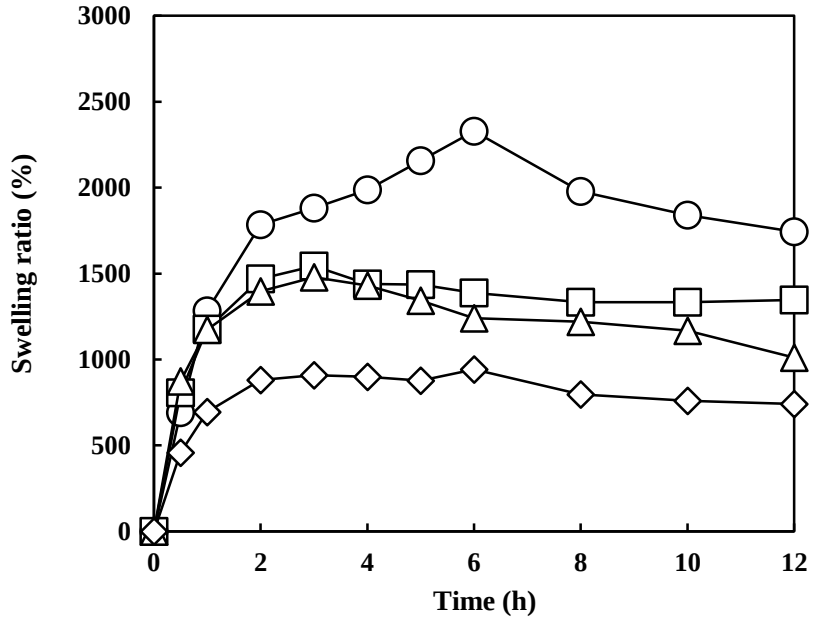

Figure 5.4. Swelling ratio of AGA gel depending on MBA concentration was plotted in PBS solution at 37°C. PAGA gel–0: ○, PAGA gel–1: □, PAGA gel–3: △, and PAGA gel–5: ◇.

The graft gel has PTMC segments, but GAT10–1 showed a high swelling ratio of 1,000%, which is similar to the PAGA gel. All PAGA gels and GAT10–1 fell through the nylon mesh bag due to weak molecular interaction. Other graft gels were much more stable, showing strong molecular interactions.

Figure 5.5(a) shows plots of swelling ratio variation based on different graft ratios. The effect of the graft ratio was examined by using GAT10–1, GAT10–5, and GAT10–10. GAT10–5 and GAT10–10 showed a maximum swelling ratio of 700 and 270% within 12 h. Furthermore, the effect of the segment length was examined by using GAT10–5, GAT20–5, and GAT50–5 (Figure 5.5(b)). GAT20–5 and GAT50–5 showed maximum swelling ratios of 380 and 105% within 18 h. Upon increasing the graft ratio and segment length, hydrophobic interactions between PTMC molecules increased. The result of swelling ratio measurement was well correlated with the graft ratio of HEAA–PTMC macromonomer and the segment length. The swelling ratio could be controlled by altering the incorporation ratio of PTMC segments and the DP of PTMC. From the results of swelling ratio experiments, the graft gels were shown to possess amphiphilic properties, even when a higher amount of hydrophobic segments was contained.

(a) Dependence on the graft ratio

(b) Dependence on the PTMC segment length

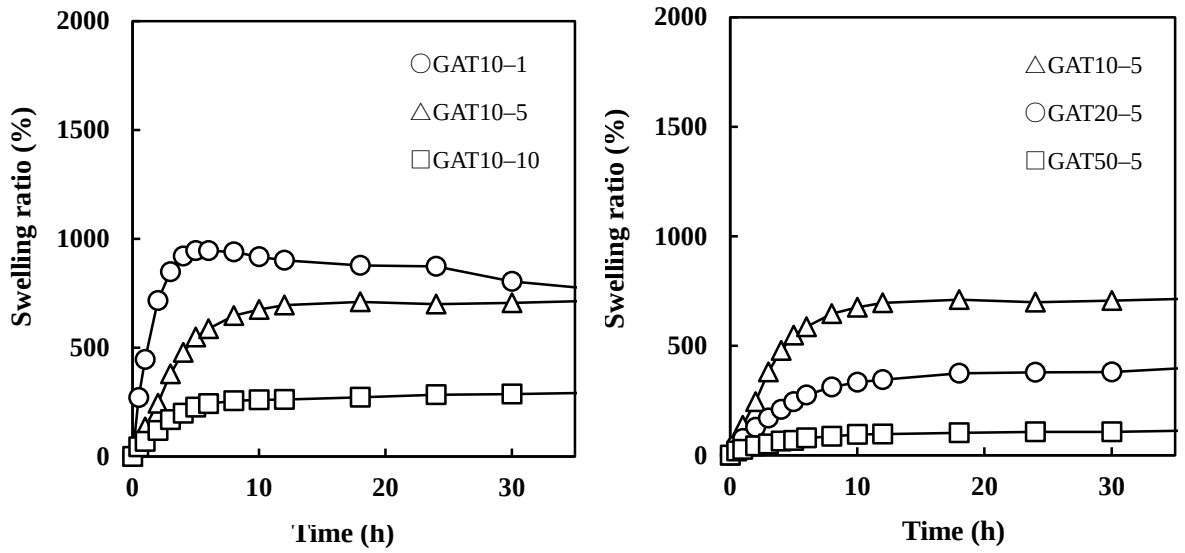

Figure 5.5. Plots of swelling ratio variation of graft gels in PBS solution with time at 37°C. (a) Dependence on the graft ratio. (b) Dependence on the PTMC segment length.

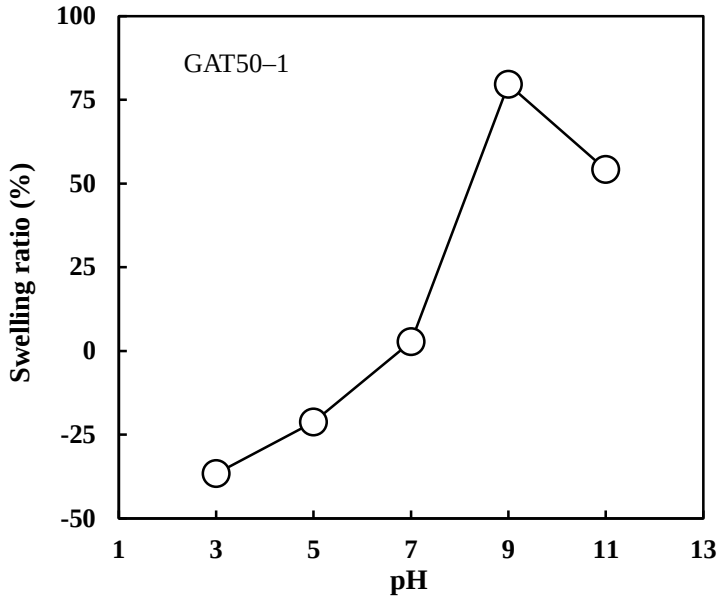

Figure 5.6. Plots of the swelling ratio change for graft gels in solution with various pH solutions at 37°C. Measurement time interval was 2 hours.

The pH sensitivity was addressed; Figure 5.6 shows results of pH dependence on the swelling ratio. Graft gel, GAT50–1, showed pH sensitivity due to the PAGA monomer unit. The carboxyl group in PAGA hydrophilic polymer backbone was protonated in an acidic environment, and the gel shrank. On the other hand, in a basic environment, PAGA from graft gels was deprotonated and the gel swelled. In pH 11, the swelling ratio decreased to dissociate network bond by alkaline hydrolysis. This swelling and shrinking behavior was observed to be reversible.

The gel was not only chemically but also physically cross-linked. One of the physical cross-linking methods was by hydrogen bonding. To confirm hydrogen bonding formation, change in the swelling ratio of GAT50–1 was observed after urea addition and heating in water (Figure 5.7). In the case of urea addition at room temperature, the swelling ratio was about 100% within 1 h and the gel state was

maintained. By heating at 70 °C without urea, the swelling ratio was changed to about 100% within 1 h and then the graft gel was gradually dissolved after 4 h. However, the swelling ratio of the graft gel was dramatically changed by both urea addition and heating. The one of the swelling ratio was observed at 220% and then the gel dissolved in a similar way after urea addition. From these results, a part of the driving forces of gel formation in the network structure was shown to be the hydrogen bonds. Urea molecules formed strong hydrogen bonding with poly(AGA), as an acrylamide derivative, reducing hydrogen bonding around the poly(AGA) segment. Moreover, hydrogen bonding is generally weak against heating. Therefore, cross-linking by hydrogen bonding was disassociated by the addition of urea and heating. This phenomenon led to dissolution of the graft gel.

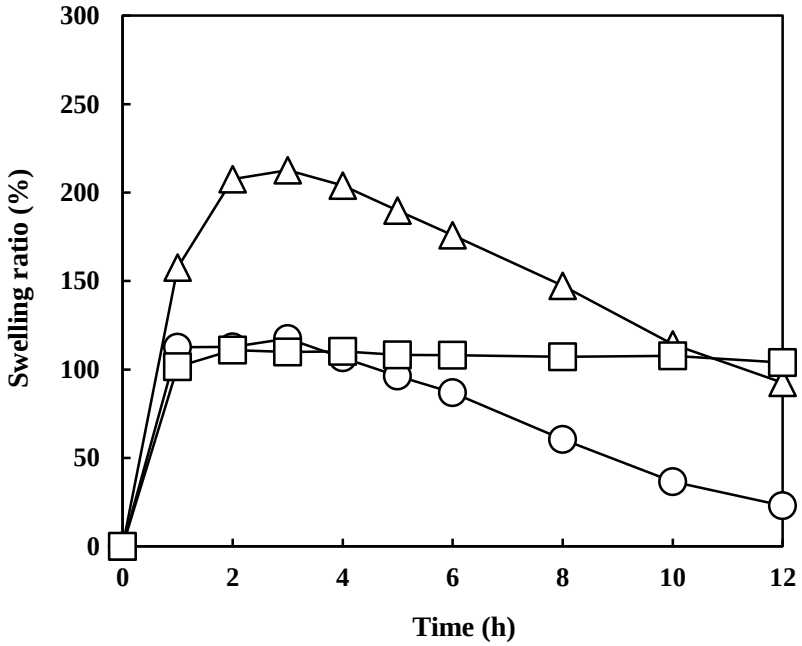

Figure 5.7. Swelling ratio of GAT50–1 plotted in urea solution, at room temperature or 70°C. Blank: ○, Urea (70°C): △, and Urea (r.t.): □.

5.3.3 Observation of Surface and Interior Morphology of Hydrogel

Figure 5.8 shows SEM images of GAT10–1, GAT10–5, GAT20–1, and GAT20–5. SEM images displayed the following components: surface skin layer and porous interior. The morphology of the hydrogel composed of PAGA as hydrophilic backbone showed only a sponge-like structure. The pore size was about 100 μm. On the other hand, when the amount of TMC units was increased in the hydrogels, the pores were much smaller (about 2 μm) or disappeared. With an increasing number of TMC units, the interior of the gel formed a solid structure. For example, PAGA gel–3 and GAT20–1 were 1.5 μm and 12 μm thick, respectively. These layers formed by PTMC segregated on the surface, and the hydrophobic PTMC prevented water molecules from penetrating. These results were based on the higher molecular mobility of amorphous PTMC segments and corresponded to the swelling ratio trend.

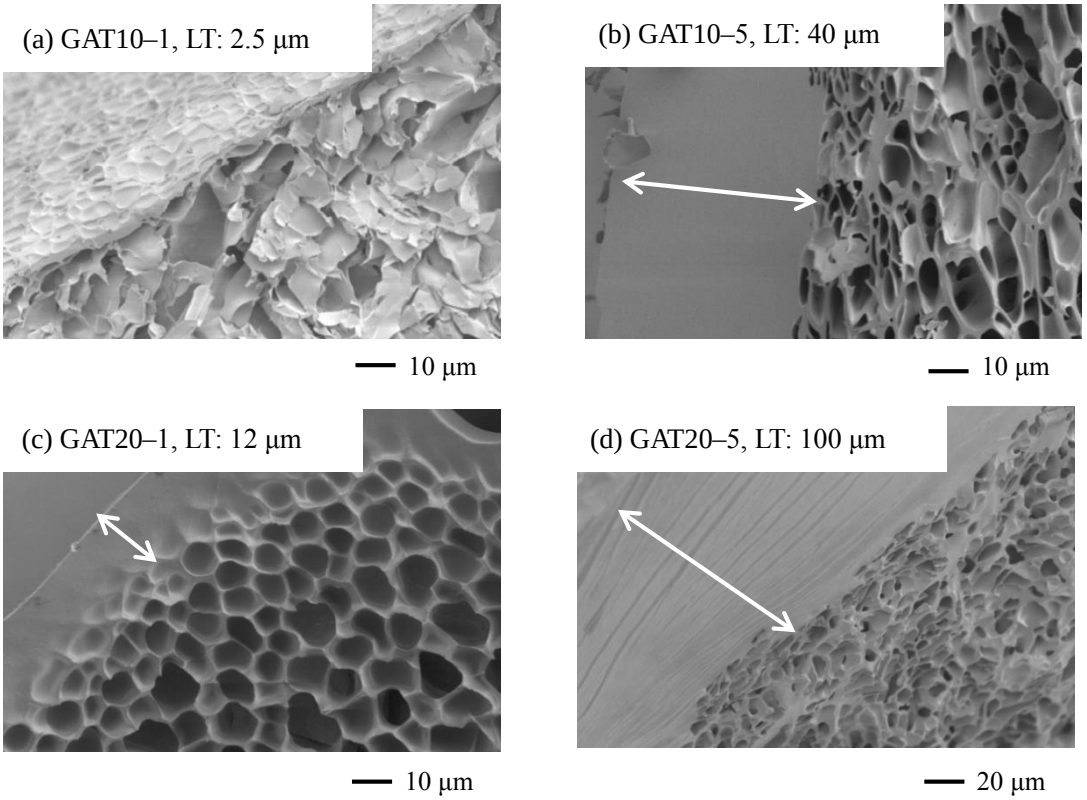

Figure 5.8. SEM pictures of graft hydrogels having different graft ratio or PTMC segment lengths. Morphologies were composed of skin layer and porous interior. (a) GAT10–1, (b) GAT10–5, (c) GAT20–1, and (d) GAT20–5.

5.3.4 Evaluation of Molecular Incorporation Using Hydrophobic Dye

In this study, BB7 was used as a hydrophobic model drug. The behavior of the supernatant of the BB7 solution containing the lyophilized hydrogel was monitored by UV–Vis spectroscopy. Measurements were performed at 0, 1, 5, 16, and 24 h. As shown in Figure 5.9, the absorbance of BB7 at 616 nm decreased in all sample tubes including the blank, PAGA gel–3, and the graft gel. In the case of the blank, the absorbance only slightly changed. On the other hand, the absorbance of PAGA gel–3 and the graft gel gradually changed at the given time. The maximum wavelength absorption changed the most in the case of PAGA gel–3 and the graft gel. The absorbance at 616 nm decreased fast in the supernatant of the graft gel mixture. In particular, the absorbance of the supernatant with GAT20–10 decreased extremely fast compared with that of other samples. From these results, it can be concluded that the adsorption of BB7 was based on the PTMC segment in the gel. BB7 dye was absorbed in the hydrophobic domain formed by PTMC segments. Figure 5.10 shows the normalized profile of the BB7 absorption on the hydrogel. The BB7 absorption increased with increasing time. In particular, GAT20–5 and GAT20–10 showed fast incorporation of BB7. Furthermore, this absorption behavior did not depend on the high swelling ratio, but the composition ratio of PTMC segment was the dominant factor. On the other hand, the plots of PAGA gel–3 and GAT20–1 showed slow absorption of BB7. Subsequently, these absorbing hydrogels were immersed into ultrapure water (Figure 5.11). BB7 diffused with time and discolored the PAGA gel–3. Thus, the BB7 molecule incorporated into the hydrogel was located in the media and diluted by the concentration gradient. In the case of the graft gels, the BB7 molecule was retained in the hydrogel upon exposure to acetone or ultrapure water over a longer period of time. The author concluded that PTMC has

absorbed BB7 by hydrophobic interactions. Therefore, BB7 in the graft gel was not affected by the external environment, by the concentration gradient. In the case of higher incorporation ratios of PTMC, the results indicated that the adsorption of BB7 was fast and active.

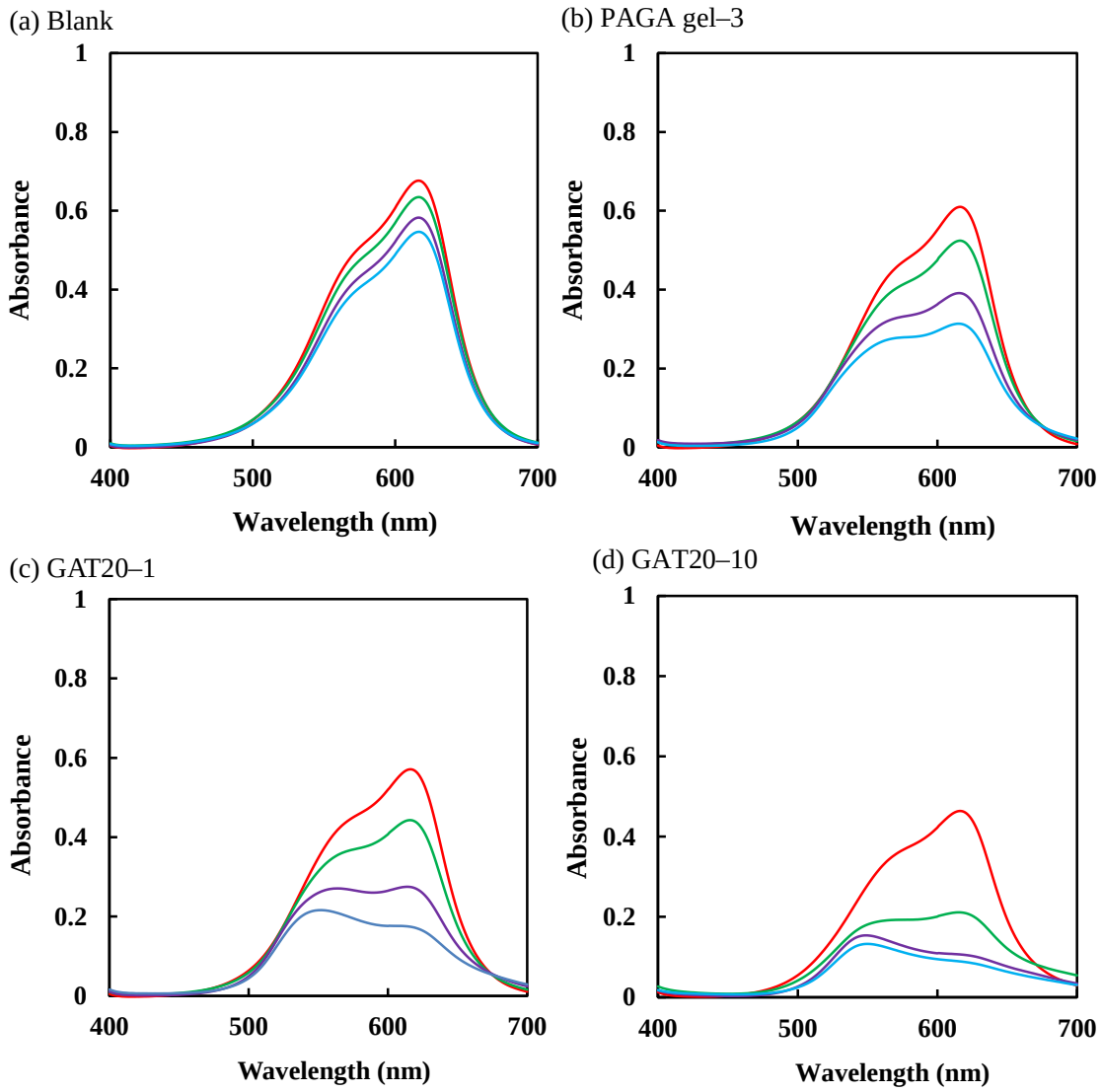

Figure 5.9. The absorption spectra of BB7 as a model drug monitored at 1, 5, 16, and 24 h, from the top spectrum, respectively. The absorbance of the supernatant of the aqueous solution containing the hydrogel, (a) blank, (b) PAGA gel–3, (c) GAT20–1, and (d) GAT20–10, was measured.

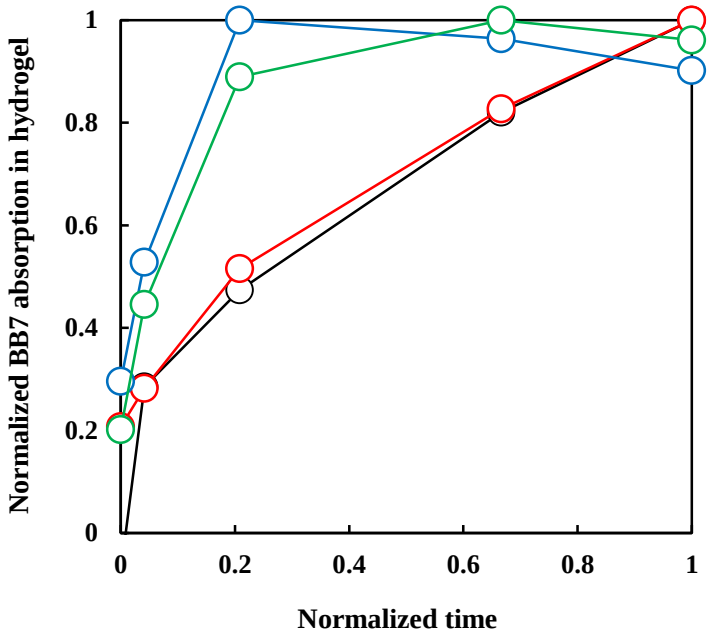

Figure 5.10. Normalized profile of BB7 absorption within the hydrogel. PAGA gel–3: ○, GAT20–1: ○, GAT20–5: ○, and GAT20–10: ○.

(a) PAGA gel (b) Graft gel

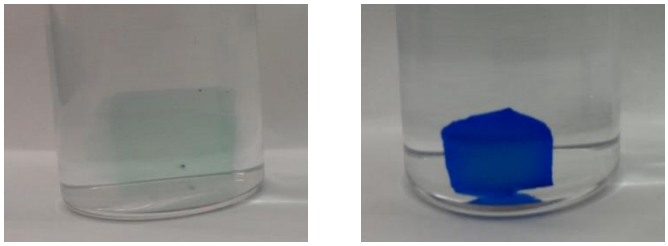

Figure 5.11. Pictures of (a) PAGA gel and (b) graft gel in water. These gels were immersed in BB7 aqueous solution for 24 h. The graft gel was retained the absorbed BB7.

5.4 Conclusions

Hydrogels having different hydrophilic-hydrophobic ratios were prepared by ring-opening polymerization and free radical polymerization. By altering the composition ratio of the PTMC macromonomer, the swelling ratio and network structure properties, such as pore size, were controlled. Upon increasing the number of TMC units in the hydrogels, pores became smaller or disappeared. The morphology of a sponge-like layer or thick skin layer was also controlled by the incorporation ratio of PTMC. The hydrophobic domain formed by PTMC was shown to incorporate hydrophobic molecules. The incorporation rate depended on the composition ratio of PTMC segments. As a result, the graft gel having variable polarity showed useful functionality. The author proposes that the graft gel is a suitable candidate for application as a molecular absorbent in the biomedical and environmental fields.

5.5 References

[1] E. Ho, A. Lowman, and M. Marcolongo, *Biomacromolecules* **2006**, *7*, 3223.

[2] H. Dai, Q. Chen, H. Qin, Y. Guan, D. Shen, Y. Hua, Y. Tang, and J. Xu, *Macromolecules* **2006**, *39*, 6584.

[3] T. Sakai, T. Matsunaga, Y. Yamamoto, C. Ito, R. Yoshid, S. Suzuki, N. Sasaki, M. Shibayama, and U. Chung, *Macromolecules* **2008**, *41*, 5379.

[4] Y. Kaneko, S. Nakamura, K. Sakai, T. Aoyagi, A. Kikuchi, Y. Sakurai, and T. Okano, *Macromolecules* **1998**, *31*, 6099.

[5] X.-D. Xu, X.-Z. Zhang, J. Yang, S.-X. Cheng, R.-X. Zhuo, and Y.-Q. Huang, *Langmuir* **2007**, *23*, 4231.

[6] F. Nederberg, B. G. G. Lohmeijer, F. Leibfarth, R. C. Pratt, J. Choi, A. P. Dove, R. M. Waymouth, and J. L. Hedrick, *Biomacromolecules* **2007**, *8*, 153.

[7] J. Mindemark, J. Hilborn, and T. Bowden, *Macromolecules* **2007**, *40*, 3515.

[8] K. Nitta, J. Miyake, J. Watanabe, and Y. Ikeda, *Trans. Mater. Res. Soc. Jpn.* **2012**, *37*, 349.

[9] H. K. Moon, Y. S. Cho, J.-K. Lee, C.-S. Ha, W.-K. Lee, and J. A. Gardella Jr., *Langmuir* **2006**, *25*, 4478.

[10] K. Makiguchi, Y. Ogasawara, S. Kikuchi, T. Satoh, and T. Kakuchi, *Macromolecules* **2013**, *46*, 1772.

Chapter 6

Preparation of Amphiphilic Polymer Gels Containing Poly(trimethylene carbonate) Segments and Evaluation of Its Molecular Incorporation Properties

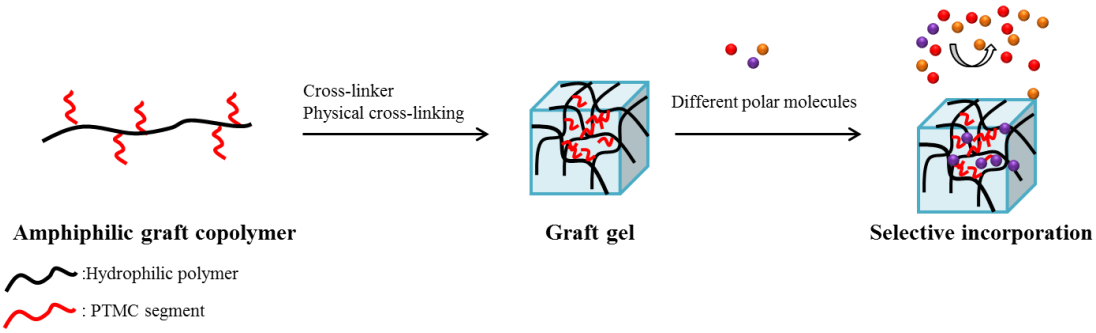

6.1 Introduction

Excellent functionality such as mechanical strength, drug loading, and biocompatibility are required for advanced materials. Moreover, amphiphilic hydrogels can incorporate hydrophobic drug molecules for application in drug delivery systems [1–7].

The author evaluated the pH responsivity graft gel by macromonomer method in Chapter 5. In this study, the author designed and synthesized an amphiphilic hydrogel containing poly(trimethylene carbonate) (PTMC) oligo segments the degree of polymerization (DP) of PTMC in the feed was between 10 and 20). The hydrophilic–hydrophobic balance was controlled by altering the length of the PTMC segments and the PTMC macromonomer composition ratio. PTMC has several favorable properties; for example, it is hydrophobic, amorphous, and biocompatible. Block copolymers containing PTMC segments have been reported to have molecular incorporation abilities as membranes and colloidal materials. The author investigated these amphiphilic hydrogels and selected three different functional monomers for use: 2-acrylamido-2-methylpropanesulfonic acid (AMPS), *N*-hydroxyethyl acrylamide (HEAA), and 2-hydroxyethyl acrylate (HEA) (Figure 6.1).

The author synthesized amphiphilic graft gels by ring-opening polymerization (ROP) and photo-polymerization. Photo-polymerization is appropriate for hydrogel synthesis because it is rapid; the hydrogel can be prepared in a few minutes without the deformation caused by heat polymerization [8, 9]. In this chapter, the author discusses our investigation into the swelling ratio and the molecular incorporation properties in the hydrophobic domain using different model molecules, such as hydrophobic dyes Basic Blue 7 and Rhodamine 6G.

(a) GAMT

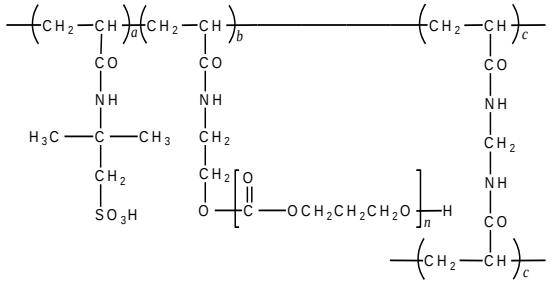

AMPS HEAA–PTMC MBA

(b) GHET

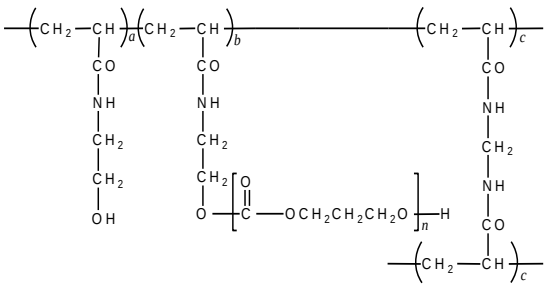

HEAA HEAA–PTMC MBA

(c) GHT

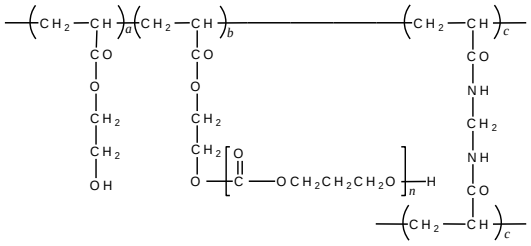

HEA HEA–PTMC MBA

Figure 6.1. Chemical structures of (a) poly(AMPS–*co*–HEAA–PTMC) (GAMT), (b) poly(HEAA–*graft*–PTMC) (GHET), and (c) poly(HEA–*graft*–PTMC) (GHT).

6.2 Experimental Section

6.2.1 Materials

Trimethylene carbonate (TMC), AMPS, HEA, and 2,2′-azobis(isobutyronitrile) (AIBN) were purchased from Tokyo Chemical Industry, Co., Ltd., Tokyo, Japan. 1,8-Diazabicyclo[5.4.0]undec-7-ene (DBU) and benzoic acid were purchased from Wako Pure Chemical Industries, Ltd., Osaka, Japan. HEAA was supplied by KOHJIN Co., Ltd., Tokyo, Japan. *N*,*N*′-Methylenebisacrylamide (MBA, Wako Pure Chemical Industries, Ltd.) was used as the cross-linker. For photo-radical polymerization, the initiator, 2,2-dimethoxy-2-phenylacetophenone (DPAP; Tokyo Chemical Industry, Co., Ltd.) was used. To investigate the drug incorporation property in the hydrogel, Basic Blue 7 (BB7) (Tokyo Chemical Industry, Co., Ltd.), Allura Red AC (Tokyo Chemical Industry, Co., Ltd.), and Rhodamine 6G (R6; Wako Pure Chemical Industries, Ltd.) were used as a model drug. Phosphate buffered saline (PBS) was purchased from Life Technologies Corp., Waltham, MA, USA. All organic solvents were used as received.

6.2.2 Synthesis of HEAA–PTMC Macromonomer

The HEAA–PTMC macromonomer was prepared according to previously reported procedure [10]. The DP of PTMC was calculated from the proton nuclear magnetic resonance (^{1}H NMR) spectrum in $CDCl_3$. The author prepared the macromonomer with approximately 10 and 20 repeating units of TMC.

6.2.3 Synthesis of HEA–PTMC Macromonomer

The HEA–PTMC macromonomer was prepared according to previously reported procedure [10]. The DP of PTMC was calculated from the ^{1}H NMR spectrum in $CDCl_3$.

The author prepared the macromonomer with approximately 10 and 20 repeating units of TMC.

6.2.4 Preparation of Poly(AMPS–*co*–HEAA–PTMC) Graft Gel

To prepare the graft gel, free radical polymerization was carried out using DPAP as initiator, AMPS, MBA, and HEAA–PTMC macromonomer (Figure 6.1(a)). Each reagent was dissolved in *N*,*N*-dimethylformamide (DMF), and these solutions were mixed. The total concentration of monomer and macromonomer was 1.5 mol/L. The concentration of DPAP was 7.5 μmol/L. Then, the mixture was poured onto glass plates separated by silicon rubber (thickness: 0.5 mm), and covered with a glass plate as a lid. This solution was polymerized by UV irradiation at 365 nm with an intensity of 3,000 mW/cm^2 for 600 s. The UV lamp was Type ZUV–C30H equipped with Type ZUV–L3H spot lens, OMRON Co., Ltd., Kyoto, Japan. The prepared hydrogel was punched out in 5 mm in diameter circles. To remove any unreacted compounds, the crude product was immersed into a DMF/water mixed solution (DMF:water = 1:1), and it was then immersed in ultrapure water. Subsequently, the prepared hydrogel was purified. The chemical structure was confirmed by FT–IR measurements. IR (in ATR mode, cm^{-1}): 3200–3500 (–C(=O)–NH–, and –OH), 1730 (–C(=O)–O–), 1550–1650 (–C(=O)–NH–), 1250 (–C–O–C–), and 1150 ($–SO_3^-$) [11, 12].

6.2.5 Preparation of Poly(HEAA–*graft*–PTMC) Graft Gel

To prepare the graft gel, free radical polymerization was carried out using DPAP as initiator, HEAA, MBA, and HEA–PTMC (Figure 6.1(b)). Each reagent was dissolved in *N*,*N*-dimethylformamide (DMF), and these solutions were mixed. The total

concentration of monomer and macromonomer was 1.5 mol/L. The concentration of DPAP was 7.5 μmol/L. Then, the mixture was poured onto glass plates separated by silicon rubber (thickness: 0.5 mm), and covered with a glass plate as a lid. This solution was polymerized by UV irradiation at 365 nm with an intensity of 3,000 mW/cm2 for 600 s. The UV lamp was Type ZUV–C30H equipped with Type ZUV–L3H spot lens, OMRON Co., Ltd., Kyoto, Japan. The prepared hydrogel was punched out in 5 mm in diameter circles. To remove any unreacted compounds, the crude product was immersed into a DMF/water mixed solution (DMF:water = 1:1), and it was then immersed in ultrapure water. Subsequently, the prepared hydrogel was purified. The Chemical structure was confirmed by FT–IR measurements. IR (in ATR mode, cm^{-1}): 3150–3550 (–C(=O)–NH–, and –OH), 1730 (–C(=O)–O–), 1550–1650 (–C(=O)–NH–), and 1230 (–C–O–C–).

6.2.6 Preparation of Poly(HEA–*graft*–PTMC) Graft Gel

To prepare the graft gel, free radical polymerization was carried out using DPAP as initiator, HEA, MBA, and HEA–PTMC (Figure 6.1(c)). Each reagent was dissolved in *N*,*N*-dimethylformamide (DMF), and these solutions were mixed. The total concentration of monomer and macromonomer was 1.5 mol/L. The concentration of DPAP was 7.5 μmol/L. Then, the mixture was poured onto glass plates separated by silicon rubber (thickness: 0.5 mm), and covered with a glass plate as a lid. This solution was polymerized by UV irradiation at 365 nm with an intensity of 3,000 mW/cm2 for 600 s. The UV lamp was Type ZUV–C30H equipped with Type ZUV–L3H spot lens, OMRON Co., Ltd., Kyoto, Japan. The prepared hydrogel was punched out in 5 mm in diameter circles. To remove any unreacted compounds, the crude product was immersed

into a DMF/water mixed solution (DMF:water = 1:1), and it was then immersed in ultrapure water. Subsequently, the prepared hydrogel was purified. The Chemical structure was confirmed by FT–IR measurements. IR (in ATR mode, cm^{-1}): 3000–3700 (–OH), 1715 (–C(=O)–O–), and 1180–1240 (–C–O–C–) [13].

6.2.7 Swelling Ratio Measurements

The prepared hydrogel was immersed into aqueous solution, and the volume of the hydrogel in its equilibrium state was measured. The swelling ratio of the hydrogel was calculated by the following equation:

$$\text{Swelling ratio} = (V_s - V_0)/V_0$$

where V_s and V_d are the volumes of the swollen hydrogel and the dried hydrogel, respectively.

6.2.8 Observation of Surface and Interior Morphology of Hydrogel

The dried hydrogel was observed by SEM. The cut hydrogel was fixed by carbon tape on a sample stage, and then electro-conductive paste (DOTITE; Fujikura Kasei Co., Ltd., Tochigi, Japan) was spotted onto the corner of the sample. The sample was sputter-coated with platinum prior to the observation.

6.2.9 Evaluation of Selective Model Drug Incorporation in Hydrogel

The author evaluated the molecular loading ability of the graft gel. Hydrophobic BB7 (solubility in water = 20 g/L), hydrophilic AR (solubility in water = 120 g/L), and

amphiphilic R6 were used as a model drug (Figure 5.2 and Figure 6.2) [14]. The water/*n*-octanol partition coefficient indicate the hydrophobicity of a molecule, and BB7 and R6 both soluble in *n*-octanol; in addition, AR and R6 were present in the water partition. Therefore, R6 is both hydrophobicity and hydrophilicity. Each organic dye aqueous solution was prepared with ultrapure water. The mixed aqueous solution of BB7 (15 μmol/L) + AR (25 μmol/L) and BB7 (10 μmol/L) + R6 (10 μmol/L). The swollen hydrogel (one disc) was immersed into each mixed dye solution at room temperature. The UV–Vis spectrum of the supernatant was monitored at given intervals. The amount of drug loading was evaluated from absorbance values obtained from UV–Vis spectroscopy. To investigate the dye release, the dye-molecule-loaded graft gels were immersed in a 10% PBS solution for 6 h. The supernatant PBS solution was then subjected to UV–Vis spectroscopy analysis.

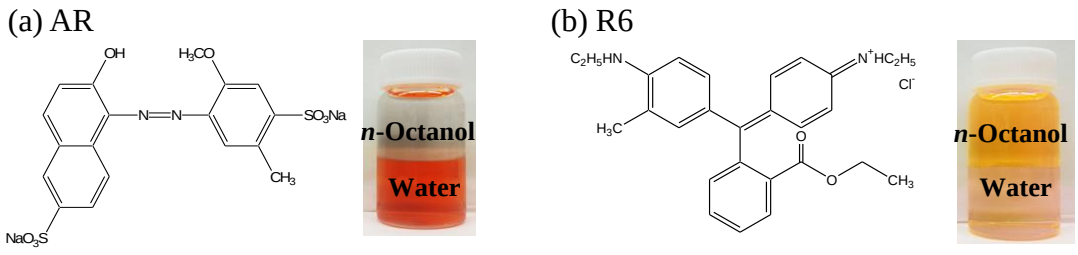

Figure 6.2. Chemical structures of (a) AR and (b) R6.

6.3 Results and Discussion

6.3.1 Synthetic Results of Graft Gels

HEAA–PTMC and HEA–PTMC were synthesized by ROP. The feed ratios of [TMC]/[HEAA] and [TMC]/[HEA] were 10 and 20, respectively. The DP of PTMC calculated by ^{1}H NMR was approximately 11 and 21. The various graft gels were prepared by photo-radical polymerization using DPAP as the initiator. The concentration of DPAP, macromonomer, and MBA were 0.5 mol%, 2 mol%, and 3 mol%, respectively. After polymerization, the graft gels were molded into a disc shape (5 mm in diameter). Unreacted chemicals such as monomer and the macromonomer were sequentially removed by immersion in DMF and ultrapure water for three days, and these solvents were replaced several times during that period. The chemical structure was confirmed by FT–IR measurement (Figure 6.3). The amide groups in AMPS and HEAA were observed as a broad absorption at 1150–1650 cm^{-1} and 3150–3550 cm^{-1}. The sulfone group in AMPS was identified stretching vibration at 1230 cm^{-1}.The stretching vibration peaks of PTMC were observed at near 1180–1240 cm^{-1} and 1715–1730 cm^{-1}. Table 6.1 summarizes the preparation condition for the graft gels. The sample codes are abbreviated as G”M”T*n*, where “M” represents the monomer, AMPS = AM, HEAA = HE, and HEA = H, and “*n*” represents the DP of PTMC. For example, GAMT10–2 refers to the graft hydrogel containing a poly(AMPS) main chain with a DP of PTMC and macromonomer composition of approximately 10 and 2 mol%, respectively.

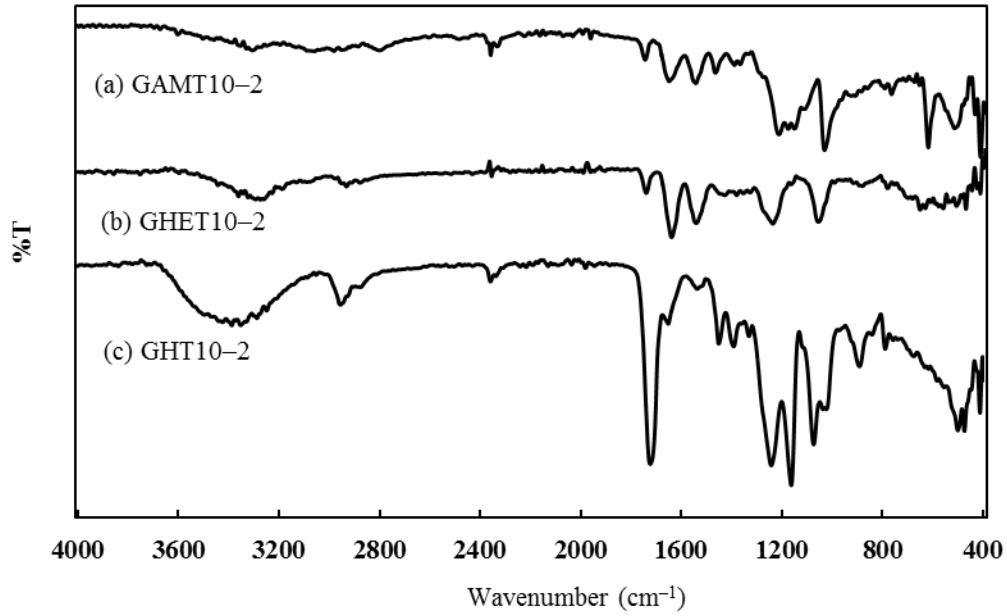

Figure 6.3. FT–IR spectra of (a) GAMT10–2, (b) GHET10–2, and (c) GHT10–2.

Table 6.1. Preparation of amphiphilic graft hydrogels

Sample	Feed ratio (mol%)				V_s/V_0
	Monomer	PTMC macromonomer (DP)		MBA	
Poly(AMPS)	97	0		3	60.8
GAMT10–2	95	2	(11)	3	46.2
GAMT20–2	95	2	(21)	3	35.8
Poly(HEAA)	97	0		3	5.1
GHET10–2	95	2	(11)	3	2.5
GHET20–2	95	2	(21)	3	2.2
Poly(HEA)	97	0		3	2.9
GHT10–2	95	2	(11)	3	1.0
GHT20–2	95	2	(21)	3	0.6

6.3.2 Change in Swelling Ratio of Graft Gel

Table 6.1 shows the swelling ratio of the hydrogel at equilibrium swelling. The hydrogel can uptake water into the network structure. Moreover, surface morphology was observed porous structure as shown Figure 6.4. The poly(AMPS) graft gel swelled, absorbing a large amount of water; however, these swollen gels are fragile due to their bulky chemical structures [11, 12].The sulfone group in the poly(AMPS) chain expands significantly due to ionic repulsion. Therefore, a large amount of water can be adsorbed into the network. The swelling ratios of poly(AMPS), GAMT10–2, and GAMT20–2 gels were approximately 60.8, 46.2, and 35.2. The swelling ratio was reduced due to the increasing hydrophobic interactions caused by the PTMC segments. The swelling ratios of poly(HEAA), GHET10–2, and GHET20–2 gels were 5.1, 2.5, and 2.2, respectively. Water uptake also decreased with increasing length of PTMC segment. Poly(HEAA) is non-ionic polymer that has a high affinity for water due to the hydroxyl and amide functional groups. In addition, the cross-linking sites of poly(HEAA) graft gel are expected to form hydrogen bonding and hydrophobic interactions besides chemical cross-linking caused by MBA. The poly(HEA) gel, GHT10–2, and GHT20–2 were clear, flexible, and had low swelling ratios: 2.9, 1.0, and 0.6. With increasing length of the PTMC segment, the swelling ratio decreased due to the poly(HEA) polymer backbone. Increasing the DP of PTMC, as in GHT, led to a hydrophobic gel, and poly(HEA) gels were more hydrophobic than the poly(AMPS) gels and poly(HEAA) gels. Poly(HEA) gels have no porous structure in Figure 6.4(c). Because, poly(HEA) gels were comparatively much hydrophobic gel than that of poly(AMPS) gels and poly(HEAA) gels. From these results of the swelling ratio and SEM photographs, the author synthesized graft gels at intended.

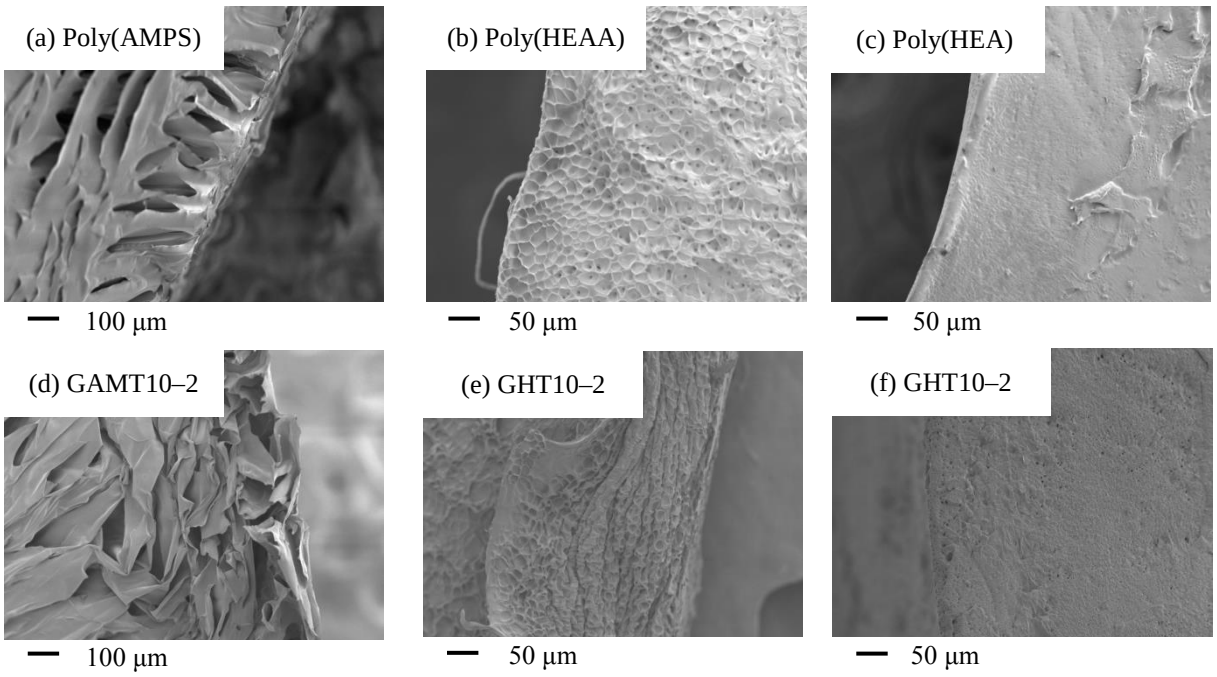

Figure 6.4. SEM images of (a) poly(AMPS), (b) poly(HEEA), (c) poly(HEA), (d) GAMT10–2, (e) GHET10–2, and (f) GHT10–2. (Scale bar: 50 or 100 μm)

6.3.3 Evaluation of Molecular Incorporation Using Various Dyes

The author analyzed the preferential or selective incorporation of various dyes in graft gels (GAMT10–2, GHET10–2, and GHT10–2). For this purpose, dyes with different solubilities were chosen (BB7, AR, and R6). The UV–Vis spectra of the supernatant solution of the hydrogel immersed in dye was monitored. Then, the amount of dye incorporated into the hydrogel was determined from wavelength of the maximum absorption.

In the case of the mixed solution of BB7 (λ_{max} = 616 nm) and AR (λ_{max} = 543 nm), the absorbance of supernatant decreased only hydrophobic dye BB7 (Figure 6.5). By solvent exchange, dye molecules and water molecule was diffused and hydrophobic BB7 was incorporated into hydrophobic domain in graft gels by hydrophobic interaction. This behavior tended to increasing relative to increase hydrogel volume, and in GAMT10–2, concentration of BB7 into hydrogel was 6.0 μmol/L at 36 h (Figure 6.5(b)). Incorporation rate of dye was increased relate to the time. The author thought that AR concentration in mixed solution barely decreased to lead to the precipitate due to complexation by pair ion effect and to incorporate a part of AR molecule into graft gel.

These molecular loading gels were immersed in PBS solution for 6 h, and these supernatant was analyzed to absorbance (Figure 6.6(a) and (b)). In the case of the BB7 and AR mixed system, the AR was only released to PBS solution and graft gel was shrunk. The release ratio of BB7 in GAMT10–2, GHET10–2, and GHT10–2 were 4.5, 1.1, and 0.0%, respectively.

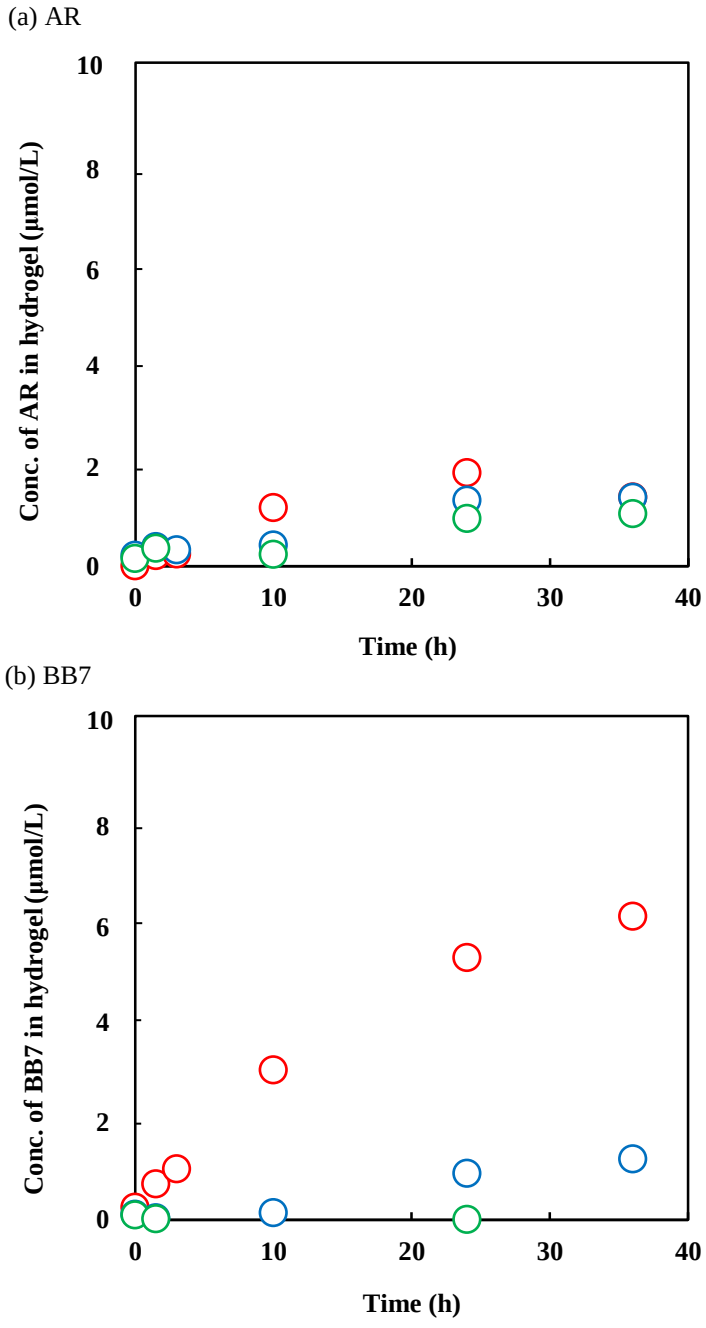

Figure 6.5. The plots of concentration of each dye, (a) AR and (b) BB7, in hydrogel versus time. GAMT10–2: ○, GHET10–2: ○, and GHT10–2: ○.

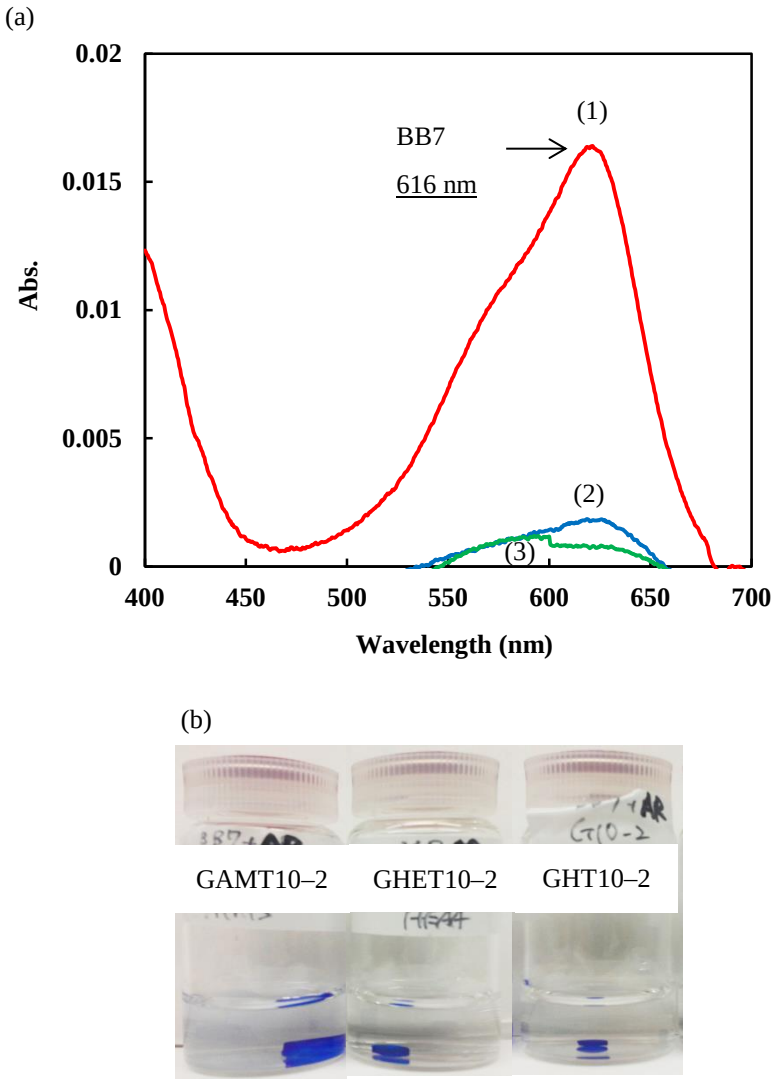

Figure 6.6. (a) Absorption spectra of BB7 monitored from the top spectrum. The absorbance of the supernatant of the PBS solution in which the graft gel was immersed for 6 h was measured. Samples were GAMT10–2: (1), GHET10–2: (2), and GHT10–2: (3). (b) Photographs of various graft gels immersed in PBS solution for 6 h.

The author analyzed the preferential or selective incorporation of various dyes in graft gels (GAMT10–2, GHET10–2, and GHT10–2). For this purpose, dyes with different aqueous solubility were chosen (BB7 and R6). The UV–Vis spectra of the supernatant solution of the hydrogel immersed in dye was monitored. Then, the amount of dye incorporated into the hydrogel was determined from wavelength of the maximum absorption. In the case of the mixed solution of BB7 (λ_{max} = 616 nm) and R6 (λ_{max} = 528 nm), on immersing GHET10–2 in the dye solution, the absorbance of supernatant decreased with time (Figure 6.7(a)). Both BB7 and R6 were incorporated into hydrophobic domains in the graft gel. Furthermore, the incorporation was active and rapid. The concentrations of BB7 in the graft gels GAMT10–2, GHET10–2, and GHT10–2 were 6.7, 5.2, and 3.9 μmol/L after 36 h, respectively (Figure 6.7(b)). The concentrations of BB7 incorporated into GAMT10–2, GHET10–2, and GHT10–2 were 8.8, 5.2, and 4.3 μmol/L after 36 h (Figure 6.7(c)). The dye loading correlated with the swelling ratio of the hydrogels. Finally, the author investigated the release behavior of incorporated dye from the graft gels by immersing the swollen hydrogels in PBS solution for 6 h. The UV–Vis spectra of the supernatants were measured, and the amount of dye released was analyzed by the changes in absorbance wavelength (Figure 6.8(a) and (b)). In the case of the BB7 and R6 mixed system, only R6 was released. The amounts of R6 released from GAMT10–2, GHET10–2, and GHT10–2 hydrogels were 60.0, 18.1, and 13.7%, respectively. Therefore, the author believe that amphiphilic R6 was incorporated into a part of hydrophilic domain, increasing the absorbance of R6. In particular, GAMT10–2, an ionic hydrogel, shrank to reduce ionic repulsion in the phosphate buffer; consequently, larger quantities of dye diffused out of the gel in comparison to the other hydrogels. Therefore, the author believes that the interaction

between hydrophobic molecules and PTMC segments is due to physical adsorption.

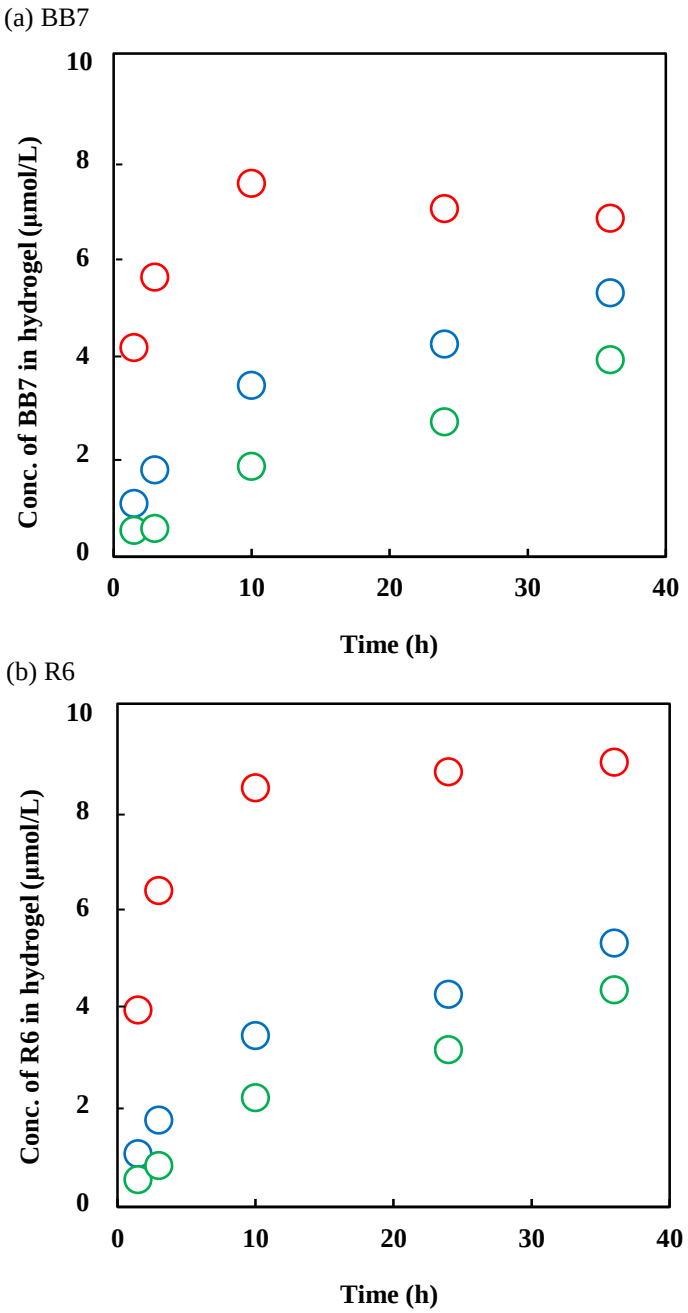

Figure 6.7. The plots of concentration of each dye, (a) BB7 and (b) R6, in the hydrogel verses time. GAMT10–2: ○, GHET10–2: ○, and GHT10–2: ○.

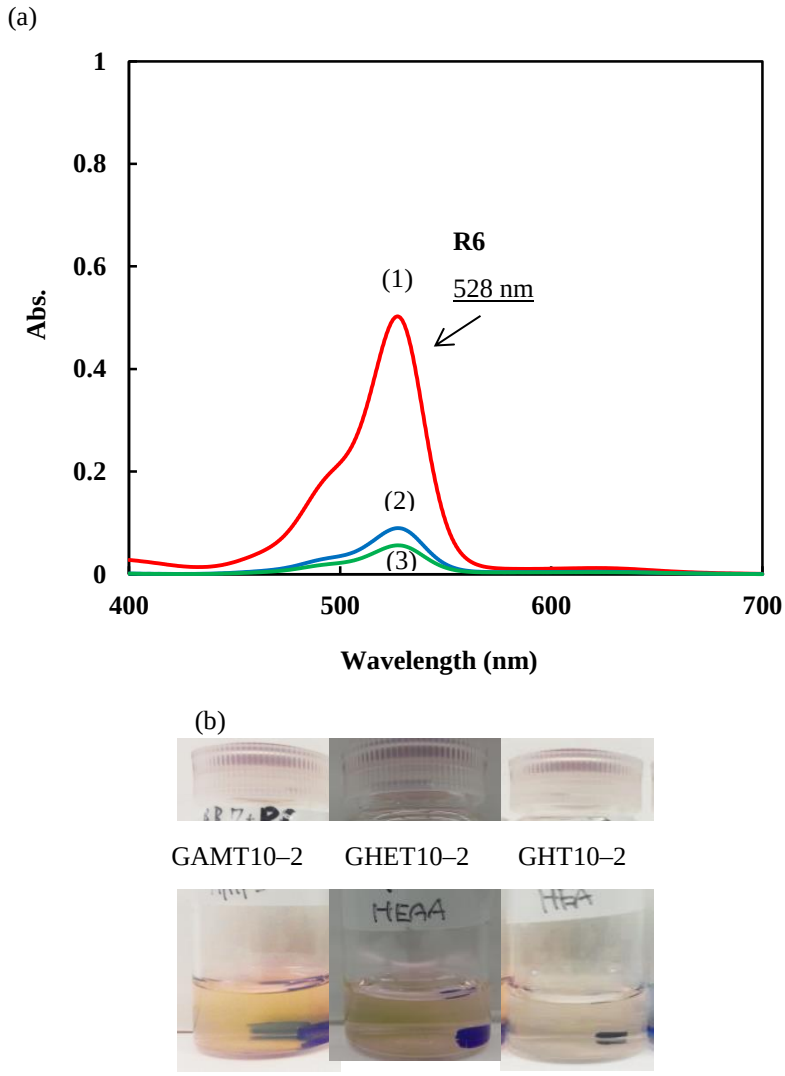

Figure 6.8. (a) Absorption spectra of R6 monitored from the top spectrum. The absorbance of the supernatant of the PBS solution in which the graft gel was immersed for 6 h was measured. Samples were GAMT10–2: (1), GHET10–2: (2), and GHT10–2: (3). (b) Photographs of various graft gels immersed in PBS solution for 6 h.

6.4 Conclusions

In this chapter, the author has reported the selective incorporation of model drugs driven by PTMC. In this study, amphiphilic graft gels with a backbone composed of different hydrophilic polymers and two lengths of PTMC side chains were prepared by photo-radical polymerization. By using different hydrophilic main chains, the swelling ratio was altered. In the bulky GAMT graft gel, the pendant sulfone group absorbed a large amount of water. In contrast, the less bulky GHET graft gel had a low swelling ratio and was clear. In incorporation tests of molecules with different solubilities in water, the low solubility BB7 was preferentially incorporated into hydrophobic PTMC and was not released on shrinkage. In contrast, amphiphilic R6 was incorporated into graft gels and was released by shrinking. The large change in swelling ratio of GAMT gel increased the number if adsorbed molecules, while the GHET gel was clear and flexible. On the other hand, GHT graft gels did not changed their volumes, and they were flexible, clear, and loaded hydrophobic dye molecule. With these properties, these graft gels are key materials for molecular separation.

6.5 References

[1] T. Kubo, S. Arimura, Y. Tominaga, T. Naito, K. Hosoya, and K. Otsuka, *Macromolecules* **2015**, *48*, 4081.

[2] A. M. Lowman and N. A. Peppas, *Macromolecules* **1997**, *30*, 4959.

[3] B. H. Lee, B. West, R. McLemore, C. Pauken, and B. L. Vernon, *Biomacromolecules* **2006**, *7*, 2059.

[4] D.-Q Wu, Y.-X. Sun, X.-D. Xu, S.-X. Cheng, X.-Z. Zhang, and R.-X. Zhuo, *Biomacromolecules* **2008**, *9*, 1155.

[5] S. A. Robb, B. H. Lee, R. McLemore, and B. L. Vernon, *Biomacromolecules* **2007**, *8*, 2294.

[6] X. Fan, M. Wang, D. Yuan, and C. He, *Langmuir* **2013**, *29*, 14307.

[7] J. Ning, G. Li, and K. Haraguchi, *Macromolecules* **2013**, *46*, 5317.

[8] D. Arunbaru, H. Shahsavan, W. Zhang, and B. Zhao, *J. Phys. Chem. B* **2012**, *117*, 441.

[9] Y. Chang, W. Yandi, W.-Y. Chen, Y.-J. Shih, C.-C. Yang, Y. Chang, Q.-D. Ling, and A. Higuchi, *Biomacromolecules* **2010**, *11*, 1101.

[10] K. Nitta, J. Miyake, J. Watanabe, and Y. Ikeda, *Trans. Mater. Res. Soc. Jpn.* **2012**, *37*, 349.

[11] J. F. StanzioneIII, R. E. Jensen, P. J. Costanzo, and G. R. Palmese, *Appl. Mater. Interfaces* **2012**, *4*, 6142.

[12] H. Pei, L. Hong, and J. Y. Lee, *Langmuir* **2007**, *23*, 5077.

[13] A. Pourjavadi and H. Salimi, *Ind. Eng. Chem. Res* **2008**, *47*, 9206.

[14] J. Watanabe, H. Kotera, and M. Akashi, *Macromolecules* **2007**, *40*, 8731.

Chapter 7

Concluding Remarks

This thesis described the various functional materials such as colloid, membrane, and hydrogel, composed of amphiphilic graft copolymer. The author designed and synthesized copolymer by macromonomer method to tune the properties. The results obtained through this work are summarized as follow.

In Chapter 2, amphiphilic graft copolymers having poly(trimethylene carbonate) (PTMC) segments were synthesized by macromonomer method. The author investigated the solution property of polymer colloid. The particle size of the poly(*N*-hydroxyethyl acrylamide–*graft*–PTMC) (PHET) aggregates in aqueous solution was indicated about 30–300 nm. Moreover, the critical association concentration (CAC) of the PHET was in the range of 2.2×10^{-3} to 8.9×10^{-2} mg/mL. The partition equilibrium constants (K_v) value was dependent on the increase in trimethylene carbonate (TMC) units. The author concluded that the particle size, CAC, and K_v values for the copolymers depended on the length of PTMC. The graft copolymer with a longer PTMC chain length underwent strong hydrophobic interactions, leading to an increase in the particle size and K_v value. The author thought that the segment having different degree of polymerization (DP) of PTMC was formed the different size hydrophobic domain.

In Chapter 3, the graft copolymers with temperature-responsive function were synthesized. By introducing *N*-isopropyl acrylamide (NIPAAm) into the PHET copolymer, the author investigated the lower critical solution temperature (LCST) and function of molecular incorporation by fluorescence probe method. By introducing

hydrophilic HEAA units into poly(NIPAAm–*graft*–PTMC) (PNT) and poly((HEAA)–*co*–NIPAAm)–*graft*–PTMC) (PHNT) showed LCST at 43.1°C and decreased particle size compared to unmodified PNT. Above the LCST, the HEAA units of the copolymer formed a shell structure in aqueous media and reorganized into a stable colloid. The CAC values of PNT and PHNT copolymers were the same values and these aggregations was composed of the number of copolymers (N_{agg} = approximately 2–4). Furthermore, near the CAC, PNT and PHNT copolymers were gradually formed stable colloids at the LCST.

PHET and PHNT aggregates formed from the graft copolymers with PTMC domains may be used as potential drug delivery vehicle for loading hydrophobic molecules.

In Chapter 4, the amphiphilic graft copolymers having different main chain, 2-hydroxyethyl acrylate (HEA) or 2-methoxyethyl acrylate (MEA), were synthesized by macromonomer method. The author investigated the wettability of polymer membrane by the static contact measurement. PTMC copolymers were indicated the low glass transition temperature, so that the mobility of PTMC segment was high at the room temperature. In polymer coated glass substrate, the surface property of polymer membrane, poly(HEA–*graft*–HEA–PTMC–*co*–poly(ethylene glycol) monomethyl ether (mPEGMA)) **(**PHPT) and poly(MEA–*co*–HEA–PTMC–*co*–mPEGMA) (PMPT), changed rapidly surface responsivity in various condition, and the wettability was controlled by altering the length of PTMC and the composition ratio. These results indicated synthesized polymer controlled the wettability of material surface by main chain polymer and composition ratio of macromonomer. However, the properties of graft copolymer containing both PTMC segment and mPEG segment were not changed.

Therefore, the biocompatible graft copolymers with rapidly surface responsivity can be used for surface modifier in biomaterial field.

In Chapter 5, the author prepared amphiphilic graft gel by heat polymerization. By altering chain length of PTMC and composition ratio of PTMC macromonomer, the swelling ratio and pore size were controlled. This graft gels were shrank, swollen, and collapsed by physical binding behavior in poly(2-acrylamidoglycolic acid) (poly(AGA)) to respond under various pH, salt, and heating. With increasing the number of TMC units in the hydrogels, the pores of dried gels became smaller or disappeared. The morphology of a sponge-like layer or thick skin layer was also controlled by hydrophobic chain length and composition ratio of macromonomer. In incorporation test, the hydrophobic domain formed by PTMC was incorporated Basic blue 7 (BB7).

In Chapter 6, the author prepared graft gels composed of various main chains by photo polymerization. By altering composition ratio of PTMC macromonomer, the swelling ratio and hydrogel morphology were controlled. The morphology of a sponge-like layer or thick skin layer was also controlled by the composition ratio of PTMC. In incorporation test, the hydrophobic domain formed by PTMC was shown to incorporate hydrophobic and amphiphilic molecules. But, low solubility BB7 was preferentially incorporated into hydrophobic domain. The incorporation rate depended on the composition ratio of PTMC segments.

From results of Chapter 5 and 6, the graft gel having variable polarity showed useful functionality. This graft gel was expected the application for drug delivery carrier and molecular separation material for further developments in the future.

In this thesis, the author focused on amphiphilic graft copolymer and attempted to development the functional material by the novel polymer design containing PTMC. In

each chapter, the author designed, synthesized, and evaluated to different materials by driven force of oligo PTMC segment. As the results, the specific properties of diverse biomaterials formation such as colloid, membrane, and hydrogel found to be appropriate for use as biomaterials. Moreover, by selecting functional monomer as polymer backbone in terms of polymer design, the graft copolymer introducing oligo PTMC segment was expected to widely apply as more intelligent material. The author hopes that these polymer designs contribute to application for the intended use in the future.

List of Publications

1. Kyohei Nitta, Junpei Miyake, Junji Watanabe, and Yoshiyuki Ikeda,
   "Gel Formation Driven by Tunable Hydrophobic Domain: Design of Acrylamide Macromonomer with Oligo Hydrophobic Segment"
   Biomacromolecules **2012**, *13*, 1002–1009.
   (Chapter 2, 3, 6)

2. Kyohei Nitta, Junpei Miyake, Junji Watanabe, and Yoshiyuki Ikeda,
   "Synthesis of Functional Macromonomers with Oligo Segment of Polycarbonate for Biomaterials"
   Transactions of the Materials Research Society of Japan **2012**, *37*, 349–352.
   (Chapter 2–6)

3. Kyohei Nitta, Junji Watanabe, and Yoshiyuki Ikeda,
   "Evaluation of Enzymatic Degradation of Gel and Colloid Formed by Poly(trimethylene carbonate) Grafted Copolymer"
   Transactions of the Materials Research Society of Japan **2013**, *38*, 629–632.
   (Chapter 2, 4, 6)

4. Kyohei Nitta, Atsushi Kimoto, Junji Watanabe, and Yoshiyuki Ikeda,
   "Characterization of Temperature-Responsive Graft Copolymer with Polycarbonate Oligo Segment"

Transactions of the Materials Research Society of Japan **2015**, *40*, 271–274.

(Chapter 3)

5. Kyohei Nitta, Atsushi Kimoto, Junji Watanabe, and Yoshiyuki Ikeda,

   “Amphiphilic graft copolymers: Effect of graft chain length and content on colloid gel”

   Biomaterials and Biomedical Engineering **2015**, *2*, 97–109.

   (Chapter 2)

6. Kyohei Nitta, Atsushi Kimoto, and Junji Watanabe,

   “Synthesis and Evaluation of Surface Property of Amphiphilic Graft Copolymer Containing Different Oligo Segments”

   in preparation.

   (Chapter 4)

7. Kyohei Nitta, Atsushi Kimoto, Junji Watanabe, and Yoshiyuki Ikeda,

   “Design and Synthesis of an Amphiphilic Graft Hydrogel Having Hydrophobic Domain Formed by Multiple Physical Interactions”

   in preparation.

   (Chapter 5)

8. Kyohei Nitta, Atsushi Kimoto, and Junji Watanabe,

   “Synthesis of Amphiphilic Polymer Gels Containing Poly(trimethylene carbonate) Segments and Evaluation of Its Molecular Incorporation Properties”

Transactions of the Materials Research Society of Japan submitted.

(Chapter 6)

List of Presentations

International Conference

1. Kyohei Nitta, Atsushi Kimoto, Junji Watanabe, and Yoshiyuki Ikeda,
   "Amphiphilic Graft Copolymers Based on Poly(trimethylene carbonate): Colloid Gel Formation and Solution Property"
   International Symposium on Nanomedicine Molecular Science 2013, Tokyo (Japan), October 2013, Poster

2. Kyohei Nitta, Atsushi Kimoto, Junji Watanabe, and Yoshiyuki Ikeda,
   "Synthesis and Swelling Behavior of Hydrogel Having Poly(trimethylene carbonate) Oligo Segment"
   IUPAC World Polymer Congress MACRO 2014, Chiang Mai (Thailand), July 2014, Poster

3. Kyohei Nitta, Atsushi Kimoto, Junji Watanabe, and Yoshiyuki Ikeda,
   "Selective Molecular Incorporation by Graft Gel Having Poly(trimethylene carbonate)"
   15th International Union of Materials Research Societies - International Conference in Asia (IUMRS-ICA 2014), Fukuoka (Japan), August 2014, Oral

4. Kyohei Nitta, Atsushi Kimoto, Junji Watanabe, and Yoshiyuki Ikeda,
   "Aggregation Properties of Temperature-Responsive Graft Copolymer with Poly(trimethylene carbonate) Oligo Segment"

250th American Chemical Society National Meeting & Exposition, Boston (Massachusetts, USA), August 2015, Poster

5. Kyohei Nitta, Atsushi Kimoto, Junji Watanabe, and Yoshiyuki Ikeda,
"Analysis of surface enrichment of graft copolymer with poly(trimethylene carbonate) and poly(ethylene glycol) oligo segment"
2015 International Chemical Congress of Pacific Basin Societies (Pacifichem 2015), Honolulu (Hawaii, USA), December 2015, Poster

Domestic Conference

1. Kyohei Nitta, Atsushi Kimoto, Junji Watanabe, and Yoshiyuki Ikeda,
"Design of Amphiphilic Graft Copolymer with Amorphous Segment on Controlled Chain Length and Application as Biomaterial"
62nd The Society of Polymer Science, Japan (SPSJ) Annual Meeting, Kyoto, May 2013, Poster

2. Kyohei Nitta, Atsushi Kimoto, Junji Watanabe, and Yoshiyuki Ikeda,
"Synthesis of copolymer having poly(trimethylene carbonate) as oligo segment and its gelation properties"
63rd SPSJ Annual Meeting, Nagoya, May 2014, Oral

3. Kyohei Nitta, Atsushi Kimoto, Junji Watanabe, and Yoshiyuki Ikeda,
"Creation of soft material having function of active molecular incorporation"

63rd SPSJ Symposium on Macromolecules, Nagasaki, September 2014, Oral

4. Kyohei Nitta, Atsushi Kimoto, Junji Watanabe, and Yoshiyuki Ikeda,
   "Preparation of amphiphilic polymer gels having poly(trimethylene carbonate) segment and its molecular incorporation property"
   64th SPSJ Annual Meeting, Sapporo, May 2015, Oral

5. Kyohei Nitta, Atsushi Kimoto, and Junji Watanabe
   "Analysis of Surface Enrichment of Amphiphilic Graft Copolymer Having Hydrophobic and Hydrophilic Segments"
   25th Materials Research Societies of Japan, Yokohama, December 2015, Oral

Acknowledgement

This study was performed at the Department of Life and Functional Material Science, Graduate School of Natural Science, Konan University, from 2010 to 2016. A part of this study was supported by Research Fellowships of the Japan Society for the Promotion of Science, from 2013 to 2016.

I would like to express my sincere gratitude to Professor Junji Watanabe of Department of Chemistry of Functional Molecules, Faculty of Science and Engineering, Konan University for his direct guidance, helpful suggestions, and hearty encouragement throughout this work.

In addition, I would like to express appreciation and thank Professor Yoshiyuki Ikeda and Lecturer Atsushi Kimoto of Department of Chemistry of Functional Molecules, Faculty of Science and Engineering, Konan University for their continuous guidance, helpful suggestions, and encouragement during this work.

I also express appreciation and thank to Professors, Associate Professor, Assistant Professor of Department of Chemistry of Functional Molecules, Faculty of Science and Engineering, Konan University for their kind advice.

I would like to express appreciation to Professors of Department of Biology, Konan University.

I also thank Mr. Kazuhisa Terao, Mr. Yuichi Takemura, Mr. Hiroki Tsunematsu, Mr. Yuta Tosaki, Ms. Akiko Tsujimoto, Mr. Shota Tsunemi, Mr. Hiroaki Sakaue, Mr. Daisuke Sakae, Mr. Ryuichi Yagi, Mr. Norihito Kambe, Mr. Yoshiatsu Hashinaga, Ms. Ayaka Ota, Ms. Marina Kawaguchi, Mr. Yugo Takata, Mr. Wataru Yakami, Mr. Kento

Onaka, Mr. Yoshitaka Sakaue, Mr. Yusuke Sawa, Mr. Yuta Maeno, Mr. Riku Koezuka, Mr. Satoshi Yamaguchi, Mr. Takahiro Ohnishi, Mr. Shunya Okayama, Mr. Hiroki Tuchii, and under graduate students as well as all members of the Material Process Laboratory for their hearty support and assistance.

Finally, I would like to express my heartfelt appreciation to my family, Toshiyuki Nitta, Keiko Nitta, Shuhei Nitta, Aisa Nitta, Suteji Arisue, Setsuko Arisue, and many others for their thoughtful attention and continuous encouragement.

March 2016

Kyohei Nitta